Topics in Heavy Particle Effective Theories

Thesis by

Matthew P. Dorsten

In Partial Fulfillment of the Requirements

for the Degree of

Doctor of Philosophy

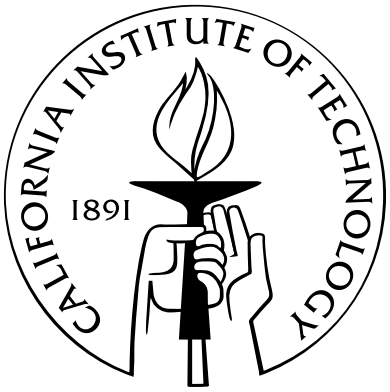

California Institute of Technology

Pasadena, California

2006

(Defended May 25, 2006)

Acknowledgments

Many thanks to my advisor, Mark Wise, for his guidance, physics-related and otherwise. I would also like to thank my collaborators on the physics projects described here: Christian Bauer, Sean Fleming, Sonny Mantry, Mike Salem, and Iain Stewart. I acknowledge the support of a Graduate Research Fellowship from the National Science Foundation and the Department of Energy under Grant No. DE-FG03-92ER40701.

Above all I must thank Rebecca, who helped me get through the whole thing.

Abstract

This thesis gives several applications of effective field theory to processes involving heavy particles. The first is a standard application of heavy quark effective theory to exclusive B decays. It involves two new sum rules discovered by Le Yaouanc *et al.* by applying the operator product expansion to the nonforward matrix element of a time-ordered product of $b \to c$ currents. They lead to the constraints $\sigma^2 > 5\rho^2/4$ and $\sigma^2 > 3(\rho^2)^2/5 + 4\rho^2/5$ on the curvature of the $\bar{B} \to D^{(*)}$ Isgur-Wise function, both of which imply the absolute lower bound $\sigma^2 > 15/16$ when combined with the Uraltsev bound $\rho^2 > 3/4$ on the slope. This thesis calculates order α_s corrections to these bounds, increasing the accuracy of the resultant constraints on the physical form factors.

The second application involves matching $\mathrm{SCET_I}$ onto $\mathrm{SCET_{II}}$ at one loop. Keeping the external fermions off their mass shell does not regulate all IR divergences in both theories. The work described here gives a new prescription to regulate infrared divergences in SCET. Using this regulator, we show that soft and collinear modes in $\mathrm{SCET_{II}}$ are sufficient to reproduce all the infrared divergences of $\mathrm{SCET_I}$. We explain the relationship between IR regulators and an additional mode proposed for $\mathrm{SCET_{II}}$.

Next we consider $t\bar{t}$ production at large energies. The production process is characterized by three disparate energy scales: the center-of-mass energy, $\sqrt{s}$; the mass, m; and the decay width, Γ; with $\sqrt{s} \gg m \gg \Gamma$. At the scale $\sqrt{s}$ we match onto massive soft-collinear effective theory (SCET). The SCET current is run from $\sqrt{s}$ to m, thereby summing Sudakov logarithms of the form $\log^n(m/\sqrt{s})$, where $n = 2, 1$. At the scale m, the top quark mass is integrated out by matching SCET jet functions onto a boosted version of heavy quark effective theory (bHQET). The jet functions in bHQET are then run from m to Γ, summing powers of single logarithms of the ratio m/Γ.

Under certain assumptions factorization formulas can be derived for differential distributions in processes involving highly energetic jets, such as jet energy distributions. As a

final topic, we show how to test these assumptions using semileptonic or radiative decays of heavy mesons, by relating the jet P^+ distribution derived under these assumptions to other differential distributions in these decays, which are better understood.

Contents

List of Figures

Chapter 1

Introduction

The main theme of this thesis is QCD. This is a theory we know a lot about indirectly. It is difficult to calculate things in hadronic physics, however. This is because of the theory's nonperturbative nature. Effective field theory is a useful way of making do with this situation. It is often used to parametrize unknown parameters and relate them to other unknown parameters through general symmetry arguments. This is a surprisingly powerful concept. It is often possible to eliminate some physics we do not understand by taking its effects from somewhere else. In this way we get around our lack of understanding.

1.1 Constraining exclusive B decay measurements

This thesis gives several applications of the ideas of effective field theory to processes involving heavy particles, that is, heavy relative to the other energy scales involved. The first is a standard application of heavy quark effective theory (HQET) to exclusive B decays. In this case, the bottom quark mass is heavy relative to the other scale in the problem, $\Lambda_{\rm QCD}$. This is a very successful theory and will be discussed more fully in the next chapter. For now, suffice it to say that it is a self-contained theory just like any other and that sum rules can be derived by relating exclusive matrix elements with the inclusive result of the optical theorem. The third chapter of this thesis discusses two new sum rules that were discovered in this way by applying the operator product expansion to the nonforward matrix element of a time-ordered product of $b \to c$ currents in the heavy quark limit of QCD. They lead to the constraints $\sigma^2 > 5\rho^2/4$ and $\sigma^2 > 3(\rho^2)^2/5 + 4\rho^2/5$ on the curvature of the $\bar{B} \to D^{(*)}$ Isgur-Wise function, which is basically just a parametrized matrix element. These constraints imply the absolute lower bound $\sigma^2 > 15/16$ when combined with the

Uraltsev bound $\rho^2 > 3/4$ on the slope of the form factor. That chapter calculates order α_s corrections to these bounds, increasing the accuracy of the resultant constraints on the physical form factors. The latter may have implications for the determination of $|V_{cb}|$ from exclusive semileptonic B meson decays.

1.2 Regulating SCET in the infrared

Soft-collinear effective theory (SCET) is another effective theory. It has many similarities with HQET. It is actually more a theory of light particles than of heavy ones. It describes the interactions of light but energetic particles. The fifth chapter of this thesis discusses a subtlety of this theory. There have been claims that its basic formulation is incomplete because it appears not to reproduce the low-energy sector of QCD, which an effective theory of QCD must do. In this chapter, we consider matching from $\mathrm{SCET_I}$, which includes ultrasoft and collinear particles, onto $\mathrm{SCET_{II}}$ with soft and collinear particles at one loop. The definitions of these different subtheories is unimportant for now. The point is that keeping the external particles off their mass shell in the matching does not regulate all infrared (IR) divergences in both theories. Usually this is sufficient to regulate any IR divergences, and it is the standard way of doing so. However, here it is not enough. We give a new prescription to regulate infrared divergences in SCET. Using this regulator, we show that soft and collinear modes in $\mathrm{SCET_{II}}$ are sufficient to reproduce all the infrared divergences of $\mathrm{SCET_I}$. We explain the relationship between IR regulators and an additional mode proposed for $\mathrm{SCET_{II}}$. This is a step toward resolving an apparent paradox that has plagued the field for some time.

1.3 Precision top quark physics

In this thesis we also consider an application of effective field theories to a perturbative process: $t\bar{t}$ production at large energies. Although the most common use for effective field theories is for parametrizing unknown aspects of nonperturbative physics, they also can be very useful in entirely perturbative processes. The reason is that the separation of scales achieved by the judicious use of effective field theories allows one to sum logarithms of the different scales that appear in a perturbative calculation. For instance, when one calculates

in a certain limit the differential cross section for top-antitop production in electron-positron scattering, three different and widely separated scales are involved. The production process is characterized by these energy scales: the center-of-mass energy, $\sqrt{s}$; the mass, m; and the decay width, Γ; with $\sqrt{s} \gg m \gg \Gamma$. Since these scales are so different, any logs of them appearing in a perturbative calculation will be quite large. This can severely diminish the accuracy of a calculation since these logs effectively increase the coupling constant. To sum them, we match at the scale $\sqrt{s}$ onto massive soft-collinear effective theory (SCET). The SCET current is run from $\sqrt{s}$ to m, thereby summing Sudakov logarithms of the form $\log^n(m/\sqrt{s})$, where $n = 2, 1$. At the scale m the top quark mass is integrated out by matching SCET jet functions onto a boosted version of heavy quark effective theory (bHQET). The jet functions in bHQET are then run from m to Γ, summing powers of single logarithms of the ratio m/Γ.

1.4 Jet definitions in SCET

The final project discussed in this thesis concerns the application of SCET to jet physics. This application typically involves some assumptions about the final state of the process. At leading order, it is easy to think of a two-jet final state as just two quarks traveling in different directions. Of course, each jet must really be a color-singlet when it is observed. Individual quarks do not fit the bill. Under certain assumptions factorization formulas can be derived for differential distributions in processes involving highly energetic jets, such as jet energy distributions. In this thesis we show how to test these assumptions using semileptonic or radiative decays of heavy mesons, by relating the jet P^+ distribution derived under these assumptions to other differential distributions in these decays, which are better understood.

1.5 Plan of the thesis

The second chapter gives a short introduction to heavy quark effective theory. This prepares the way for the third chapter, which is an application of this effective theory to the extraction of $|V_{cb}|$ from exclusive semileptonic B decays. The fourth chapter introduces soft-collinear effective theory, the subject of the remaining chapters. The fifth chapter uses this theory

(as well as parts of heavy quark effective theory) to sum logs that arise in perturbative calculations of top-antitop production. The sixth chapter discusses the definition of hadronic jets in soft-collinear effective theory. It explores a way to test the validity of these definitions.

Chapter 2

Heavy quark effective theory

This chapter is a brief review of some of the aspects of heavy quark effective theory (HQET). It follows the book by Manohar and Wise [1]. This review will be useful for introducing the next chapter as well as for the later chapters involving soft-collinear effective theory. HQET describes the interactions of heavy quarks (usually the bottom or charm quarks) with the soft degrees of freedom they hadronize with. For instance, a B meson has for valence quarks a b quark and a light quark. There are also lots of sea quarks and gluons that serve to keep the meson bound together. These soft degrees of freedom typically have momenta on the order of $\Lambda_{\rm QCD}$, the scale of nonperturbative strong dynamics. This scale is dynamically generated by QCD, and its inverse gives the typical size of a hadron containing no more than one heavy quark.

2.1 Basics

Consider the B meson system: a heavy bottom quark with mass m_b and a light quark with mass $m \sim \Lambda_{\rm QCD}$. The momentum exchanged between the heavy quark and the light degrees of freedom is of order $\Lambda_{\rm QCD}$. This momentum exchange can only change the velocity of the heavy quark by an amount of order

$$\Delta v = \Delta p/m_b \sim \Lambda_{\rm QCD}/m_b\,. \tag{2.1}$$

In the heavy-quark limit, $m_Q \to \infty$, the velocity change goes to zero. One can say that the velocity of a heavy quark in this situation is a good quantum number. As a result, in HQET the velocity of a heavy quark labels its field, as we will see below.

The QCD Lagrangian for a quark field $q(x)$ with mass m_Q is

$$\mathcal{L} = \bar{Q}(x)(i\not{D} - m_Q)Q(x)\,. \tag{2.2}$$

Here D_μ is the covariant derivative, which we define as

$$D_\mu = \partial_\mu - igT^a A^a_\mu\,. \tag{2.3}$$

This Lagrangian determines the standard quark propagator:

$$\frac{i(\not{p} + m_Q)}{p^2 - m_Q^2 + i\epsilon}\,. \tag{2.4}$$

HQET describes nearly on-shell heavy quarks since their interactions with the light degrees of freedom do not change the velocity, as described above. We can see this by parametrizing the heavy quark momentum as

$$p^\mu = m_Q v^\mu + k^\mu\,, \tag{2.5}$$

where the so-called residual momentum k is small relative to the heavy quark mass: $k^\mu \sim \Lambda_{\rm QCD}$. We choose the velocity such that it squares to unity: $v^2 = 1$. In particular, this parametrization of the momentum shows that

$$p^2 - m_Q^2 = 2m_Q v\cdot k + k^2 \ll m_Q^2\,, \tag{2.6}$$

which confirms the statement above. Because the residual momentum is small relative to the heavy quark mass, the heavy quark remains nearly on-shell despite its interactions with the other stuff inside the hadron.

We can substitute this momentum parametrization into the quark propagator above to get its simplification in the heavy-quark limit:

$$\frac{i(1 + \not{v})}{2v\cdot k + i\epsilon}\,, \tag{2.7}$$

where the k^2 term in the denominator has been dropped as higher order. This is the propagator appropriate in the heavy-quark limit to describe small fluctuations of the heavy quark around its on-shell limit. Note that the propagator is proportional to the projection

operator

$$\frac{1+\not{v}}{2}\,. \tag{2.8}$$

This leads to an important property of HQET to be discussed below.

2.2 Leading-order in the heavy quark expansion

Now let us construct the HQET Lagrangian. This is useful for understanding the implications of HQET, as well as for understanding soft-collinear effective theory, which is discussed below. We start by writing the QCD quark field $Q(x)$ as

$$Q(x) = e^{-im_Q v\cdot x}\left[Q_v(x) + \mathcal{Q}_v(x)\right]\,, \tag{2.9}$$

where the projected fields are defined as

$$\begin{aligned} Q_v(x) &= e^{im_Q v\cdot x}\frac{1+\not{v}}{2}Q(x)\,, &(2.10)\\ \mathcal{Q}_v(x) &= e^{im_Q v\cdot x}\frac{1-\not{v}}{2}Q(x)\,. &(2.11)\end{aligned}$$

The exponential in front of $Q(x)$ has the effect of subtracting the large part of the heavy quark's momentum, so that the remaining piece, Q_v, just describes fluctuations around the on-shell limit. The next section will show that $\mathcal{Q}_v$ is suppressed by $\Lambda_{\rm QCD}/m_Q$ relative to the Q_v field. Assuming this for now and dropping the $\mathcal{Q}_v$ field, substituting Eq. (2.9) into the QCD Lagrangian gives the leading-order HQET Lagrangian:

$$\mathcal{L} = \bar{Q}_v(x)(iv\cdot D)Q_v(x)\,. \tag{2.12}$$

It is easy to see that the heavy quark propagator obtained from this Lagrangian matches what we wrote down before in Eq. (2.7) by taking the large m_Q limit of the standard QCD propagator.

Note the effect of the projector in the field definitions:

$$\begin{aligned} \frac{1+\not{v}}{2}Q_v(x) &= Q_v(x)\,, &(2.13)\\ \frac{1+\not{v}}{2}\mathcal{Q}_v(x) &= 0\,. &(2.14)\end{aligned}$$

This is a result of the fact that $v^2 = 1$. The presence of this projector in the heavy quark propagator results in a modification of the interaction between heavy quarks and gluons. In QCD the vertex is $igT^a\gamma^\mu$. Since this vertex is always sandwiched between two heavy quark propagators, the effective vertex is just v^μ. This can be seen as follows:

$$\frac{1+\not{v}}{2}\gamma^\mu\frac{1+\not{v}}{2} = v^\mu\frac{1+\not{v}}{2}\,. \tag{2.15}$$

This fact alones produces a major simplication in the interactions of heavy quarks with gluons. Since the vertices of heavy quark effective theory have no Dirac matrices, the interactions leave heavy quark spin unchanged!

2.3 Lagrangian beyond leading order in $1/m_Q$

The HQET Lagrangian beyond leading order in $\Lambda_{\rm QCD}/m_Q$ can be derived in the same way as the leading-order Lagrangian above. Simply inserting the identity in Eq. (2.9) into the standard QCD Lagrangian gives

$$\mathcal{L} = \bar{Q}_v(iv\cdot D)Q_v - \bar{\mathcal{Q}}_v(iv\cdot D + 2m_Q)\mathcal{Q}_v + \bar{Q}_v i\not{D}\mathcal{Q}_v + \bar{\mathcal{Q}}_v i\not{D}Q_v\,, \tag{2.16}$$

where we have used the identities $\not{v}Q_v = Q_v$ and $\not{v}\mathcal{Q}_v = -\mathcal{Q}_v$. The appearance of the term $2m_Q$ in the kinetic term for the $\mathcal{Q}_v$ field confirms the claim above. This field produces higher-energy excitations than the Q_v field and can be integrated out. Varying the Lagrangian with respect to $\bar{\mathcal{Q}}_v(x)$ gives the equation that allows us to do this at tree level:

$$\mathcal{Q}_v(x) = -\frac{i\not{D}}{i\not{D} - 2m_Q}Q_v(x)\,. \tag{2.17}$$

We can substitute this formula into the Lagrangian above to integrate out the $\mathcal{Q}_v$ field. The result is

$$\mathcal{L} = \bar{Q}_v(x)(iv\cdot D)Q_v(x) + \bar{Q}_v(x)i\not{D}\left(\frac{1}{i\not{D} - 2m_Q}\right)i\not{D}Q_v(x)\,. \tag{2.18}$$

Since derivatives acting on the Q_v field scale like $\Lambda_{\rm QCD}$ the last term can be further expanded to yield

$$\begin{aligned} \mathcal{L} &= \bar{Q}_v(x)(iv\cdot D)Q_v(x) + \bar{Q}_v(x)\frac{(i\not{D})^2}{2m_Q}Q_v(x) && (2.19)\\ &= \bar{Q}_v(x)(iv\cdot D)Q_v(x) + \bar{Q}_v(x)\left[\frac{(iD)^2+\sigma_{\mu\nu}G^{\mu\nu}}{2m_Q}\right]Q_v(x)\,, && (2.20)\end{aligned}$$

where we have used the fact that

$$\gamma^\mu\gamma^\nu = \frac{1}{2}\{\gamma^\mu,\gamma^\nu\} + \frac{1}{2}[\gamma^\mu,\gamma^\nu] = g^{\mu\nu} + i\sigma^{\mu\nu}\,. \qquad (2.21)$$

Higher-order terms can be calculated by expanding Eq. (2.17) in the Lagrangian and keeping higher-order terms. Here we only kept the first term in the expansion.

The expression for the subleading-order HQET Lagrangian shows several things. The first is simply that the heavy quark spin symmetry is broken by these higher-order terms. The term involving $\sigma_{\mu\nu}$ contains Dirac matrices and therefore no longer preserves the heavy quark spin. A second point to notice from the subleading Lagrangian is an understanding of the origin of corrections to heavy quark symmetry. The leading-order HQET Lagrangian gives a heavy quark propagating freely without interactions. The first correction term (the one with D^2) looks just like a kinetic energy term, and the second correction term (the one with $\sigma_{\mu\nu}$) is a magnetic moment interaction term. These terms support the intuitive picture of heavy quark symmetry that we have been discussing.

Chapter 3

Perturbative corrections to sum rules

In this chapter we discuss heavy quark effective theory sum rules and the perturbative improvement. It is shown how these sum rules can be useful in the extraction of $|V_{cb}|$ from B meson decays. Much of this chapter appeared in Ref. [2].

3.1 Sum rules and $|V_{cb}|$

Heavy quark effective theory (HQET) [3] provides a model-independent method of extracting the CKM matrix element $|V_{cb}|$ from exclusive semileptonic B meson decays. The $\bar{B} \to D^{(*)} l\bar{\nu}$ differential decay rates are given by

$$\begin{aligned}
\frac{\mathrm{d}\Gamma}{\mathrm{d}w}(\bar{B} \to D^* l\bar{\nu}) &= \frac{G_F^2 |V_{cb}|^2 m_B^5}{48\pi^3}\, r_*^3 (1-r_*)^2 \sqrt{w^2-1}\,(w+1)^2 \\
&\quad \times \left[1 + \frac{4w}{w+1}\frac{1-2wr_*+r_*^2}{(1-r_*)^2}\right] \mathcal{F}_{D^*}(w)^2 \ , \\
\frac{\mathrm{d}\Gamma}{\mathrm{d}w}(\bar{B} \to D l\bar{\nu}) &= \frac{G_F^2 |V_{cb}|^2 m_B^5}{48\pi^3}\, r^3 (1+r)^2 (w^2-1)^{3/2} \mathcal{F}_D(w)^2 \ ,
\end{aligned} \tag{3.1}$$

where $r_{(*)} = m_{D^{(*)}}/m_B$ and $w = v \cdot v'$ is the product of the $\bar{B}$ and $D^{(*)}$ four-velocities. Heavy quark symmetry [4] relates $\bar{B} \to D^{(*)} l\bar{\nu}$ form factors to the corresponding Isgur-Wise function, with the result $\mathcal{F}_{D^*}(w) = \mathcal{F}_D(w) = \xi(w)$ in the heavy-quark limit of QCD. Since $\xi(w)$ is absolutely normalized to unity at zero recoil (i.e., $w = 1$) [4, 5, 6, 7], experimental data determine $|V_{cb}|$ without recourse to model-specific assumptions.

This procedure has several sources of uncertainty. First, the identity $\mathcal{F}_{D^{(*)}}(1) = 1$ receives both perturbative corrections and corrections suppressed by the heavy b and c

quark masses. The former are known to order α_s^2 [8], with unknown higher-order corrections likely less than 1%, but the latter depend on four subleading Isgur-Wise functions and have been estimated only with phenomenological models and quenched lattice QCD.

Another source of error is the extrapolation of measured form factors to zero recoil, where the rates vanish. Linear fits of $\mathcal{F}_{D^{(*)}}(w)$ underestimate the zero-recoil value by about 3%, an effect mostly due to the curvature [9]. Using nonlinear shapes for $\mathcal{F}_{D^{(*)}}(w)$ reduces this error, and therefore constraints on second and higher derivatives at zero-recoil are welcome. Dispersive constraints [10, 11] relate second and sometimes higher derivatives to the first and are commonly used.

HQET sum rules provide a complementary way of constraining the $\mathcal{F}_{D^{(*)}}(w)$ shapes. New sum rules for the curvature and higher derivatives of the Isgur-Wise function were derived in Refs. [12, 13, 14]. Equating the result of inserting a complete set of intermediate states in the nonforward matrix element of a time-ordered product of HQET currents with the operator product expansion (OPE) gives a generic sum rule depending on the products of the velocities of the initial, final, and intermediate states. These are denoted respectively by v_i, v_f, and v' (the intermediate states all have the same velocity v' in the infinite-mass limit), and the products are denoted by

$$w_{if} = v_i \cdot v_f \quad , \quad w_i = v_i \cdot v' \quad , \quad w_f = v_f \cdot v' \, , \tag{3.2}$$

or generically w_x. These parameters are constrained to lie within the range [12]

$$w_i, w_f, w_{if} \geq 1 \, , \quad w_i w_f - \sqrt{(w_i^2-1)(w_f^2-1)} \leq w_{if} \leq w_i w_f + \sqrt{(w_i^2-1)(w_f^2-1)} \, , \tag{3.3}$$

and differentiating the generic sum rule with respect to them at $w_x = 1$ (read: $w_i = w_f = w_{if} = 1$) produces a class of sum rules for derivatives of the Isgur-Wise function at zero recoil. The sum rules of Refs. [12, 13, 14] were derived at tree level in the heavy-quark limit. The present chapter includes the order α_s corrections to the new sum rules and uses them to derive bounds on the curvatures of $\mathcal{F}_{D^{(*)}}(w)$ including α_s and $\Lambda_{\rm QCD}/m_{c,b}$ corrections. Including these corrections to the heavy-quark limit is important for meaningful comparison with data and dispersive constraints.

3.2 Derivation of the generic sum rule

The derivation of the generic sum rule follows a well-known formalism [15, 16, 17, 18]. It begins with the consideration of the time-ordered product of two arbitrary heavy-heavy currents

$$T_{fi}(\varepsilon) \;=\; \frac{i}{2m_B}\int d^4x\; e^{-iq\cdot x}\,\langle B_f(p_f)|\,T\{J_f(0),J_i(x)\}\,|B_i(p_i)\rangle \tag{3.4}$$

as a complex function of $\varepsilon = E_M - E_i - q^0$ at fixed $\vec{q}$, where $E_M = \sqrt{m_M^2 + |\vec{p}_i + \vec{q}|^2}$ is the minimum possible energy of the charmed hadronic state that J_i can create at fixed $\vec{q}$. The currents have the form

$$J_f(x) = \bar{b}(x)\Gamma_f c(x)\ ,\ J_i(y) = \bar{c}(y)\Gamma_i b(y) \tag{3.5}$$

for any Dirac matrices $\Gamma_{i,f}$. Only the choices $\Gamma_{i,f} = \not{v}_{i,f}$ and $\Gamma_{i,f} = \not{v}_{i,f}\gamma_5$ are explored here, but in principle others lead to different sum rules. The B states are ground state $\bar{B}$ or $\bar{B}^*$ mesons and have the standard relativistic normalization. As in the derivation of the Uraltsev sum rule [19], the initial and final states do not necessarily have the same velocity. Considering the *nonforward* matrix element of the time-ordered product is a crucial generalization in deriving the new sum rules [12].

From Eq. (3.4) one proceeds by splitting up the two time-orderings and inserting complete sets of intermediate charm states. The result is

$$\begin{aligned} T_{fi}(\varepsilon) \;&=\; \frac{1}{2m_B}\sum_{X_c}(2\pi)^3\delta^3(\vec{q}+\vec{p}_i-\vec{p}_{X_c})\frac{\langle B_f|J_f(0)|X_c\rangle\langle X_c|J_i(0)|B_i\rangle}{\varepsilon + E_{X_c} - E_M - i0^+} \\ &-\; \frac{1}{2m_B}\sum_{X_{\bar{c}bb}}(2\pi)^3\delta^3(\vec{q}-\vec{p}_f+\vec{p}_{X_{\bar{c}bb}})\frac{\langle B_f|J_i(0)|X_{\bar{c}bb}\rangle\langle X_{\bar{c}bb}|J_f(0)|B_i\rangle}{\varepsilon + E_i + E_f - E_M - E_{X_{\bar{c}bb}} + i0^+}\ , \end{aligned} \tag{3.6}$$

where the sums include phase space factors such as $d^3p/(2\pi)^3 2E_X$. Again, T_{fi} has been written as above to call attention to the full generality possible for deriving sum rules by this method, but here both B_i and B_f will be taken to be $\bar{B}$ mesons to avoid the considerable complication of the $\bar{B}^*$ polarization. In addition, HQET states and currents will be used henceforth since the goal is sum rules for the derivatives of the Isgur-Wise function. Deriving the bounds in the effective theory also makes the calculation of perturbative corrections

much easier.

The function $T_{fi}(\varepsilon)$ has two cuts along the real axis, as shown in Fig. 3.1. The important one here, running from $-\infty$ to the origin, comes from the first time-ordering and corresponds to intermediate states with a c quark or a c quark, a b quark, and a $\bar{b}$ quark. The cut associated with the other time-ordering begins near $2m_c$ and corresponds to states with two b quarks and a $\bar{c}$ quark. Since $T_{fi}(\varepsilon)$ is perturbatively calculable only when smeared over a large enough range of ε [20], it is multiplied by a weight function W_Δ and integrated around the contour shown in the figure. The scale Δ gives the extent of the smearing and therefore should be well above $\Lambda_{\rm QCD}$. The contour chosen eliminates all but the intermediate states with heavy quark content c by avoiding the second cut and pinching the first at $\varepsilon = -2m_b$. Crossing the contour assumes local duality at the scale m_b, but if $\Delta < m_b$ the weight function will be quite small here. This will be clear with the specific weight function used below. Assuming it is analytic in the shaded region of Fig. 3.1, the result is

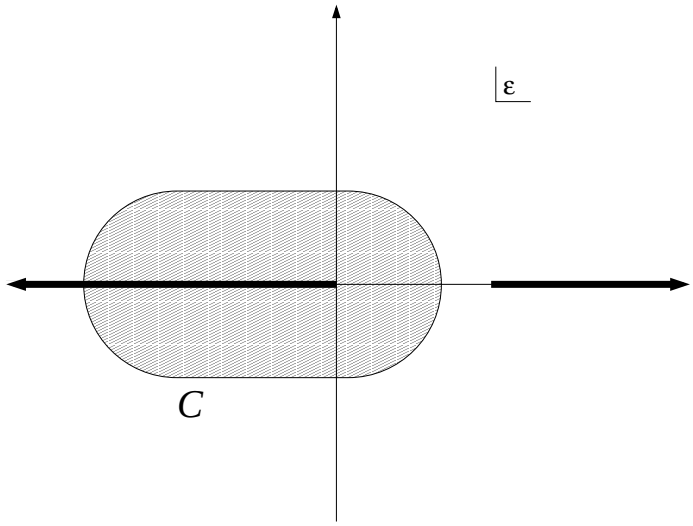

Figure 3.1: The cuts of T_{fi} in the complex ε plane. The depicted contour picks up only contributions from the left-hand cut, which corresponds to physical states with a charm quark. The states given by the right-hand cut do not contribute here.

$$\frac{1}{2\pi i}\int_C d\varepsilon\, W_\Delta(\varepsilon)\, T_{fi}(\varepsilon) \;=\; \sum_{X_c} W_\Delta(E_M - E_{X_c}) \frac{\langle \bar{B}(v_f)|J_f|X_c(v')\rangle\langle X_c(v')|J_i|\bar{B}(v_i)\rangle}{4v'^0} \;, \quad (3.7)$$

where the delta function has been used to perform the phase-space integral and the HQET state normalization convention has been used to eliminate mass factors in the denominator.

The intermediate X_c states carry four-momentum $p_{X_c} = m_{X_c} v' = p_i + q$.

Choice of the weight function is governed by well-known concerns [18, 16]. In practice one uses $W_\Delta(\varepsilon) = \theta(\Delta + \varepsilon)$, which is the $n \to \infty$ limit of the set of functions

$$W_\Delta^{(n)}(\varepsilon) = \frac{\Delta^{2n}}{\varepsilon^{2n} + \Delta^{2n}} \tag{3.8}$$

for $\varepsilon < 0$. But since the weight function must be analytic within the contour, the use of these is strictly correct only for small $n > 1$. In this case the poles at $\varepsilon = \sqrt[2n]{-1}\,\Delta$ are a distance of order Δ away from the cut, and the contour can be deformed away without getting too close to the cut and relying on local duality at a scale below m_b. This is not true of the $n \to \infty$ limit, in which the poles approach the cut and the contour must pinch the cut at the scale Δ instead of m_b. This is a problem because the contribution at Δ is weighted much more heavily than that at m_b, and thus the results will depend more strongly on the assumption of local duality. However, an explicit calculation shows that the results here do not depend on n, just as the authors of Ref. [18] found in their derivation of corrections to the Bjorken sum rule. This is not true in other cases, such as the Voloshin sum rule [18]. The weight function in what follows can therefore be considered a simple step function excluding states with excitation energies greater than Δ. Although increasing Δ includes more states and weakens the bounds, the cutoff energy must be chosen large enough to make perturbative QCD appropriate. Choosing $\Delta \gtrsim 2$ GeV should therefore be sufficient.

The sum rule is derived by performing an operator product expansion on the time-ordered product of currents on the left-hand side of Eq. (3.7) while writing out the right-hand side explicitly in terms of excited-state Isgur-Wise functions. The leading-order OPE relevant for B matrix elements consists of a single dimension-three operator, $\bar{b}_{v_f} \Gamma_f (1 + \not{v}') \Gamma_i b_{v_i}$. Higher-dimension operators will be neglected here, as they give corrections suppressed by powers of $\Lambda_{\rm QCD}/\Delta$ or $\Lambda_{\rm QCD}/m_{c,b}$. The order α_s corrections to the Wilson coefficient of the leading operator are given by a matching calculation involving the diagrams in Figs. 3.2 and 3.3. The generic sum rule resulting from this is

$$\begin{aligned} &\frac{1}{4}\xi(w_{if})[1 + \alpha_s F(w_i, w_f, w_{if})]\,\mathrm{Tr}\left[(1 + \not{v}_f)\,\Gamma_f (1 + \not{v}')\,\Gamma_i (1 + \not{v}_i)\right] \\ &\qquad = \sum_{X_c} W_\Delta(E_M - E_{X_c}) \langle \bar{B}(v_f)|J_f|X_c(v')\rangle\langle X_c(v')|J_i|\bar{B}(v_i)\rangle \ , \end{aligned} \tag{3.9}$$

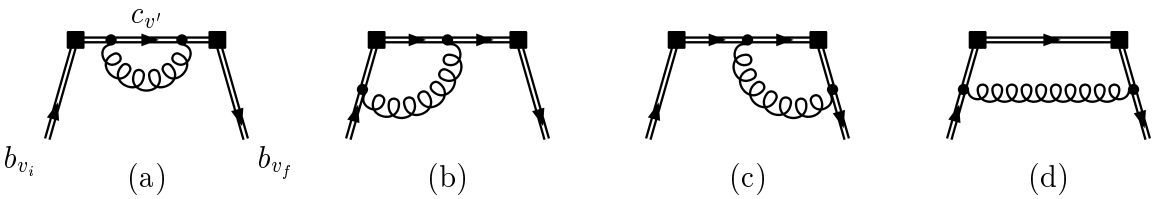

Figure 3.2: Diagrams contributing to the order α_s corrections to the sum rules. The squares indicate insertions of the currents J_i and J_f, respectively. The current J_i inserts momentum q, while the current J_f carries away momentum q' sufficient to leave the final b-quark with velocity v_f. The velocity-labeled quark fields are those of the heavy quark effective theory.

where the function F contains the one-loop corrections. In principle, F could be defined to include perturbative corrections of all orders. The form of the corrected sum rule would be the same since HQET vertices are spin-independent. The right-hand side is written out explicitly in the next section.

Working in the rest frame of the intermediate hadrons (i.e., $v'^0 = 1$) and using the $\overline{\rm MS}$ scheme with dimensional regularization and a finite gluon mass m, the contributions to $\alpha_s F$ of the graphs in Figs. 3.2(a)–3.2(d) are, respectively,

$$\frac{2\alpha_s}{3\pi}\left(2 - \ln\frac{4\Delta^2}{\mu^2}\right) \ , \tag{3.10}$$

$$\frac{2\alpha_s}{3\pi} w_i \left\{ \frac{\ln\left(w_i + \sqrt{w_i^2-1}\right)}{\sqrt{w_i^2-1}} \ln\frac{4\Delta^2}{\mu^2} + \int_0^1 dx\, \frac{2\ln x - \ln[1+2x(1-x)(w_i-1)]}{1+2x(1-x)(w_i-1)} \right\} \ , \tag{3.11}$$

$$\frac{2\alpha_s}{3\pi} w_f \left\{ \frac{\ln\left(w_f + \sqrt{w_f^2-1}\right)}{\sqrt{w_f^2-1}} \ln\frac{4\Delta^2}{\mu^2} + \int_0^1 dx\, \frac{2\ln x - \ln[1+2x(1-x)(w_f-1)]}{1+2x(1-x)(w_f-1)} \right\} \ , \tag{3.12}$$

$$-\frac{4\alpha_s}{3\pi} w_{if} \int_0^1 dx\, dy\, dz\, \delta(x+y+z-1) \frac{\theta(z-\sqrt{a}m/\Delta)}{a\sqrt{z^2 - am^2/\Delta^2}} \ , \tag{3.13}$$

where $a = 1 + 2xy(w_{if}-1) + 2xz(w_i-1) + 2yz(w_f-1)$, and α_s is evaluated at subtraction point μ. The contribution of Fig. 3.2(d) cannot easily be simplified further, but this is no limitation since the sum rules require only the first few terms of F in an expansion about $w_x = 1$. The graph in Fig. 3.3 contributes with a minus sign to the matching calculation for the Wilson coefficient, since it gives the renormalization of the leading operator in the

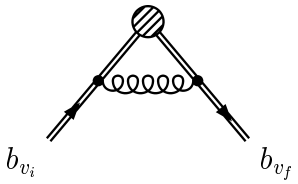

Figure 3.3: One-loop renormalization of the leading operator in the operator product expansion of T_{fi}. The blob indicates an insertion of this operator, $\bar{b}_{v_f}\Gamma_f(1+\not{v}')\Gamma_i b_{v_i}$. The external lines are bottom quarks in the heavy quark effective theory.

OPE, and so its contribution to $\alpha_s F$ is

$$\frac{2\alpha_s}{3\pi}\frac{w_{if}}{\sqrt{w_{if}^2-1}}\ln\left(w_{if}+\sqrt{w_{if}^2-1}\right)\ln\frac{\mu^2}{m^2}\ . \tag{3.14}$$

This infrared divergence cancels that of the graph in Fig. 3.2(d), leaving $\alpha_s F$ independent of the regulating gluon mass.

From the results above, it is not hard to show that $F(1,w,w) = F(w,1,w) = 0$. This important characteristic of the perturbative corrections is true to all orders in α_s, as can easily be seen. In the limits $v_i = v'$ and $v_f = v'$, one of the currents in the time-ordered product is a conserved current associated with heavy quark flavor symmetry and its matrix elements receive no perturbative corrections. Because HQET loop graphs do not change the matrix structures of inserted operators, perturbative corrections to matrix elements of the other current cancel those of the leading operator in the OPE. Therefore, the function analogous to F including perturbative corrections of all orders will still vanish in these limits.

The sum rules derived here are primarily of interest near zero recoil, making it convenient to expand F about $w_x = 1$ with the definitions

$$\begin{aligned}\alpha_s F(w_i,w_f,w_{if}) \;=\;& b_{if1}(w_{if}-1)+b_{i1}(w_i-1)+b_{f1}(w_f-1)+\frac{1}{2}b_{if2}(w_{if}-1)^2\\ &+\frac{1}{2}b_{i2}(w_i-1)^2+\frac{1}{2}b_{f2}(w_f-1)^2+b_{i2f}(w_i-1)(w_f-1)\\ &+b_{i2if}(w_i-1)(w_{if}-1)+b_{f2if}(w_f-1)(w_{if}-1)+\cdots\ .\end{aligned} \tag{3.15}$$

There is no zeroth-order term since $F(1,1,1) = 0$. This follows from the identities $F(1,w,w) =$

$F(w,1,w)=0$, which also imply

$$b_{f1}+b_{if1}=b_{i1}+b_{if1}=0\ , \tag{3.16}$$

$$b_{f2}+2b_{f2if}+b_{if2}=b_{i2}+2b_{i2if}+b_{if2}=0\ . \tag{3.17}$$

These relations between derivatives of the perturbative corrections can be checked at order α_s with the explicit values

$$\begin{aligned}
b_{if1}=-b_{f1}=-b_{i1} &= \frac{4\alpha_s}{9\pi}\left(\frac{5}{3}-\ln\frac{4\Delta^2}{\mu^2}\right)\ ,\\
b_{i2}=b_{f2} &= \frac{4\alpha_s}{15\pi}\left(\frac{2}{5}-\ln\frac{4\Delta^2}{\mu^2}\right)\ ,\\
b_{if2} &= \frac{4\alpha_s}{15\pi}\left(-\frac{12}{5}+\ln\frac{4\Delta^2}{\mu^2}\right)\ ,\\
b_{i2if}=b_{f2if} &= \frac{4\alpha_s}{15\pi}\ ,\\
b_{i2f} &= -\frac{4\alpha_s}{45\pi}\ .
\end{aligned} \tag{3.18}$$

The derivatives above are all specific to the rest frame of intermediate hadrons. This is the frame used henceforth. In other frames (e.g., $v_i^0=1$) the weight function depends on the w_x parameters, and the sum rules are more complicated but not qualitatively different.

3.3 Vector and axial vector sum rules

When specific matrices $\Gamma_{i,f}$ are chosen, the generic sum rule in Eq. (3.9) can be written out explicitly in terms of excited-state Isgur-Wise functions using Falk's description of HQET states of arbitrary spin [21]. The choice $\Gamma_{i,f}=\not{v}_{i,f}$ yields [13]

$$\begin{aligned}
&\xi(w_{if})\left[1+\alpha_s F(w_i,w_f,w_{if})\right](1+w_i+w_f+w_{if})\\
=\ &(w_i+1)(w_f+1)\sum_{\ell=0}\frac{\ell+1}{2\ell+1}S_\ell(w_i,w_f,w_{if})\sum_n \tau^{(\ell)(n)}_{\ell+1/2}(w_i)\tau^{(\ell)(n)}_{\ell+1/2}(w_f)W_\Delta(m_M-m^{(\ell)(n)}_{\ell+1/2})\\
&+\sum_{\ell=1}S_\ell(w_i,w_f,w_{if})\sum_n \tau^{(\ell)(n)}_{\ell-1/2}(w_i)\tau^{(\ell)(n)}_{\ell-1/2}(w_f)W_\Delta(m_M-m^{(\ell)(n)}_{\ell-1/2})\ ,
\end{aligned} \tag{3.19}$$

where the weight function now bounds excitation *mass* because $v'^0=1$. The functions $\tau^{(\ell)(n)}_{\ell\pm1/2}(w)$ are $\bar{B}\to D^{(\ell)(n)}_{\ell\pm1/2}$ Isgur-Wise functions, where $\ell\pm1/2$ is the spin of the light degrees

of freedom, $(-1)^{\ell+1}$ is the parity of the state, and the label n counts "radial excitations." This name is inspired by the nonrelativistic constituent quark model, but these states can be anything carrying the other quantum numbers, including continuum contributions, for which n would be a continuous parameter and the sums integrals. In that case, the functions $\tau^{(\ell)(n)}_{\ell\pm1/2}(w)$ would not be Isgur-Wise functions but other B decay form factors. This possibility will be downplayed here, with the assumption that such contributions are small in the bounds derived here. Experimental input on $B \to D\pi l\bar{\nu}$, for example, is needed to evaluate this assumption.

The quark model also offers an interpretation of ℓ as the orbital angular momentum between the light antiquark and the heavy quark. The relation of this notation to that of Isgur and Wise [22] for the lower values of ℓ is given by

$$\tau^{(0)(n)}_{1/2}(w) = \xi^{(n)}(w) \quad , \quad \tau^{(1)(n)}_{1/2}(w) = 2\,\tau^{(n)}_{1/2}(w) \quad , \quad \tau^{(1)(n)}_{3/2}(w) = \sqrt{3}\,\tau^{(n)}_{3/2}(w) \; . \tag{3.20}$$

The function S_ℓ takes into account the polarization of an intermediate state with integral spin ℓ and is defined as

$$S_\ell = v_{i\nu_1}\cdots v_{i\nu_\ell} v_{f\mu_1}\cdots v_{f\mu_\ell} \sum_\lambda \varepsilon^{*\nu_1\cdots\nu_\ell}_{(\lambda)} \varepsilon^{\mu_1\cdots\mu_\ell}_{(\lambda)} \; , \tag{3.21}$$

where $\varepsilon^{\mu_1\cdots\mu_\ell}$ is the polarization tensor of the intermediate state. The sum runs over the $2\ell+1$ polarizations. This quantity was reduced in Ref. [12] to the relatively simple form

$$S_\ell(w_i, w_f, w_{if}) = \sum_{k=0}^{\ell/2} C_{\ell,k} (w_i^2-1)^k (w_f^2-1)^k (w_i w_f - w_{if})^{\ell-2k} \, , \tag{3.22}$$

with the coefficient

$$C_{\ell,k} = (-1)^k \frac{(\ell!)^2}{(2\ell)!} \frac{(2\ell-2k)!}{k!(\ell-k)!(\ell-2k)!} \; . \tag{3.23}$$

Using this formula it is easy to show that Eq. (3.19) reduces to

$$2(1+w)\xi(w)[1+\alpha_s F(1,w,w)] = 2(1+w)\xi(w) \tag{3.24}$$

in the limit $v_i = v'$, confirming that $F(1,w,w) = 0$ to all orders. The limit $v_f = v'$ gives $F(w,1,w) = 0$.

The axial sum rule (i.e., Eq. (3.9) with $\Gamma_{i,f} = \not{v}_{i,f}\gamma_5$) can be written out explicitly in the same way [13]:

$$\begin{aligned} & \xi(w_{if})\left[1+\alpha_s F(w_i,w_f,w_{if})\right](-1+w_i+w_f-w_{if}) \\ = \;& (w_i-1)(w_f-1)\sum_{\ell=1}\frac{\ell}{2\ell-1}S_{\ell-1}(w_i,w_f,w_{if})\sum_n \tau^{(\ell)(n)}_{\ell-1/2}(w_i)\tau^{(\ell)(n)}_{\ell-1/2}(w_f)W_\Delta(m_M-m^{(\ell)(n)}_{\ell-1/2}) \\ & +\sum_{\ell=0}S_{\ell+1}(w_i,w_f,w_{if})\sum_n \tau^{(\ell)(n)}_{\ell+1/2}(w_i)\tau^{(\ell)(n)}_{\ell+1/2}(w_f)W_\Delta(m_M-m^{(\ell)(n)}_{\ell+1/2})\ . \end{aligned} \tag{3.25}$$

As in the vector sum rule, the masses of the intermediate states are denoted by $m^{(\ell)(n)}_{\ell\pm1/2}$. The limits $v_i = v'$ and $v_f = v'$ are trivial for the axial sum rule.

The doublets with spin of the light degrees of freedom $s_l = \ell + 1/2$ and $s_l = \ell - 1/2$ contain states with angular momentum ℓ, $\ell+1$ and $\ell-1$, ℓ, respectively. But only one member of each doublet contributes to the sum rules in Eqs. (3.19) and (3.25) because of the choice of currents. This explains the appearance of only one polarization function for each doublet in the vector and axial vector sum rules.

The zero-recoil normalization of the $\bar{B} \to D^{(*)}$ Isgur-Wise function allows one to write

$$\xi(w) = 1 - \rho^2(w-1) + \frac{\sigma^2}{2}(w-1)^2 - \cdots\ . \tag{3.26}$$

The axial and vector sum rules (i.e., Eqs. (3.19) and (3.25)) give expressions for ρ^2, σ^2, and higher derivatives of $\xi(w)$ when differentiated with respect to the parameters w_x at $w_x = 1$. Different combinations of derivatives yield different relations. In the $v'^0 = 1$ frame, the sum rules are invariant under the interchange of w_i and w_f, and it is therefore sufficiently general to consider only derivatives with respect to w_{if} and $w = w_i = w_f$. Because of this simplification, this chapter only uses derivatives of the vector and axial sum rules of the sort

$$\left.\frac{\partial^{p+q}}{\partial w_{if}^p \partial w^q}\right|_{w_{if}=w=1}\ . \tag{3.27}$$

Derivatives of the vector sum rule with $p+q=2$ give expressions for σ^2, while the extra factors of (w_x-1) in the axial rule require $p+q=3$ for curvature relations.

As an illustration of the method, one can easily derive the Bjorken [23, 22] and Uraltsev [19] sum rules with order α_s corrections. For this it is only necessary to consider $p+q=1$ in the vector rule and $p+q=2$ in the axial rule. Taking the vector sum rule first, the

equation given by the $p = 0$, $q = 1$ derivative is trivial, but $p = 1$, $q = 0$ gives the Bjorken sum rule with one-loop corrections [18]:

$$\rho^2(\mu) = \frac{1}{4} + \frac{4\alpha_s}{9\pi}\left(\frac{5}{3} - \ln\frac{4\Delta^2}{\mu^2}\right) + 2\sum_n^{\Delta}\left[\tau_{3/2}^{(n)}(1)\right]^2 + \sum_n^{\Delta}\left[\tau_{1/2}^{(n)}(1)\right]^2 \ . \tag{3.28}$$

This equation has been written in the familiar notation of Isgur and Wise using Eq. (3.20). The upper limit Δ on the sums stands for a factor of the weight function $W_\Delta(m_M - m_{X_c})$, which serves to cut off the sums. Without it the results are divergent, as can be seen by attempting to take the $\Delta \to \infty$ limit in the order α_s corrections. Note that the subtraction-point dependence is the same on both sides of the equation, since Isgur-Wise functions are independent of μ at zero recoil while their slopes depend on it logarithmically [24]. This equation should be evaluated near $\mu = \Delta$ to avoid large logarithms in the perturbative expansion.

The lower bound resulting from ignoring the sums in Eq. (3.28) is similar to one derived in Ref. [25] but somewhat weaker. As discussed in Ref. [18], this is the result of using different weight functions. That of Ref. [25] is effectively given by the phase space of b decay and falls off faster with ε, thus reducing the contribution of the intermediate states to the sum rule and strengthening the resultant lower bound. A similar effect could be achieved here by using a smaller value for Δ, but as discussed above this makes the use of perturbative QCD less reliable.

The $p = 0$, $q = 2$ derivative of the axial equation also gives the Bjorken sum rule. The $p = 2$, $q = 0$ and $p = 1$, $q = 1$ derivatives give the same result, which, when combined with the Bjorken rule, gives the traditional form of the Uraltsev sum rule:

$$\sum_n^{\Delta}\left[\tau_{3/2}^{(n)}(1)\right]^2 - \sum_n^{\Delta}\left[\tau_{1/2}^{(n)}(1)\right]^2 = \frac{1}{4} - b_{if1} - \frac{1}{2}(b_{i1} + b_{f1}) = \frac{1}{4} \ , \tag{3.29}$$

where Eq. (3.20) has again been used. This equation receives no unsuppressed perturbative corrections. (There are in fact perturbative corrections suppressed by $\Lambda_{\rm QCD}^2/\Delta^2$ [19], but such corrections are being neglected here.) In this particular derivation of the Uraltsev rule, this is the result of the relation in Eq. (3.16) between the first derivatives of F. But another derivation from different derivatives of the axial and vector sum rules gives α_s corrections proportional to $F(1,1,1) = 0$. It appears that the Uraltsev rule is always

protected from perturbative corrections by the general identities $F(1,w,w) = F(w,1,w) = 0$. This convergent sum rule indicates that $\tau_{1/2}^{(n)}(1)$ and $\tau_{3/2}^{(n)}(1)$ become equal as $n \to \infty$.

Combined with Eq. (3.28), the Uraltsev rule improves the Bjorken bound significantly:

$$\rho^2(\mu) = \frac{3}{4} + b_{if1}(\mu) + 3\sum_n^\Delta \left[\tau_{1/2}^{(n)}(1)\right]^2 > \frac{3}{4} + \frac{4\alpha_s}{9\pi}\left(\frac{5}{3} - \ln\frac{4\Delta^2}{\mu^2}\right) \ . \tag{3.30}$$

Because the Uraltsev rule is not corrected, the corrections to this improved bound are just those of the original Bjorken bound. In particular, they are not substantially increased, as one might expect from the drastic improvement to the bound.

Constraints on the curvature of the Isgur-Wise function are obtained from higher derivatives of the same equations. The three second derivatives of the vector equation and the four third derivatives of the axial can be reduced to five linearly independent relations, as demonstrated in Ref. [14]. Complete with the one-loop corrections derived here, they are

$$\rho^2 = -\frac{4}{5}\sum_n^\Delta \tau_{3/2}^{(1)(n)}(1)\tau_{3/2}^{(1)(n)'}(1) + \frac{3}{5}\sum_n^\Delta \tau_{1/2}^{(1)(n)}(1)\tau_{1/2}^{(1)(n)'}(1) + \frac{2}{5}b_{if1} \ , \tag{3.31}$$

$$\sigma^2 = -\sum_n^\Delta \tau_{3/2}^{(1)(n)}(1)\tau_{3/2}^{(1)(n)'}(1) + b_{if1}\rho^2 - b_{if2} - \frac{1}{2}\left(b_{i2if} + b_{f2if}\right) \ , \tag{3.32}$$

$$\sigma^2 = 2\sum_n^\Delta \left[\tau_{5/2}^{(2)(n)}(1)\right]^2 + 2b_{if1}\rho^2 - b_{if2} \ , \tag{3.33}$$

$$\sigma^2 = \frac{5}{4}\rho^2 + \frac{5}{4}\sum_n^\Delta \left[\tau_{3/2}^{(2)(n)}(1)\right]^2 + 2b_{if1}\rho^2 - b_{if2} - \frac{5}{4}b_{if1} \ , \tag{3.34}$$

$$\begin{aligned}\sigma^2 = {} & \frac{4}{5}\rho^2 + \frac{3}{5}\sum_n^\Delta \left[\tau_{1/2}^{(0)(n)'}(1)\right]^2 + \frac{4}{5}b_{if1}\rho^2 - \frac{4}{5}b_{if1} - \frac{6}{5}\left(b_{i2if} + b_{f2if}\right) \\ & - \frac{8}{5}b_{if2} - \frac{3}{10}\left(b_{i2} + 2b_{i2f} + b_{f2}\right) \ .\end{aligned} \tag{3.35}$$

The last two equations give the bounds of Ref. [14], complete with order α_s corrections. Only a couple of orbital excitations occur and in positive-definite form, allowing the derivation

of nontrivial lower bounds. Using the values of Eqs. (3.18) gives

$$\sigma^2(\mu) > \frac{5}{4}\rho^2(\mu)\left(1+\frac{32\alpha_s}{27\pi}-\frac{32\alpha_s}{45\pi}\ln\frac{4\Delta^2}{\mu^2}\right)-\frac{193\alpha_s}{675\pi}+\frac{13\alpha_s}{45\pi}\ln\frac{4\Delta^2}{\mu^2}\ , \tag{3.36}$$

$$\sigma^2(\mu) > \frac{3}{5}\left[\rho^2(\mu)\right]^2+\frac{4}{5}\rho^2(\mu)\left(1+\frac{20\alpha_s}{27\pi}-\frac{4\alpha_s}{9\pi}\ln\frac{4\Delta^2}{\mu^2}\right) - \frac{148\alpha_s}{675\pi}+\frac{4\alpha_s}{45\pi}\ln\frac{4\Delta^2}{\mu^2}\ , \tag{3.37}$$

where the identity $\tau_{1/2}^{(0)(0)'}(1) = -\rho^2$ has been used. As demonstrated below in the derivation of physical bounds, the subtraction-point dependence is the same on both sides of these inequalities.

3.4 Physical bounds

When combined with α_s and $\Lambda_{\rm QCD}/m_{c,b}$ corrections from matching HQET onto the full theory, the curvature bounds derived above imply bounds on the zero-recoil derivatives of the functions $\mathcal{F}_{D^{(*)}}(w)$. It is convenient to expand these functions about the zero-recoil point according to

$$\mathcal{F}_{D^{(*)}}(w) = \mathcal{F}_{D^{(*)}}(1)\left[1-\rho^2_{D^{(*)}}(w-1)+\frac{\sigma^2_{D^{(*)}}}{2}(w-1)^2-\cdots\right]\ . \tag{3.38}$$

A simple matching calculation, taken from Ref. [24], yields the relations between the Isgur-Wise derivatives and those of the physical shape functions:

$$\rho^2_{D^{(*)}} = \rho^2(\mu)+\frac{4\alpha_s}{9\pi}\ln\frac{m_c^2}{\mu^2}+\frac{\alpha_s}{\pi}\left(\delta^{(\alpha_s)}_{D^{(*)}}-\frac{20}{27}\right)+\frac{\bar\Lambda}{2m_c}\delta^{(1/m)}_{D^{(*)}}\ ,$$

$$\sigma^2_{D^{(*)}} = \sigma^2(\mu)+2\rho^2(\mu)\left[\frac{4\alpha_s}{9\pi}\ln\frac{m_c^2}{\mu^2}+\frac{\alpha_s}{\pi}\left(\delta^{(\alpha_s)}_{D^{(*)}}-\frac{20}{27}\right)\right]+\frac{4\alpha_s}{15\pi}\ln\frac{m_c^2}{\mu^2} + \frac{\alpha_s}{\pi}\left(\Delta^{(\alpha_s)}_{D^{(*)}}-\frac{16}{25}\right)+\frac{\bar\Lambda}{2m_c}\Delta^{(1/m)}_{D^{(*)}}\ . \tag{3.39}$$

The perturbative corrections are model independent. The parameters $\delta_{D^{(*)}}^{(\alpha_s)}$ and $\Delta_{D^{(*)}}^{(\alpha_s)}$ are given by

$$\begin{aligned}
\delta_{D^*}^{(\alpha_s)} &= \frac{2(1-z)(11+2z+11z^2)+24(2-z+z^2)z\ln z}{27(1-z)^3} = 0.24 \ , \\
\delta_{D}^{(\alpha_s)} &= \frac{2(1-z)(23-34z+23z^2)+12(3-3z+2z^2)z\ln z}{27(1-z)^3} = 1.20 \ , \\
\Delta_{D^*}^{(\alpha_s)} &= -\frac{8(47+17z+252z^2+17z^3+47z^4)}{675(1-z)^4} \\
&\quad - \frac{4(5+125z-55z^2+95z^3-18z^4)z\ln z}{135(1-z)^5} = -1.16 \ , \\
\Delta_{D}^{(\alpha_s)} &= \frac{4(47-258z+302z^2-258z^3+47z^4)}{225(1-z)^4} \\
&\quad - \frac{8(5-5z+5z^2-z^3)z^2\ln z}{15(1-z)^5} = 0.63 \ ,
\end{aligned} \tag{3.40}$$

where $z = m_c/m_b$, and the approximation $r_{(*)} \approx z$ has been made in the order α_s corrections. These values agree with those calculated in Ref. [26]. The numerical values are for $m_c = 1.4$ GeV and $m_b = 4.8$ GeV.

The nonperturbative corrections cannot currently be calculated model-independently because they depend on the four subleading Isgur-Wise functions that parameterize first-order corrections to the heavy-quark limit, $\chi_{1-3}(w)$ and $\eta(w)$. But they can be estimated using QCD sum rules [27] (and, in principle, lattice QCD). In the notation of Neubert [24], the nonperturbative corrections are

$$\begin{aligned}
\delta_{D^*}^{(1/m)} &= -2\chi_1'(1)(1+z) - \frac{4}{3}\chi_2(1)(1-3z) + 4\chi_3'(1)(1-3z) \\
&\quad - \frac{5}{6}(1+z) - \frac{1-2z+5z^2}{3(1-z)}\eta(1) \approx -2.1 \ , \\
\delta_{D}^{(1/m)} &= -2(1+z)\left[\chi_1'(1) - 2\chi_2(1) + 6\chi_3'(1)\right] + \frac{2(1-z)^2}{1+z}\eta'(1) \approx -1.3 \ , \\
\Delta_{D^*}^{(1/m)} &= \rho^2\left[-2\eta(1)\frac{1-2z+5z^2}{3(1-z)} - \frac{5}{3}(1+z)\right] + 2(1+z)\chi_1''(1) - \frac{8(1-6z+z^2)\chi_2(1)}{9(1-z)^2} \\
&\quad + \frac{8}{3}(1-3z)\chi_2'(1) - 4(1-3z)\chi_3''(1) - \frac{\eta(1)(5-28z+18z^2-52z^3+25z^4)}{9(1-z)^3} \\
&\quad + \frac{2\eta'(1)(1-2z+5z^2)}{3(1-z)} - \frac{(1+z)(25-42z+25z^2)}{18(1-z)^2} \approx -2.6\rho^2 - 1.7 \ , \\
\Delta_{D}^{(1/m)} &= 4\rho^2\eta'(1)\frac{(1-z)^2}{1+z} + 2(1+z)\left[\chi_1''(1) - 4\chi_2'(1) + 6\chi_3''(1)\right] - 2\eta''(1)\frac{(1-z)^2}{1+z} \\
&\approx -0.3 \ ,
\end{aligned} \tag{3.41}$$

where the primes denote d/dw. In these corrections ρ^2 can be taken to be $\rho^2_{D^{(*)}}$, since the results here do not include corrections of order $\alpha_s\Lambda_{\rm QCD}/m_{c,b}$. The parts of these expressions for $\Delta^{(1/m)}_{D^*}$ and $\Delta^{(1/m)}_{D}$ proportional to ρ^2 disagree with those of Ref. [26].[1] The numerical estimates are based on the approximate values $\eta(1)=0.6$, $\eta'(1)=0$, $\chi_1'(1)=0.3$, $\chi_2(1)=-0.04$, $\chi_2'(1)=0.03$, and $\chi_3'(1)=0.02$ [27]. The values $\eta''(1)=\chi_1''(1)=\chi_3''(1)=0$ and $z=0.29$ were also used. Since these values are model-dependent with large uncertainties, the numerical estimates of the nonperturbative corrections should be interpreted with caution. Reliable lattice results would be a welcome check on such large QCD sum rule estimates of these corrections.

Combining the bounds of Eqs. (3.36) and (3.37) with Eqs. (3.39) gives the physical bounds

$$\begin{aligned}
\sigma^2_{D^{(*)}} &> \frac{5}{4}\rho^2_{D^{(*)}}\left(1+\frac{8\alpha_s}{5\pi}\delta^{(\alpha_s)}_{D^{(*)}}+\frac{32\alpha_s}{45\pi}\ln\frac{m_c^2}{4\Delta^2}\right)-\frac{13\alpha_s}{45\pi}\ln\frac{m_c^2}{4\Delta^2}-\frac{5\alpha_s}{4\pi}\delta^{(\alpha_s)}_{D^{(*)}}+\frac{\alpha_s}{\pi}\Delta^{(\alpha_s)}_{D^{(*)}} \\
&\quad -\frac{5}{4}\frac{\bar\Lambda}{2m_c}\delta^{(1/m)}_{D^{(*)}}+\frac{\bar\Lambda}{2m_c}\Delta^{(1/m)}_{D^{(*)}}\ , \qquad (3.42)\\
\sigma^2_{D^{(*)}} &> \frac{3}{5}\left(\rho^2_{D^{(*)}}\right)^2+\frac{4}{5}\rho^2_{D^{(*)}}\left(1+\frac{4\alpha_s}{9\pi}\ln\frac{m_c^2}{4\Delta^2}+\frac{\alpha_s}{\pi}\delta^{(\alpha_s)}_{D^{(*)}}-\frac{3}{2}\frac{\bar\Lambda}{2m_c}\delta^{(1/m)}_{D^{(*)}}\right)-\frac{4\alpha_s}{45\pi}\ln\frac{m_c^2}{4\Delta^2} \\
&\quad -\frac{4\alpha_s}{15\pi}-\frac{4\alpha_s}{5\pi}\delta^{(\alpha_s)}_{D^{(*)}}+\frac{\alpha_s}{\pi}\Delta^{(\alpha_s)}_{D^{(*)}}-\frac{4}{5}\frac{\bar\Lambda}{2m_c}\delta^{(1/m)}_{D^{(*)}}+\frac{\bar\Lambda}{2m_c}\Delta^{(1/m)}_{D^{(*)}}\ . \qquad (3.43)
\end{aligned}$$

Numerically, these inequalities are

$$\begin{aligned}
\sigma^2_{D^*} &> \frac{5}{4}\rho^2_{D^*}[1-0.11(0.16)_p-0.3_{np}]-0.081(0.059)_p+0.1_{np}\ ,\\
\sigma^2_{D^*} &> \frac{3}{5}\left(\rho^2_{D^*}\right)^2+\frac{4}{5}\rho^2_{D^*}[1-0.066(0.101)_p+0.08_{np}]-0.14(0.13)_p-0.003_{np}\ ,\\
\sigma^2_{D} &> \frac{5}{4}\rho^2_{D}[1+0.041(-0.014)_p+0.0_{np}]-0.025(0.0028)_p+0.2_{np}\ ,\\
\sigma^2_{D} &> \frac{3}{5}\left(\rho^2_{D}\right)^2+\frac{4}{5}\rho^2_{D}[1+0.025(-0.0089)_p+0.3_{np}]-0.039(0.032)_p+0.1_{np}\ , \qquad (3.44)
\end{aligned}$$

where the values $\alpha_s=0.3$ (in the $\overline{\rm MS}$ scheme around 2 GeV) and $\bar\Lambda=0.4$ GeV have been used. The perturbative corrections, with subscript p, are for two values of Δ. The results for $\Delta=2$ GeV are first, and those for $\Delta=3$ GeV are in parentheses. The nonperturbative corrections are labeled by a subscript np.

Equations (3.42) and (3.43) imply absolute bounds when combined with the corrected

[1] The authors of Ref. [26] have confirmed these findings. They report that the numerical result in their Eq. (19) for the difference $(\sigma^2_D-\sigma^2_{D^*})/2$ changes from $0.17+0.20\rho^2$ to $0.17+0.29\rho^2$.

form of the Uraltsev bound,

$$\rho^2_{D^{(*)}} > \frac{3}{4} + \frac{4\alpha_s}{9\pi}\ln\frac{m_c^2}{4\Delta^2} + \frac{\alpha_s}{\pi}\delta^{(\alpha_s)}_{D^{(*)}} + \frac{\bar{\Lambda}}{2m_c}\delta^{(1/m)}_{D^{(*)}} \ , \tag{3.45}$$

which comes from Eq. (3.30) and the first of Eqs. (3.39), and the tree-level Voloshin bound [28], $\rho^2 \lesssim 3/4$. A lower bound is required for terms proportional to $\rho^2_{D^{(*)}}$ with positive coefficients, and an upper bound is required for those with negative coefficients. The latter are corrections, so the upper bound is only needed at tree level. Note that an upper bound is required to estimate the greatest impact the corrections could have on the bound.

Inserting these inequalities into Eq. (3.42) gives

$$\sigma^2_{D^{(*)}} > \frac{15}{16} + \frac{14\alpha_s}{15\pi}\ln\frac{m_c^2}{4\Delta^2} + \frac{3\alpha_s}{2\pi}\delta^{(\alpha_s)}_{D^{(*)}} + \frac{\alpha_s}{\pi}\Delta^{(\alpha_s)}_{D^{(*)}} + \frac{\bar{\Lambda}}{2m_c}\Delta^{(1/m)}_{D^{(*)}} \ , \tag{3.46}$$

where $\rho^2_{D^{(*)}}$ is replaced by 3/4 in $\Delta^{(1/m)}_{D^{(*)}}$. The absolute bound produced in the same way from Eq. (3.43) happens to be identical at leading order and weaker only by the addition of $-4\alpha_s/15\pi$ after perturbative and $\Lambda_{\rm QCD}/m_{c,b}$ corrections are included. Using the numerical estimates above, the bounds in Eq. (3.46) are

$$\begin{aligned} \sigma^2_{D^*} &> 0.94 - 0.26(0.34)_p - 0.5_{np} \ , \\ \sigma^2_{D} &> 0.94 + 0.045(-0.027)_p - 0.04_{np} \ , \end{aligned} \tag{3.47}$$

where the corrections are labeled as described above.

When considering the bounds in Eqs. (3.45) and (3.46) and their dependence on Δ, one must bear in mind that the logarithms in the perturbative corrections are only small if Δ, m_b, and m_c are roughly of the same order. That is the accuracy of the results obtained here. For instance, Eq. (3.39) is valid for μ on the order of $m_{c,b}$, while Eqs. (3.36) and (3.37) are valid for μ near Δ. Therefore, taking the $\Delta \to \infty$ limit does not make sense in the absolute bounds. To understand the behavior of the bounds in this limit, one would need to sum the logarithms of m_c^2/Δ^2. Since these logarithms are not large for the values of Δ used here, this extra step has been omitted.

The sum rule bounds derived here should be compared with the dispersive constraints usually used to guide the extrapolation of measured form factors to zero recoil. These con-

straints are derived by computing the vacuum expectation value of a time-ordered product of $b \to c$ currents in the perturbative regime and then using analyticity to learn about the semileptonic regime. The result is equated with a spectral function sum of resonances (i.e., a sum of positive quantities). Much as in the derivation of the sum rules here, focusing on specific resonances yields form factor constraints. A typical example is shown in Fig. 3.4. The slope and curvature must lie within the ellipse, a constraint that is well approximated by a linear relation between the slope and curvature. Data are fit as a function of w for $|V_{cb}|\mathcal{F}_{D^{(*)}}(1)$ and $\rho^2_{D^{(*)}}$, and the second derivative at zero recoil is related to the slope according to this relation. For the process $\bar{B}^0 \to D^+\ell^-\bar{\nu}$, Belle used the relation $\sigma_D^2/2 = 1.05\rho_D^2 - 0.15$ [11] to find $\sigma_D^2 = 2.06 \pm 0.46 \pm 0.29$, where the first uncertainty is statistical and the second systematic [29]. This value is consistent with the bound above.

Rather than $\mathcal{F}_{D^*}(w)$, one typically fits the shape of the axial vector form factor $h_{A_1}(w)$, which is defined, for example, in Ref. [26]. Like $\mathcal{F}_{D^*}(w)$, it is equal to the Isgur-Wise function $\xi(w)$ in the heavy-quark limit. Its curvature is defined as in Eq. (3.38) and satisfies the bound in Eq. (3.46), with perturbative and nonperturbative corrections given by

$$\begin{aligned}
\delta_{A_1}^{(\alpha_s)} &= \frac{2(1-z)(17-4z+17z^2)+6(9-3z+4z^2)z\ln z}{27(1-z)^3} = 0.65 \ , \\
\delta_{A_1}^{(1/m)} &= -2(1+z)\chi_1'(1) + 4z\chi_2(1) + 4\chi_3'(1)(1-3z) + z\eta(1) - \frac{1+z}{2} \approx -1.3 \ , \\
\Delta_{A_1}^{(\alpha_s)} &= \frac{4(1-z)(27-203z-68z^2-203z^3+27z^4)-120(10+5z^2-z^3)z^2\ln z}{225(1-z)^5} = 0.24 \ , \\
\Delta_{A_1}^{(1/m)} &= \rho^2[2z\eta(1)-1-z] + 2\chi_1''(1)(1+z) - 8z\chi_2'(1) - 4\chi_3''(1)(1-3z) \\
&\quad + z\eta(1) - 2z\eta'(1) - \frac{1+z}{2} \approx -0.9\rho^2 - 0.5 \ ,
\end{aligned} \tag{3.48}$$

where the numerical estimates are based on the values used above. These values produce the absolute bound

$$\sigma_{A_1}^2 > .94 - 0.071(0.14)_p - 0.2_{np} \tag{3.49}$$

on the curvature of $h_{A_1}(w)$. This should be compared with the value found by Belle by the procedure described above for the process $\bar{B}^0 \to D^{*+}e^-\bar{\nu}$. Using the relation $\sigma_{A_1}^2/2 = 1.08\rho_{A_1}^2 - 0.23$ [11], Belle found $\sigma_{A_1}^2 = 2.44 \pm 0.37 \pm 0.41$, where the first uncertainty is statistical and the second systematic [30]. This value is also consistent with the bound produced here. A plot comparing dispersive constraints and sum rule bounds for this form

factor would be similar to Fig. 3.4, but with the sum rule bounds comparatively somewhat weaker.

3.5 Summary

This chapter has presented order α_s corrections to two new sum rules derived in Refs. [12, 13, 14] in the context of HQET. Section 3.2 repeated the tree-level derivation of a generic sum rule depending on three velocity transfer variables and included one-loop corrections. Section 3.3 studied the axial vector and vector sum rules that result from choosing specific currents in the generic equation. These led to α_s-corrected versions of the sum rules of Le Yaouanc *et al.* for the curvature of the Isgur-Wise function. There were no corrections suppressed by the heavy quark masses because the infinite-mass limit was used. Section 3.4 translated these HQET bounds into bounds on physical form factors by including perturbative and finite-mass corrections associated with matching HQET onto the full theory. Numerical estimates were given and compared with experimental values and dispersive constraints. The bounds produced here are less powerful than dispersive constraints but may provide an important check on those constraints.

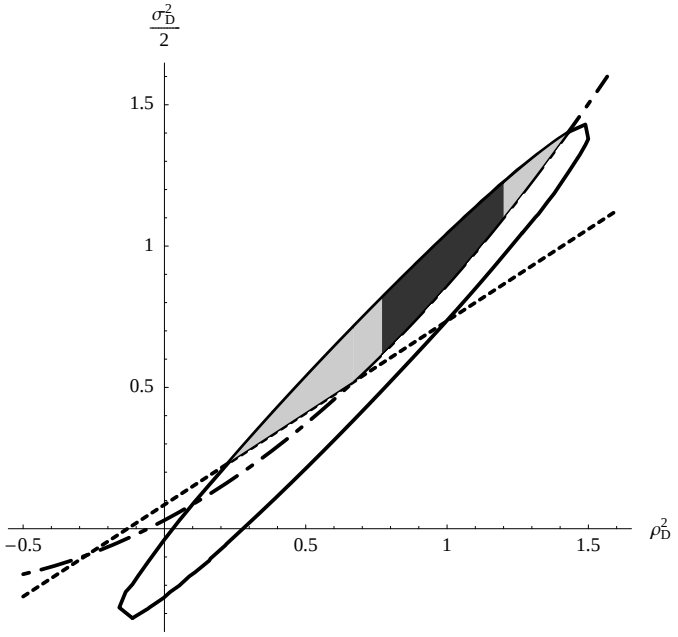

Figure 3.4: Dispersive constraints on $\mathcal{F}_D$ derivatives combined with the corrected sum rule bounds derived here at $\Delta = 2$ GeV. The interior of the ellipse is the region allowed by the dispersion relations. Including the curvature bounds, given by the area above the dashed curves, further restricts the allowed region to the shaded area. The darker region is obtained by also including the Bjorken and Voloshin bounds. Both perturbative and nonperturbative corrections are included.

Chapter 4

Soft-collinear effective theory

This is a brief review of some of the aspects of soft-collinear effective theory (SCET). Its logic follows the unpublished notes of C. Bauer [31]. This will be an introduction to the remaining topics of the thesis, each of which involves SCET in a fundamental way. Just like HQET, SCET describes the interactions of quarks in a very specific situation. For HQET, the quarks were heavy and were considered only inside hadrons. In SCET, for the most part we consider light quarks with large energy relative to the scale of strong dynamics, $\Lambda_{\rm QCD}$. For instance, a typical application is to $b \to s\gamma$ decays in the region of phase space in which the strange quark has energy on the order of the bottom quark mass, m_b, but still has small invariant mass. The fundamental point is that the light quark has large energy but small mass and hence travels almost along the lightcone.

4.1 Basics

Making the statement above more formal, we introduce a power counting parameter similar to the power counting parameter in HQET, $\Lambda_{\rm QCD}/m_Q$. Here we denote it λ for generality and define

$$p^2 = Q^2\lambda^2 \ll Q^2\,, \tag{4.1}$$

where Q is the large scale in the process under question. Typical values for λ are $\sqrt{\Lambda_{\rm QCD}/m_b}$ or sometimes $\Lambda_{\rm QCD}/m_b$. To be general, for now we will not specify what λ is. Now we will follow the same steps as in the introduction to HQET above. Start with the QCD quark Lagrangian, this time for zero mass. (It is possible to add a quark mass, but this is a

separate topic to be discussed in a later section.)

$$\mathcal{L} = \bar{\psi}(x) i \not{D} \psi(x) \,. \tag{4.2}$$

The quark propagator that results from this Lagrangian is the following:

$$\frac{i \not{p}}{p^2 + i\epsilon} \,. \tag{4.3}$$

We will expand this propagator just as in the HQET case by enforcing our SCET power counting. To understand what this power counting should be, decompose the quark momentum as follows:

$$p^\mu = \frac{1}{2} \bar{n}\cdot p \, n^\mu + \frac{1}{2} n \cdot p \, \bar{n}^\mu + p_\perp^\mu \,. \tag{4.4}$$

This parametrization is useful for processes occurring near the lightcone. The lightlike unit vectors above satisfy the following conditions:

$$n^2 = \bar{n}^2 = 0 \,, \tag{4.5}$$

$$n \cdot \bar{n} = 2 \,. \tag{4.6}$$

For convenience, we will choose these vectors to be $n^\mu = (1, 0, 0, 1)$ and $\bar{n}^\mu = (1, 0, 0, -1)$. Other choices are possible, but this is as good as any, assuming that we are talking about an energetic quark moving along the z-axis. This means it is mostly in the n direction. Using these lightcone coordinates, the invariant mass of the particle is given by

$$p^2 = \bar{n}\cdot p \, n \cdot p + p_\perp^2 \,. \tag{4.7}$$

The momentum scaling of the collinear quark discussed above gives the following scaling of the momentum lightcone components:

$$p^\mu \sim Q(\lambda^2, 1, \lambda) \,, \tag{4.8}$$

where the first component is $n{\cdot}p$, the second component is $\bar{n}{\cdot}p$, and the last component is $p_\perp$. The last component actually stands for the two components of momentum perpendicular to the z-axis. They have the same scaling, by assumption, and so they are grouped together.

The less energetic degrees of freedom the collinear quarks interact with are called ultrasoft, or usoft. (There are also soft modes, but these will not concern us here.) They have a characteristic scaling very different from the collinear degrees of freedom:

$$p^\mu_{\rm us} \sim Q\lambda^2 \,. \tag{4.9}$$

This means that all their components scale the same way, just like the soft degrees of freedom in HQET. Just as the light degress of freedom in HQET could not change the velocity of a heavy quark, the usoft degrees of freedom here cannot change the scaling of the collinear quark's momentum. To include this fact in the formalism, we parametrize the collinear momentum as

$$p^\mu = \tilde{p}^\mu + k^\mu \,, \tag{4.10}$$

where the so-called label momentum is defined as

$$\tilde{p}^\mu = \frac{1}{2}\bar{n}\cdot p\, n^\mu + p^\mu_\perp \,, \tag{4.11}$$

and the residual momentum is denoted k. Only k is affected by interactions with usoft particles.

With these definitions and scalings in hand, we can proceed with the expansion of the quark propagator. Putting all these scalings into Eq. (4.3) and keeping only the leading-order piece gives

$$i\frac{\not{n}}{2}\frac{\bar{n}\cdot p}{\bar{n}\cdot p n\cdot k + p_\perp^2 + i\epsilon} \,. \tag{4.12}$$

When we derive the leading-order SCET Lagrangian in the next section, it will be easy to confirm this form of the propagator.

4.2 Lagrangian

The SCET Lagrangian can be derived in a way very similar to the derivation of the HQET Lagrangian. As in that case, we start by factoring out the large momentum components from the field. In the SCET case it is necessary to sum over the label momentum in this process. This is what one would naturally expect, because the field gives a continuous spectrum of momenta when it creates particles, but it was unnecessary in the HQET case

because of a "velocity superselection rule." This is the same as the statement that the velocity of a heavy quark cannot be changed by interactions with soft particles. It makes the sum over velocities unnecessary since there will always be a delta function present to collapse the sum.

However, here the sum is necessary, and we write

$$\psi(x) = \sum_{\tilde{p}} e^{-i\tilde{p}\cdot x}\psi_{n,p}(x)\,. \tag{4.13}$$

We can check that this does what we want by acting on the original field with a derivative:

$$\begin{aligned} i\not{D}\psi(x) &= i\not{D}\sum_{\tilde{p}} e^{-i\tilde{p}\cdot x}\psi_{n,p}(x) \\ &= \sum_{\tilde{p}} e^{-i\tilde{p}\cdot x}(\not{p}+i\not{D})\psi_{n,p}(x)\,. \end{aligned} \tag{4.14}$$

This shows the order of a derivative acting on the newly defined $\psi_{n,p}$ field:

$$i\not{D}\psi_{n,p}(x) = \not{k}\psi_{n,p}(x)\,. \tag{4.15}$$

This is what we were trying to accomplish by pulling out the exponential prefactor involving the large momentum components. Derivatives acting on the new field scale like the residual momentum.

Let us now write the Lagrangian in Eq. (4.2) in terms of the $\psi_{n,p}$ fields:

$$\mathcal{L} = \sum_{\tilde{p},\tilde{p}'} \bar{\psi}_{n,p'} e^{-i(\tilde{p}-\tilde{p}')\cdot x}(\not{p}+i\not{D})\psi_{n,p}(x)\,. \tag{4.16}$$

Just as in the HQET case where subtracting out the exponential prefactor was not sufficient to get rid of large fluctuations, here $\psi_{n,p}$ contains two large components and two small components. We must integrate out the large components just like the $\mathcal{Q}_v$ field in HQET and then write the Lagrangian only in terms of the components giving small fluctuations around the SCET limit. Write the two different components as

$$\psi_{n,p} = \xi_{n,p} + \xi_{\bar{n},p}\,, \tag{4.17}$$

where they are defined once again in terms of projection operators:

$$\xi_{n,p} = \frac{\not{n}\bar{\not{n}}}{4}\psi_{n,p}\,, \tag{4.18}$$

$$\xi_{\bar{n},p} = \frac{\bar{\not{n}}\not{n}}{4}\psi_{n,p}\,. \tag{4.19}$$

These new fields satisfy the following relations:

$$\frac{\not{n}\bar{\not{n}}}{4}\xi_{n,p} = \xi_{n,p}\,, \quad \not{n}\xi_{n,p} = 0\,, \tag{4.20}$$

$$\frac{\bar{\not{n}}\not{n}}{4}\xi_{\bar{n},p} = \xi_{\bar{n},p}\,, \quad \bar{\not{n}}\xi_{\bar{n},p} = 0\,. \tag{4.21}$$

In terms of these fields, the Lagrangian can be written as

$$\mathcal{L} = \sum_{\tilde{p},\tilde{p}'} e^{-i(\tilde{p}-\tilde{p}')\cdot x} \quad \Big[\ \bar{\xi}_{n,p'}(x)\frac{\bar{\not{n}}}{2} in\cdot D\xi_{n,p}(x) + \bar{\xi}_{\bar{n},p'}(x)\frac{\not{n}}{2}(\bar{n}\cdot p + i\bar{n}\cdot D)\xi_{\bar{n},p}(x)$$
$$+\ \bar{\xi}_{n,p'}(x)(\not{p}_\perp + i\not{D}_\perp)\xi_{\bar{n},p}(x) + \bar{\xi}_{\bar{n},p'}(x)(\not{p}_\perp + i\not{D}_\perp)\xi_{n,p}(x)\Big]\,. \tag{4.22}$$

Varying this Lagrangian with respect to $\bar{\xi}_{\bar{n},p}$ gives the equation of motion for the large components:

$$\xi_{\bar{n},p}(x) = \frac{1}{\bar{n}\cdot p + i\bar{n}\cdot D}(\not{p}_\perp + i\not{D}_\perp)\xi_{n,p}(x)\,. \tag{4.23}$$

Just as in our HQET derivation, this equation can be used to eliminate the $\xi_{\bar{n},p}$ field from the Lagrangian at tree level. The result is

$$\mathcal{L} = \sum_{\tilde{p},\tilde{p}'} e^{-i(\tilde{p}-\tilde{p}')\cdot x}\bar{\xi}_{n,p'}(x)\left[in\cdot D + (\not{p}_\perp + i\not{D}_\perp)\frac{1}{\bar{n}\cdot p + i\bar{n}\cdot D}(\not{p}_\perp + i\not{D}_\perp)\right]\frac{\bar{\not{n}}}{2}\xi_{n,p}(x)\,. \tag{4.24}$$

To get the leading-order SCET Lagrangian, this expression still needs to be expanded in our power counting parameter λ. To do this, though, we need to distinguish between different kinds of gluon fluctuations. There are both collinear and ultrasoft gluons to worry about, and this is one of the things that make SCET so much more complicated than HQET. In HQET, there is only one kind of gluon fluctuation, the $\Lambda_{\rm QCD}$ gluon. The two different types of gluon field have the following scaling:

$$A_n^{c,\mu} \sim Q(\lambda^2, 1, \lambda)\,, \quad A_{\rm us}^{\mu} \sim Q\lambda^2\,. \tag{4.25}$$

The ultrasoft scaling shows that its contributions to $D_\perp$ and $\bar{n}\cdot D$ are subleading and can be dropped at this order. In contrast, the collinear gluon still has large fluctuations that must be removed just as we did for the collinear quark:

$$A_n^c(x) = \sum_{\tilde{p}} e^{-i\tilde{p}\cdot x} A_{n,p}^c(x)\,. \tag{4.26}$$

This fact must be kept in mind. While the large fluctuations of the collinear quark field have been fully removed from our Lagrangian, the same is not true of the collinear gluons. Derivatives acting on these fields can still be large.

For now, let us proceed and write the Lagrangian with the ultrasoft gluons dropped where possible:

$$\mathcal{L} = \sum_{\tilde{p},\tilde{p}'} e^{i\tilde{p}'\cdot x}\bar{\xi}_{n,p'}(x)\left[in\cdot D + (\not{p}_\perp + i\not{D}_\perp^c)\frac{1}{\bar{n}\cdot p + i\bar{n}\cdot D^c}(\not{p}_\perp + i\not{D}_\perp^c)\right]\frac{\not{\bar{n}}}{2}e^{-i\tilde{p}\cdot x}\xi_{n,p}(x)\,. \tag{4.27}$$

The derivatives labeled with a superscript c contain only collinear gluon field and the derivatives without a superscript contain both collinear and ultrasoft gluon fields. Note that only one term in the Lagrangian above contains interactions of the collinear quark field with ultrasoft gluons. It is the one place where the ultrasoft gluon field is not subleading. This feature will be crucial in what follows.

4.3 Label operators

An unfortunate fact about the notation used above in the expression for the Lagrangian is that all partial derivatives are meant to act only on the exponentials containing label momenta and not on the fields themselves. The following explains what we mean. The partial derivatives are supposed to act according to

$$\bar{n}\cdot\partial \sum_{\tilde{p}} e^{-i\tilde{p}\cdot x}\xi_{n,p} = \sum_{\tilde{p}} e^{-i\tilde{p}\cdot x}\bar{n}\cdot p\,\xi_{n,p}\,. \tag{4.28}$$

This is not intuitive, and a better notation was invented in Ref. [36]. The so-called label operators do exactly what we want, as can be seen in the following. The label operator

acting on a field just gives the large component of its label:

$$\bar{n}\cdot\mathcal{P}\xi_{n,p} = \bar{n}\cdot p\xi_{n,p}\,. \tag{4.29}$$

Now define the following convenient but deceptive notation to hide the sum over labels:

$$\xi_n \equiv \sum_{\tilde{p}} e^{-i\tilde{p}\cdot x}\xi_{n,p}\,, \tag{4.30}$$

and we can see what the label operator is good for. Acting on this field, it gives just the sort of expression that appears in the Lagrangian:

$$\begin{aligned}\bar{n}\cdot\mathcal{P}\xi_n &= \bar{n}\cdot\mathcal{P}\sum_{\tilde{p}} e^{-i\tilde{p}\cdot x}\xi_{n,p} \\ &= \sum_{\tilde{p}} e^{-i\tilde{p}\cdot x}\bar{n}\cdot p\xi_{n,p}\,.\end{aligned} \tag{4.31}$$

Using this, we can rewrite our expression for the Lagrangian in a much simpler way:

$$\mathcal{L} = \bar{\xi}_n(x)\left(in\cdot D + i\not{D}^c_\perp\frac{1}{i\bar{n}\cdot D^c}i\not{D}^c_\perp\right)\frac{\not{\bar{n}}}{2}\xi_n(x)\,. \tag{4.32}$$

This expression allows us to easily verify the collinear quark propagator derived above by expanding the QCD propagator with the SCET power counting.

The following definitions of the covariant derivatives should be noted:

$$\bar{n}\cdot D^c = \bar{n}\cdot\mathcal{P} - igT^a\bar{n}\cdot A^c\,, \tag{4.33}$$

$$D^c_\perp = \mathcal{P}_\perp - igT^a A^c_\perp\,, \tag{4.34}$$

$$n\cdot D = n\cdot\partial - igT^a n\cdot A^c - igT^a n\cdot A^{\rm us}\,. \tag{4.35}$$

These are not quite what one might expect, but they are correct for our purposes.

4.4 Gauge invariance

The Lagrangian as written above is still not quite right. To see what is wrong and how to correct it, we must first understand gauge invariance in the context of SCET. First, recall

SU(3) gauge transformations of the fields in QCD:

$$\psi(x) \;\to\; \psi'(x) = U(x)\psi(x)\,, \tag{4.36}$$

$$A^\mu(x) \;\to\; A'^\mu(x) = U(x)A^\mu U^\dagger(x) + \frac{i}{g}U(x)\partial^\mu U^\dagger(x)\,, \tag{4.37}$$

where $U(x)$ is an SU(3) Wilson line. Since SCET splits up the gluon fields into two different kinds, collinear and ultrasoft, it is natural that there should be two different kinds of gauge transformation as well. Since ultrasoft fluctuations are at a much lower momentum scale (or a much larger distance scale) than the collinear fluctuations, we can think of the ultrasoft gauge field as a classical background field for the collinear degrees of freedom. With this picture in mind, it is clear that the ultrasoft fields should transform under ultrasoft gauge transformations just as they do in QCD:

$$\psi_{\rm us}(x) \;\to\; \psi'_{\rm us}(x) = U(x)_{\rm us}\psi_{\rm us}(x)\,, \tag{4.38}$$

$$A^\mu_{\rm us}(x) \;\to\; A'^\mu_{\rm us}(x) = U(x)_{\rm us}A^\mu_{\rm us}U^\dagger_{\rm us}(x) + \frac{i}{g}U_{\rm us}(x)\partial^\mu U^\dagger_{\rm us}(x)\,. \tag{4.39}$$

At the same time, the collinear fields should transform under collinear gauge transformations just as they do in QCD in background field gauge:

$$\xi_n(x) \;\to\; \xi'_n(x) = \mathcal{U}_n(x)\xi_n(x)\,, \tag{4.40}$$

$$A^\mu_n(x) \;\to\; A'^\mu_n(x) = \mathcal{U}_n(x)A^\mu_n\mathcal{U}^\dagger_n(x) + \frac{i}{g}\mathcal{U}_n(x)\mathcal{D}^\mu\mathcal{U}^\dagger_n(x)\,. \tag{4.41}$$

Here we have defined a different kind of covariant derivative to take into account the label operators:

$$\mathcal{D}^\mu = \frac{1}{2}\bar{n}\cdot\mathcal{P}n^\mu + \mathcal{P}^\mu_\perp + \frac{1}{2}n\cdot D\bar{n}^\mu\,, \tag{4.42}$$

where the regular covariant derivative contains only the ultrasoft gluon field:

$$n\cdot D = n\cdot\partial + ign\cdot A_{\rm us}\,. \tag{4.43}$$

Finally, under ultrasoft gauge transformations, the collinear fields transform as

$$\xi_n(x) \;\to\; \xi_n'(x) = U_{\rm us}(x)\xi_n(x)\,, \tag{4.44}$$

$$A_n^\mu(x) \;\to\; A_n'^\mu(x) = U_{\rm us}(x)A_n^\mu(x)U_{\rm us}^\dagger\,. \tag{4.45}$$

With all these definitions and transformations established, we are ready to deal with gauge invariance in SCET. First define a collinear Wilson line made up only of collinear gluons:

$$W_n(x) = P\exp\left(-ig\int_x^\infty ds\bar{n}\cdot A_c(\bar{n}s)\right)\,. \tag{4.46}$$

From the properties established above, it transforms under collinear gauge transformations according to

$$W_n(x) \to W_n'(x) = \mathcal{U}_n(x)W_n(x)\,, \tag{4.47}$$

and under ultrasoft gauge transformations according to

$$W_n(x) \to W_n'(x) = U_{\rm us}(x)W_n(x)U_{\rm us}^\dagger(x)\,. \tag{4.48}$$

Now we note that the problem with the form of the Lagrangian above is that it is not gauge invariant because of the derivative term in the denominator. We can fix that problem now by adding the terms required by gauge invariance. The following identity can be shown without too much trouble:

$$\bar{n}\cdot\mathcal{P} + g\bar{n}\cdot A^c = W_n\bar{n}\cdot\mathcal{P}W_n^\dagger\,. \tag{4.49}$$

This identity shows us what we need to add to the Lagrangian to make it gauge invariant:

$$\mathcal{L} = \bar{\xi}_n(x)\left(in\cdot D + i\not{D}_\perp^c W_n(x)\frac{1}{i\bar{n}\cdot\mathcal{P}}W_n^\dagger(x)i\not{D}_\perp^c\right)\frac{\not{\bar{n}}}{2}\xi_n(x)\,. \tag{4.50}$$

The Wilson lines make explicit the fact that the original Lagrangian contained interactions of collinear quarks with an arbitrary number of collinear gluons, all at the same order in the power counting parameter λ. This fact also make SCET quite a bit more complicated than HQET.

4.5 Collinear-ultrasoft decoupling

Now we are prepared to derive probably the most important property of SCET: collinear-ultrasoft decoupling. It is this property that makes SCET's factorization proofs possible. Recall first that the only coupling between collinear quarks and ultrasoft gluons in the leading-order SCET Lagrangian came from the $n\cdot D$ covariant derivative. It turns out that this simple coupling can be removed by a field redefinition. This field redefinition is given by the following:

$$\begin{aligned} \xi_n(x) &= Y_n(x)\xi_n^{(0)}(x)\,, && (4.51)\\ A_n(x) &= Y_n(x)A_n^{(0)}(x)Y_n^\dagger(x)\,, && (4.52)\\ W_n(x) &= Y_n(x)W_n^{(0)}(x)Y_n^\dagger(x)\,, && (4.53) \end{aligned}$$

where the ultrasoft Wilson line above is defined in analogy with the collinear Wilson line:

$$Y_n(x) = P\exp\left(-ig\int_x^\infty ds n\cdot A_{\rm us}(ns)\right)\,. \tag{4.54}$$

It can be shown that this Wilson line satisfies

$$(n\cdot\partial + ign\cdot A_{\rm us})Y_n = Y_n n\cdot\partial\,. \tag{4.55}$$

This relation allows us to write the Lagrangian in terms of the redefined fields and remove the collinear-ultrasoft coupling:

$$\mathcal{L} = \bar\xi_n^{(0)}(x)\left(in\cdot D^c + i\not{D}_\perp^c W_n^{(0)}(x)\frac{1}{i\bar n\cdot\mathcal{P}}W_n^{(0)\dagger}(x)i\not{D}_\perp^c\right)\frac{\not{\bar n}}{2}\xi_n^{(0)}(x)\,. \tag{4.56}$$

It must be noted, however, that although the coupling has been removed from the Lagrangian, the effects have not disappeared. The same field redefinitions must be applied to any external operators considered, and this is where the effects turn up. These operators change to include more Wilson lines. But this facilitates the proof of many factorization theorems.

An interesting sidenote is that this trick will work for HQET as well. After all, there is a very similar heavy quark coupling to soft gluons in its leading-order Lagrangian. It is

possible to perform a similar field redefinition and remove this coupling. In HQET, this fact is unfortunately not as useful.

Chapter 5

Infrared regulators in SCET

This chapter discusses the important question of whether soft-collinear effective theory reproduces the low-energy sector of QCD—as it must. Much of this chapter appeared in Ref. [32].

5.1 Introduction

Soft-collinear effective theory [33, 34, 35, 36] describes the interactions of soft and ultrasoft (usoft) particles with collinear particles. Using lightcone coordinates in which a general four-momentum is written as $p^\mu = (p^+, p^-, p^\perp) = (n\cdot p, \bar{n}\cdot p, p^\perp)$, where n and $\bar{n}$ are four-vectors on the lightcone ($n^2 = \bar{n}^2 = 0$, $n \cdot \bar{n} = 2$), these three degrees of freedom are distinguished by the scaling of their momenta:

$$\begin{aligned} &\text{collinear:} && p_c^\mu \sim Q(\lambda^2, 1, \lambda), \\ &\text{soft:} && p_s^\mu \sim Q(\lambda, \lambda, \lambda), \\ &\text{usoft:} && p_{us}^\mu \sim Q(\lambda^2, \lambda^2, \lambda^2). \end{aligned} \tag{5.1}$$

The size of the expansion parameter λ is determined by the typical off-shellness of the collinear particles in a given problem. For example, in inclusive decays one typically has $p_c^2 \sim Q^2\lambda^2 \sim Q\Lambda_{\rm QCD}$, from which it follows that $\lambda = \sqrt{\Lambda_{\rm QCD}/Q}$. For exclusive decays, however, one needs collinear particles with $p_c^2 \sim \Lambda_{\rm QCD}^2$, giving $\lambda = \Lambda_{\rm QCD}/Q$. One is usually interested in describing the interactions of these collinear degrees of freedom with non-perturbative degrees of freedom at rest, which satisfy $p^\mu \sim (\Lambda_{\rm QCD}, \Lambda_{\rm QCD}, \Lambda_{\rm QCD})$. Thus inclusive processes involve interactions of collinear and usoft degrees of freedom, while exclusive decays are described by interactions of collinear and soft degrees of freedom The

theory describing the former set of degrees of freedom is called $\mathrm{SCET_I}$, while the latter theory is called $\mathrm{SCET_{II}}$ [37].

Interactions between usoft and collinear degrees of freedom are contained in the leading-order Lagrangian of $\mathrm{SCET_I}$,

$$\mathcal{L}_{\rm I} = \bar{\xi}_n \left[in\cdot D + i\not{D}_c^\perp \frac{1}{i\bar{n}\cdot D_c} i\not{D}_c^\perp \right] \frac{\not{\bar{n}}}{2} \xi_n \,, \tag{5.2}$$

and are well understood. The only interaction between collinear fermions and usoft gluons is from the derivative

$$iD^\mu = iD_c^\mu + gA_{us}^\mu \,. \tag{5.3}$$

These interactions can be removed from the leading-order Lagrangian by the field redefinition [36]

$$\begin{aligned} \xi_n = Y_n \xi_n^{(0)} \,, \quad A_n = Y_n A_n^{(0)} Y_n^\dagger \,, \\ Y_n(x) = \mathrm{P} \exp\left(ig \int_{-\infty}^0 ds\, n\cdot A_{us}(x+ns) \right) \,. \end{aligned} \tag{5.4}$$

However, the same field redefinition has to be performed on the external operators in a given problem, and this reproduces the interactions with the usoft degrees of freedom. Consider for example the heavy-light current, which in $\mathrm{SCET_I}$ is given by

$$J_{hl}^I(\omega) = \left[\bar{\xi}_n W_n \right]_\omega \Gamma h_v \,, \tag{5.5}$$

where h_v is the standard field of heavy quark effective theory [1], the Wilson line W_n is required to ensure collinear gauge invariance [35] and ω is the large momentum label of the gauge invariant $[\bar{\xi}_n W_n]$ collinear system. Written in terms of the redefined fields, this current is

$$J_{hl}^I(\omega) = \left[\bar{\xi}_n^{(0)} W_n^{(0)} \right]_\omega \Gamma \left[Y_n^\dagger h_v \right] \,. \tag{5.6}$$

For exclusive decays, we need to describe the interactions of soft with collinear particles. This theory is called $\mathrm{SCET_{II}}$ [37]. Since adding a soft momentum to a collinear particle

takes this particle off its mass shell $(p_c + p_s)^2 \sim (Q\lambda, Q, Q\lambda)^2 \sim Q^2\lambda \sim Q\Lambda_{\rm QCD}$, there are no couplings of soft to collinear particles in the leading-order Lagrangian.[1] Thus, the Lagrangian is given by [39, 40]

$$\mathcal{L}_{\rm II} = \bar{\xi}_n \left[in\cdot D_c + i\not{D}_c^\perp \frac{1}{i\bar{n}\cdot D_c} i\not{D}_c^\perp \right] \frac{\bar{\not{n}}}{2} \xi_n \,. \tag{5.7}$$

In this theory, the heavy-light current is given by

$$J_{hl}^{II}(\omega,\kappa) = \left[\bar{\xi}_n^{(0)} W_n^{(0)}\right]_\omega \Gamma \left[S_n^\dagger h_v\right]_\kappa \,, \tag{5.8}$$

where S_n is a soft Wilson line in the n direction defined by

$$S_n(x) = \mathrm{P} \exp\left(ig \int_{-\infty}^0 ds\, n\cdot A_s(x+ns) \right) \,. \tag{5.9}$$

This is the most general current invariant under collinear and soft gauge transformations.

This chapter is organized as follows: We first consider matching the heavy-light current in $\mathrm{SCET_I}$ onto the heavy-light current in $\mathrm{SCET_{II}}$ using off-shell fermions. While the terms logarithmic in the off-shellness do not agree in the two theories, we argue that this is due to unregulated IR divergences in $\mathrm{SCET_{II}}$. We then discuss IR regulators in SCET in more detail. We first identify the problems with the common SCET regulators and then propose a new regulator that addresses these issues. Using this regulator we then show that soft and collinear modes in $\mathrm{SCET_{II}}$ are sufficient to reproduce the IR divergences of $\mathrm{SCET_I}$ and explain the relationship between IR regulators and an additional mode proposed for $\mathrm{SCET_{II}}$ [40].

5.2 Matching from $\mathrm{SCET_I}$ onto $\mathrm{SCET_{II}}$

The only difference between $\mathrm{SCET_I}$ and $\mathrm{SCET_{II}}$ is the typical off-shellness of the collinear degrees of freedom in the theory. The theory $\mathrm{SCET_I}$ allows fluctuations around the classical momentum with $p_c^2 \sim Q\Lambda_{\rm QCD}$, while the theory $\mathrm{SCET_{II}}$ allows fluctuations with only $p_c^2 \sim \Lambda_{\rm QCD}^2$. Since both theories expand around the same limit, $\mathrm{SCET_{II}}$ can be viewed as a low-energy effective theory of $\mathrm{SCET_I}$. Therefore, one can match from the theory $\mathrm{SCET_I}$ onto

[1] At higher orders, higher-dimensional operators with at least two soft and two collinear particles can appear.

Figure 5.1: Diagrams in $\mathrm{SCET_I}$ contributing to the matching. The solid square denotes an insertion of the heavy-light current.

$\mathrm{SCET_{II}}$ by integrating out the $\mathcal{O}(\sqrt{Q\Lambda_{\mathrm{QCD}}})$ fluctuations.

To illustrate this matching, we consider the heavy-light current. Using the definitions of this current given in Eqs. (5.5) and (5.8), we can write

$$J^I_{hl}(\omega) = \int d\kappa \; C(\omega,\kappa) \; J^{II}_{hl}(\omega,\kappa)\,. \tag{5.10}$$

At tree level one finds trivially

$$C(\omega,\kappa) = 1\,. \tag{5.11}$$

In fact, this Wilson coefficient remains unity to all orders in perturbation theory, as was argued in Ref. [38].

To determine the matching coefficient at one loop, we calculate matrix elements of the current in the two theories. There are two diagrams in $\mathrm{SCET_I}$, shown in Fig. 5.1. For on-shell external states, we find for the two integrals

$$\begin{aligned} iA^{Ia} &= g^2 C_F \mu^{4-d} \int \frac{\mathrm{d}^d k}{(2\pi)^d} \frac{1}{[-n\cdot k + i0][-v\cdot k + i0][k^2 + i0]}\,, & (5.12)\\ iA^{Ib} &= 2g^2 C_F \mu^{4-d} \int \frac{\mathrm{d}^d k}{(2\pi)^d} \frac{\bar{n}\cdot(p_c - k)}{[-\bar{n}\cdot k + i0][k^2 - 2p_c\cdot k + i0][k^2 + i0]}\,. & (5.13) \end{aligned}$$

The diagrams in $\mathrm{SCET_{II}}$ are shown in Fig. 5.2. For on-shell external states the two integrals are exactly the same as in $\mathrm{SCET_I}$:

$$\begin{aligned} iA^{IIa} &= g^2 C_F \mu^{4-d} \int \frac{\mathrm{d}^d k}{(2\pi)^d} \frac{1}{[-n\cdot k + i0][-v\cdot k + i0][k^2 + i0]}\,, & (5.14)\\ iA^{IIb} &= 2g^2 C_F \mu^{4-d} \int \frac{\mathrm{d}^d k}{(2\pi)^d} \frac{\bar{n}\cdot(p_c - k)}{[-\bar{n}\cdot k + i0][k^2 - 2p_c\cdot k + i0][k^2 + i0]}\,. & (5.15) \end{aligned}$$

Figure 5.2: Diagrams in $\mathrm{SCET_{II}}$ contributing to the matching.

Since the integrands are exactly the same, the loop diagrams will precisely cancel in the matching calculation. Thus we find that the Wilson coefficient $C(\omega,\kappa)$ remains unity, even at one loop. This confirms the arguments in [38] to this order.

The fact that both of these integrals are scaleless and therefore zero might bother some readers. The vanishing of these diagrams is due to the cancellation of collinear, infrared (IR) and ultraviolet (UV) divergences. Introducing an IR regulator will separate these divergences, and the UV will be regulated by dimensional regularization. In Ref. [33] a small off-shellness was introduced to regulate the IR divergences of $\mathrm{SCET_I}$. In Refs. [40] the divergence structure of $\mathrm{SCET_{II}}$ was studied keeping both the heavy and the collinear fermions off-shell. Using this IR regulator, the authors of Refs. [40] argued that $\mathrm{SCET_{II}}$ does not reproduce the IR divergences of $\mathrm{SCET_I}$ and introduced a new mode in $\mathrm{SCET_{II}}$ to fix this problem. To gain more insight into their argument, we will go through their calculation in some detail.

In $\mathrm{SCET_I}$ the first diagram is

$$\begin{aligned}
A_{p_c}^{Ia} &= -ig^2 C_F \mu^{4-d} \int \frac{\mathrm{d}^d k}{(2\pi)^d} \frac{1}{[\tilde{p}_c - n\cdot k + i0][v\cdot(p_s-k)+i0][k^2+i0]} \\
&= -\frac{g^2 C_F}{2\pi}(4\pi)^{1-d/2}\Gamma\left(2-\frac{d}{2}\right)\mu^{4-d}\int_0^\infty \mathrm{d}n\cdot k\,(n\cdot k-\tilde{p}_c)^{-1}\,n\cdot k^{d/2-2}\,(n\cdot k - 2v\cdot p_s)^{d/2-2} \\
&= \frac{\alpha_s C_F}{4\pi}\bigg[-\frac{1}{\epsilon^2}+\frac{2}{\epsilon}\log\frac{-\tilde{p}_c}{\mu}-2\log^2\frac{-\tilde{p}_c}{\mu}+2\log\left(1-\frac{2v\cdot p_s}{\tilde{p}_c}\right)\log\frac{2v\cdot p_s}{\tilde{p}_c} \\
&\quad + 2\,\mathrm{Li}_2\left(\frac{2v\cdot p_s}{\tilde{p}_c}\right)-\frac{3\pi^2}{4}\bigg],
\end{aligned} \tag{5.16}$$

where $d = 4-2\epsilon$ and

$$\tilde{p}_c = \frac{p_c^2}{\bar{n}\cdot p_c}\,. \tag{5.17}$$

In going from the first line to the second, we closed the $\bar{n}\cdot k$ contour below, thus restricting

$n\cdot k$ to positive values, and performed the Euclidean $k_\perp$ integral. The second diagram gives

$$\begin{aligned} A_{p_c}^{Ib} &= -2ig^2 C_F \mu^{4-d} \int \frac{\mathrm{d}^d k}{(2\pi)^d} \frac{\bar{n}\cdot(p_c - k)}{[-\bar{n}\cdot k + i0][(k-p_c)^2 + i0][k^2 + i0]} \\ &= \frac{\alpha_s C_F}{4\pi} \left[\frac{2}{\epsilon^2} + \frac{2}{\epsilon} - \frac{2}{\epsilon} \log \frac{-p_c^2}{\mu^2} + \log^2 \frac{-p_c^2}{\mu^2} - 2\log \frac{-p_c^2}{\mu^2} + 4 - \frac{\pi^2}{6} \right] . \end{aligned} \tag{5.18}$$

In this diagram it is necessary to choose $d < 4$ for the $k_\perp$ integral, but one requires $d > 4$ for the $\bar{n}\cdot k$ integral. In the former integral, dimensional regularization regulates the divergence at $k_\perp = \infty$, while in the latter it regulates the divergence at $\bar{n}\cdot k = 0$. Both of these divergences have to be interpreted as UV, as discussed in section 5.3. Each diagram contains a mixed UV-IR divergence of the form $\log p_c^2/\epsilon$. This mixed divergence cancels in the sum of the two diagrams and we find, after also adding the wave function contributions,

$$\begin{aligned} A_{p_c}^{I} &= \frac{\alpha_s C_F}{4\pi} \left[\frac{1}{\epsilon^2} + \frac{2}{\epsilon} \log \frac{\mu}{\bar{n}\cdot p_c} + \frac{5}{2\epsilon} + \log^2 \frac{-p_c^2}{\mu^2} - 2\log^2 \frac{-\tilde{p}_c}{\mu} - \frac{3}{2} \log \frac{-p_c^2}{\mu^2} - 2\log \frac{-2v\cdot p_s}{\mu} \right. \\ &\quad \left. + 2\log\left(1 - \frac{2v\cdot p_s}{\tilde{p}_c}\right) \log \frac{2v\cdot p_s}{\tilde{p}_c} + 2\mathrm{Li}_2\left(\frac{2v\cdot p_s}{\tilde{p}_c}\right) + \frac{11}{2} - \frac{11\pi^2}{12} \right] . \end{aligned} \tag{5.19}$$

Now consider the $\mathrm{SCET_{II}}$ diagrams. The second is identical to the one in $\mathrm{SCET_I}$:

$$A_{p_c}^{IIb} = A_{p_c}^{Ib} . \tag{5.20}$$

The first diagram, however, is different and we find

$$\begin{aligned} A_{p_c}^{IIa} &= -ig^2 C_F \mu^{4-d} \int \frac{\mathrm{d}^d k}{(2\pi)^d} \frac{1}{[-n\cdot k + i0][v\cdot(p_s - k) + i0][k^2 + i0]} \\ &= -\frac{g^2 C_F}{2\pi} \mu^{4-d} \int_0^\infty \mathrm{d}n\cdot k \int \frac{\mathrm{d}^{d-2} k_\perp}{(2\pi)^{d-2}} \frac{1}{n\cdot k\,(k_\perp^2 + n\cdot k^2 - 2v\cdot p_s\, n\cdot k)} \\ &= -\frac{\alpha_s C_F}{2\pi} (4\pi)^{2-d/2} \Gamma\left(2 - \frac{d}{2}\right) \mu^{4-d} \int_0^\infty \mathrm{d}n\cdot k\, n\cdot k^{d/2-3} (n\cdot k - 2v\cdot p_s)^{d/2-2} . \end{aligned} \tag{5.21}$$

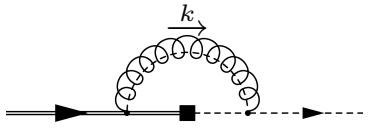

Figure 5.3: Contribution of the additional $\mathrm{SCET_{II}}$ mode proposed in Refs. [40].

Note that convergence of this integral at $n\cdot k = \infty$ requires $d < 4$, whereas convergence at $n\cdot k = 0$ requires $d > 4$. In this case dimensional regularization is regulating both a UV divergence at $n\cdot k = \infty$, as well as the divergence at $n\cdot k = 0$, which is IR in nature, as we will discuss in section 5.3. Using the variable transformation $x = n\cdot k/(n\cdot k - 2v\cdot p_s)$ to relate this integral to a beta function [41] one finds

$$A_{p_c}^{IIa} = \frac{\alpha_s C_F}{4\pi}\left[\frac{1}{\epsilon^2} - \frac{2}{\epsilon}\log\frac{-2v\cdot p_s}{\mu} + 2\log^2\frac{-2v\cdot p_s}{\mu} + \frac{5\pi^2}{12}\right]. \tag{5.22}$$

Adding the two diagrams together with the wave function contributions gives

$$\frac{\alpha_s C_F}{4\pi}\left[\frac{3}{\epsilon^2} - \frac{2}{\epsilon}\log\frac{2v\cdot p_s\, p_c^2}{\mu^3} + \frac{5}{2\epsilon} + \log^2\frac{-p_c^2}{\mu^2} + 2\log^2\frac{-2v\cdot p_s}{\mu} - \frac{3}{2}\log\frac{-p_c^2}{\mu^2}\right.$$
$$\left. - 2\log\frac{-2v\cdot p_s}{\mu} + \frac{11}{2} + \frac{\pi^2}{4}\right]. \tag{5.23}$$

We can see that in the sum of the two diagrams the terms proportional to $\log p_c^2/\epsilon$ or $\log vp_s/\epsilon$ do not cancel as they did in $\mathrm{SCET_I}$. Furthermore, the finite terms logarithmic in p_c^2 or $v\cdot p_s$ do not agree with the corresponding terms in the $\mathrm{SCET_I}$ result. This fact prompted the authors of Refs. [40] to conclude that $\mathrm{SCET_{II}}$ does not reproduce the IR divergences of $\mathrm{SCET_{II}}$ and that a new mode is needed in the latter effective theory. However, as we mentioned above, there are problems with IR effects in this diagram. In fact, as we will show in great detail in the next section, the off-shellness of the fermions does not regulate all IR divergences in this diagram. This means that the fact that the terms logarithmic in the fermion off-shellness do not agree between $\mathrm{SCET_I}$ and $\mathrm{SCET_{II}}$ does not imply that the IR divergences are not reproduced correctly since some $1/\epsilon$ poles are IR in origin.

We also calculate the diagram in $\mathrm{SCET_{II}}$ containing the additional mode proposed in Refs. [40]. The new messenger mode has momenta scaling as

$$p_{sc}^\mu \sim (\Lambda_{\mathrm{QCD}}^2/Q, \Lambda_{\mathrm{QCD}}, \Lambda_{\mathrm{QCD}}^{3/2}/Q^{1/2})\,. \tag{5.24}$$

(Note that the invariant mass of this term satisfies $p_{sc}^2 \ll \Lambda_{\mathrm{QCD}}^2$.) The diagram is shown in

Fig. 5.3 and we find

$$\begin{aligned} A_{p_c}^{IIc} &= -2ig^2 C_F \mu^{4-d} \int \frac{\mathrm{d}^d k}{(2\pi)^d} \frac{1}{[\tilde{p}_c - n\cdot k + i0][2v\cdot p_s - \bar{n}\cdot k + i0][k^2 + i0]} \\ &= \frac{\alpha_s C_F}{4\pi} \left[-\frac{2}{\epsilon^2} + \frac{2}{\epsilon} \log \frac{2v\cdot p_s\, \tilde{p}_c}{\mu^2} - \log^2 \frac{2v\cdot p_s\, \tilde{p}_c}{\mu^2} - \frac{\pi^2}{2} \right] . \end{aligned} \tag{5.25}$$

Adding this term to the Eq. (5.23) cancels the terms proportional to $\log(2v\cdot p_s\, p_c^2/\mu^3)/\epsilon$ and we find

$$\begin{aligned} A_{p_c}^{II} &= \frac{\alpha_s C_F}{4\pi} \left[\frac{1}{\epsilon^2} + \frac{2}{\epsilon} \log \frac{\mu}{\bar{n}\cdot p_c} + \frac{5}{2\epsilon} + \log^2 \frac{-p_c^2}{\mu^2} - \frac{3}{2} \log \frac{-p_c^2}{\mu^2} - 2 \log \frac{-2v\cdot p_s}{\mu} \right. \\ &\quad \left. + 2 \log^2 \left(\frac{-2v\cdot p_s}{\mu} \right) - \log^2 \left(\frac{2v\cdot p_s \tilde{p}_c}{\mu^2} \right) + \frac{11}{2} - \frac{\pi^2}{4} \right] . \end{aligned} \tag{5.26}$$

This result still does not agree with the $\mathrm{SCET_I}$ expression in Eq. (5.19). However, the off-shellness in $\mathrm{SCET_{II}}$ satisfies $\tilde{p}_c \ll v\cdot p_s$. In this limit the $\mathrm{SCET_I}$ result in Eq. (5.19) agrees with the $\mathrm{SCET_{II}}$ result in Eq. (5.26).

5.3 Infrared regulators in SCET

5.3.1 Problems with known IR regulators

One of the most important properties of $\mathrm{SCET_I}$ is the field redefinition given in Eq. (5.4), which decouples the usoft from the collinear fermions. It is the crucial ingredient for proving factorization theorems. Furthermore, only after performing this field redefinition is it simple to match from $\mathrm{SCET_I}$ onto $\mathrm{SCET_{II}}$, since one can identify the Wilson line Y_n in $\mathrm{SCET_I}$ with the Wilson line S_n in $\mathrm{SCET_{II}}$. However, it is a well-known fact that field redefinitions only leave on-shell Green functions invariant [42]. Hence, the off-shellness of the collinear quark p_c^2 used to regulate the IR in $\mathrm{SCET_I}$ takes away our ability to perform this field redefinition. Since no field redefinition is performed on the heavy quark, one is free to give it an off-shellness.

IR divergences appear in individual diagrams, but they cancel in the set of diagrams contributing to a physical observable. More specifically, the IR divergences in virtual loop diagrams are cancelled against those in real emissions, which physically have to be included due to finite detector resolutions. From this it is obvious that the IR divergences in the

heavy-light current originate from regions of phase space where either the gluon three-momentum $|\mathbf{k}|$ or the angle θ between the gluon and the light fermion goes to zero. Other divergences arise if the three-momentum of the gluon goes to infinity or θ goes to π. These divergences are UV. To check if the IR divergences match between the two theories one has to use an IR regulator that regulates all IR divergences in both theories. To get insight into the behavior of the three-momentum and the angle, it will be instructive to perform the required loop integrals by integrating over k_0 using the method of residues, and then integrating over the magnitude of the three-momentum and the solid angle. This will allow us to identify clearly the IR divergences as described above. Let us illustrate this method by showing that all $1/\epsilon$ divergences in the $\mathrm{SCET_I}$ one-loop calculation of the previous section are UV. For the first diagram we find

$$\begin{aligned} A_{p_c}^{Ia} &= -ig^2 C_F \mu^{4-d} \int \frac{\mathrm{d}^d k}{(2\pi)^d} \frac{1}{[\tilde{p}_c - n\cdot k + i0][v\cdot(p_s - k) + i0][k^2 + i0]} \\ &= -\frac{g^2 C_F}{2} \frac{\Omega_{d-2}}{(2\pi)^{d-1}} \mu^{4-d} \int_0^\infty \mathrm{d}|\mathbf{k}| |\mathbf{k}|^{d-2} \\ &\quad \times \int_{-1}^1 \mathrm{d}\cos\theta \, \sin^{d-4}\theta \frac{1}{(|\mathbf{k}|(1-\cos\theta) - \tilde{p}_c)\,(|\mathbf{k}| - v\cdot p_s)|\mathbf{k}|} \,. \end{aligned} \tag{5.27}$$

Performing the remaining integrals, we of course reproduce the result obtained previously, but this form demonstrates that all divergences from regions $|\mathbf{k}| \to 0$ and $(1-\cos\theta) \to 0$ are regulated by the infrared regulators and thus all $1/\epsilon$ divergences are truly UV.

The second diagram is

$$\begin{aligned} A_{p_c}^{Ib} &= -2ig^2 C_F \mu^{4-d} \int \frac{\mathrm{d}^d k}{(2\pi)^d} \frac{\bar{n}\cdot(p_c - k)}{[-\bar{n}\cdot k + i0][(p_c - k)^2 + i0][k^2 + i0]} \\ &= -2ig^2 C_F \left[I_1 + I_2\right] , \end{aligned} \tag{5.28}$$

where I_1 and I_2 are the integrals with the $\bar{n}p$ and the $\bar{n}k$ terms in the numerator, respectively. The integral I_2 is standard and we find

$$I_2 = \frac{i}{16\pi^2} \left[\frac{1}{\epsilon} - \log\frac{-p_c^2}{\mu^2} + 2\right] , \tag{5.29}$$

where ϵ regulates only UV divergences. For the first integral we again perform the k_0

integral by contours and we find

$$
\begin{aligned}
I_1 &= \frac{i\bar{n}\cdot p_c}{2}\frac{\Omega_{d-2}}{(2\pi)^{d-1}}\mu^{4-d}\int_0^\infty \mathrm{d}|\mathbf{k}||\mathbf{k}|^{d-2}\int_{-1}^1 \mathrm{d}\cos\theta\,\sin^{d-4}\theta \\
&\quad\Bigg[-\frac{1}{\mathbf{k}^2(1+\cos\theta)[2|\mathbf{k}|(p_0-|\mathbf{p}|\cos\theta)-p_c^2]} \\
&\quad+\frac{1}{a[p_0+a+|\mathbf{k}|\cos\theta][2p_0^2+2p_0a-2|\mathbf{k}||\mathbf{p}|\cos\theta-p_c^2]}\Bigg]\,,
\end{aligned}
\tag{5.30}
$$

where

$$
p_c=(p_0,\mathbf{p})\,,\qquad a=\sqrt{\mathbf{k}^2+\mathbf{p}^2-2|\mathbf{k}||\mathbf{p}|\cos\theta}\,. \tag{5.31}
$$

From this expression we can again see that all IR singularities from $|\mathbf{k}|\to 0$ and $(1-\cos\theta)\to 0$ are regulated by the off-shellness, and all remaining divergences are UV. Note furthermore that in the limit $|\mathbf{k}|\to\infty$, with unrestricted θ, the two terms cancel each other, so that there is no usual UV divergence. This agrees with the fact that there are five powers of k in the denominator of the integrand in Eq. (5.28). However, in the limit $|\mathbf{k}|\to\infty$ with $|\mathbf{k}|(1+\cos\theta)\to 0$ the second term of Eq. (5.30) remains finite, whereas the first term develops a double divergence. Thus, it is this region of phase space that gives rise to the double pole in this diagram. The presence of the square roots makes the evaluation of the remaining integrals difficult, but we have checked that we reproduce the divergent terms of the result given in Eq. (5.18).

From the above discussion it follows that the off-shellness of the external fermions regulates all the IR divergences, and that the $1/\epsilon$ divergences all correspond to divergences of UV origin. The situation is different in $\mathrm{SCET_{II}}$, since the off-shellness of the light quark does not enter diagram (a). We find

$$
\begin{aligned}
A_{p_c}^{IIa} &= -ig^2C_F\mu^{4-d}\int\frac{\mathrm{d}^dk}{(2\pi)^d}\frac{1}{[-n\cdot k+i0][v\cdot(p_s-k)+i0][k^2+i0]} \\
&= -\frac{g^2C_F}{2}\frac{\Omega_{d-2}}{(2\pi)^{d-1}}\mu^{4-d}\int_0^\infty \mathrm{d}|\mathbf{k}||\mathbf{k}|^{d-2} \\
&\quad\times\int_{-1}^1 \mathrm{d}\cos\theta\,\sin^{d-4}\theta\frac{1}{\mathbf{k}^2(1-\cos\theta)(|\mathbf{k}|-v\cdot p_s)}\,.
\end{aligned}
\tag{5.32}
$$

The IR divergence originating from the limit $(1-\cos\theta)\to 0$ is not regulated by the off-shellness. Thus part of the $1/\epsilon$ divergences in Eq. (5.22) are of IR origin. In other words,

the fact that the terms logarithmic in the off-shellness in the $\mathrm{SCET_I}$ amplitude Eq. (5.19) are not reproducing the corresponding terms in the $\mathrm{SCET_{II}}$ amplitude Eq. (5.23) does not imply that the IR divergences do not match between the two theories. In order to check whether the IR divergences of the two theories match, one needs a regulator that regulates all IR divergences in both $\mathrm{SCET_I}$ and $\mathrm{SCET_{II}}$.

As an alternative IR regulator one could try to use a small gluon mass. Consider the first diagram in $\mathrm{SCET_I}$ again, this time with a gluon mass. We find

$$\begin{aligned} A_m^{Ia} &= -ig^2 C_F \mu^{4-d} \int \frac{\mathrm{d}^d k}{(2\pi)^d} \frac{1}{[-n\cdot k + i0][v\cdot(p_s-k)+i0][k^2-m^2+i0]} \\ &= -\frac{g^2 C_F}{2} \frac{\Omega_{d-2}}{(2\pi)^{d-1}} \mu^{4-d} \int_0^\infty \mathrm{d}|\mathbf{k}||\mathbf{k}|^{d-2} \\ &\quad \times \int_{-1}^1 \mathrm{d}\cos\theta \, \sin^{d-4}\theta \frac{1}{(\mathbf{k}^2+m^2-v\cdot p_s\sqrt{\mathbf{k}^2+m^2})(\sqrt{\mathbf{k}^2+m^2}-|\mathbf{k}|\cos\theta)} \,. \end{aligned} \tag{5.33}$$

Again, all divergences $|\mathbf{k}| \to 0$ and $(1-\cos\theta) \to 0$ are regulated by the gluon mass, but in the limit $|\mathbf{k}| \to \infty$ with $|\mathbf{k}|(1-\cos\theta) \to 0$ the integrand becomes

$$\frac{|\mathbf{k}|^{d-4} \sin^{d-4}\theta}{|\mathbf{k}|(1-\cos\theta)+\frac{m^2}{2|\mathbf{k}|}} \,, \tag{5.34}$$

so that the term that could potentially regulate the $(1-\cos\theta) \to 0$ divergence goes to zero as $|\mathbf{k}| \to \infty$. This is why a gluon mass cannot be used to regulate the IR of SCET.

5.3.2 A new regulator for SCET

The gluon mass is not an appropriate IR regulator for SCET because it appears in the combination $m^2/|\mathbf{k}|$ in the expression (5.34). Instead of using a gluon mass, consider adding the terms [2]

$$\begin{aligned} \mathcal{L}_{\mathrm{reg}}^{c} &= -\frac{\delta}{2} A_\mu^c \bar{\mathcal{P}} A_c^\mu \\ \mathcal{L}_{\mathrm{reg}}^{(u)s} &= -\frac{\delta}{2} A_\mu^{(u)s} i\bar{n}\cdot\partial A_{(u)s}^\mu \end{aligned} \tag{5.35}$$

[2] An alternative regulator has been introduced in Ref. [43]. In that paper a quark mass is used in conjunction with an "analytic" regulator, which regulates the $(1-\cos\theta) \to 0$ divergence. The conclusions about the soft-collinear mode in Ref. [40] are similar to the ones drawn here. However, we believe that a regulator such as the one introduced here is advantageous, since it can naturally be defined at the level of the Lagrangian, and a single dimensionful parameter regulates all IR divergences.

to the collinear and (u)soft gluon Lagrangians. Here, $\bar{\mathcal{P}}$ is the label operator that picks out the large momentum label of the collinear gluon field. Both of these terms are generated if a similar term is added to the full QCD gluon action before constructing SCET. Note that these terms preserve the invariance of the theory under the field redefinitions given in Eq. (5.4).

The infinitesimal, dimensionful parameter δ suffices to regulate all IR divergences in SCET, unlike the gluon mass. Following the same steps as in Eq. (5.33). We find

$$\begin{aligned} A_\delta^{Ia} &= -\frac{g^2 C_F}{2}\frac{\Omega_{d-2}}{(2\pi)^{d-1}}\mu^{4-d}\int_0^\infty \mathrm{d}|\mathbf{k}||\mathbf{k}|^{d-2} \\ &\quad \times \int_{-1}^{1}\mathrm{d}\cos\theta\, \sin^{d-4}\theta \frac{8}{b(\delta+b)(\delta+b-2|\mathbf{k}|\cos\theta)}\,, \end{aligned} \tag{5.36}$$

where

$$b = \sqrt{4\mathbf{k}^2+\delta^2+4|\mathbf{k}|\delta\cos\theta}\,. \tag{5.37}$$

Obviously, the parameter δ regulates the divergences $|\mathbf{k}| \to 0$ and $(1-\cos\theta) \to 0$, just as the gluon mass did. Expanding around the limit $|\mathbf{k}| \to \infty$ with $|\mathbf{k}|(1-\cos\theta) \to 0$ the integrand becomes

$$\frac{|\mathbf{k}|^{d-4}\sin^{d-4}\theta}{|\mathbf{k}|(1-\cos\theta)+\delta}\,, \tag{5.38}$$

and this IR region is therefore regulated as well. Even though δ is enough to regulate all IR divergences in SCET, we will keep the heavy quark off its mass-shell for later convenience.

Performing the integrals using the method above is difficult. While performing the k_0 integration using the method of residues gives insight into the divergence structure of the loop integrals, it is simpler to perform the integrals using the variables $n\cdot k$ and $\bar{n}\cdot k$ instead.

The first diagram in $\mathrm{SCET_I}$ with this new regulator is then given by

$$\begin{aligned} A_\delta^{Ia} &= -ig^2 C_F \mu^{4-d} \int \frac{\mathrm{d}^d k}{(2\pi)^d} \frac{1}{[-n\cdot k + i0][-v\cdot k + v\cdot p_s + i0][k^2 - \delta \bar{n}\cdot k + i0]} \\ &= -\frac{g^2 C_F}{2\pi} (4\pi)^{1-d/2} \Gamma\left(2 - \frac{d}{2}\right) \mu^{4-d} \int_\delta^\infty \mathrm{d}n\cdot k \; n\cdot k^{-1} \, (n\cdot k - \delta)^{d/2-2} \, (n\cdot k - 2v\cdot p_s)^{d/2-2} \\ &= \frac{\alpha_s C_F}{4\pi} \bigg[-\frac{1}{\epsilon^2} + \frac{2}{\epsilon} \log\frac{\delta}{\mu} - 2\log^2\frac{\delta}{\mu} + 2\log\left(1 - \frac{2v\cdot p_s}{\delta}\right) \log\frac{2v\cdot p_s}{\delta} \\ &\quad + 2\,\mathrm{Li}_2\left(1 - \frac{2v\cdot p_s}{\delta}\right) - \frac{3\pi^2}{4} \bigg] . \end{aligned} \tag{5.39}$$

Similarly, it is possible to show that the parameter δ regulates all IR divergences in the second diagram, for which we find

$$\begin{aligned} A_\delta^{Ib} &= -2ig^2 C_F \mu^{4-d} \int \frac{\mathrm{d}^d k}{(2\pi)^d} \frac{\bar{n}\cdot(p_c - k)}{[-\bar{n}\cdot k + i0][k^2 - 2k\cdot p_c + i0][k^2 - \delta \bar{n}\cdot k + i0]} \\ &= \frac{\alpha_s C_F}{4\pi} \left[\frac{2}{\epsilon^2} + \frac{2}{\epsilon} - \frac{2}{\epsilon} \log\frac{\delta\,\bar{n}\cdot p_c}{\mu^2} + \log^2\frac{\delta\,\bar{n}\cdot p_c}{\mu^2} - 2\log\frac{\delta\,\bar{n}\cdot p_c}{\mu^2} + 4 - \frac{\pi^2}{6} \right] . \end{aligned} \tag{5.40}$$

The mixed UV-IR divergences cancel in the sum of the two diagrams,

$$\begin{aligned} A_\delta^{I} &= \frac{\alpha_s C_F}{4\pi} \bigg[\frac{1}{\epsilon^2} + \frac{2}{\epsilon} \log\frac{\mu}{\bar{n}\cdot p_c} + \frac{5}{2\epsilon} + \log^2\frac{\delta \bar{n}\cdot p_c}{\mu^2} - 2\log^2\frac{\delta}{\mu} - \frac{3}{2}\log\frac{\delta \bar{n}\cdot p_c}{\mu^2} \\ &\quad - 2\log\frac{\delta - 2v\cdot p_s}{\mu} + 2\log\left(1 - \frac{2v\cdot p_s}{\delta}\right) \log\frac{2v\cdot p_s}{\delta} \\ &\quad + 2\mathrm{Li}_2\left(1 - \frac{2v\cdot p_s}{\delta}\right) + \frac{11}{2} - \frac{11\pi^2}{12} \bigg] , \end{aligned} \tag{5.41}$$

and one can show that this result agrees with full QCD.

Since the regulator is in the gluon action, it is the same for $\mathrm{SCET_I}$ and $\mathrm{SCET_{II}}$, and the two diagrams in $\mathrm{SCET_{II}}$ are identical to those in $\mathrm{SCET_I}$ since the integrands are exactly equal:

$$A_\delta^{II} = A_\delta^{I} . \tag{5.42}$$

Therefore, the IR divergences in $\mathrm{SCET_{II}}$ are exactly the same as those in $\mathrm{SCET_I}$.

While in $\mathrm{SCET_I}$ it is possible to choose the scaling $\delta \sim Q\lambda^2$ such that both the contributions to the collinear and the usoft gluon action are leading order in the power counting, the same is not true in $\mathrm{SCET_{II}}$. Choosing $\delta \sim Q\lambda^2$ to make the IR regulator leading order

in collinear gluon Lagrangian makes it suppressed by one power of λ in the soft Lagrangian. This can be understood physically, since in going from $\mathrm{SCET_I}$ to $\mathrm{SCET_{II}}$ the typical scaling of the (u)soft momenta remains of order Λ_{QCD}, while the off-shellness of the collinear particles is lowered. However, the IR divergence from $n\cdot k \to 0$ corresponds to $(1-\cos\theta)\to 0$, and the typical cutoff on $(1-\cos\theta)$ is set by the collinear scales. Since $n\cdot k_c \ll n\cdot k_s$ it is natural that any cutoff κ regulating the $n\cdot k_s \to 0$ divergence will satisfy $\kappa \ll n\cdot k_s$. This is not a problem, since the IR regulator does not introduce a new scale into the effective theory.

If one insists on keeping the scaling in the soft gluon Lagrangian manifest, one is forced to drop the regulator term. In this case, the diagram (a) in $\mathrm{SCET_{II}}$ no longer includes the IR regulator δ and is therefore not regulated properly. The calculation then reduces to the result given in Eq. (5.22). Part of the $1/\epsilon$ divergences in this result are from true UV divergences, but others are due to the unregulated $(1-\cos\theta)\to 0$ IR divergences, which arise from physics at the scale $n\cdot k \sim Q\lambda^2$. These IR divergences can be recovered by adding a diagram containing a gluon scaling as $n\cdot k \sim Q\lambda^2$, $\bar n\cdot k \sim Q\lambda$. Requiring $n\cdot k\,\bar n\cdot k \sim k_\perp^2$, this is the soft collinear messenger mode introduced in [40]. The resulting diagram (c) gives

$$\begin{aligned} A_\delta^{IIc} &= -2ig^2 C_F \mu^{4-d}\int\frac{\mathrm{d}^d k}{(2\pi)^d}\frac{1}{[-n\cdot k+i0][2v\cdot p_s-\bar n\cdot k+i0][k^2-\delta\bar n\cdot k+i0]} \\ &= \frac{\alpha_s C_F}{4\pi}\left[-\frac{2}{\epsilon^2}+\frac{2}{\epsilon}\log\frac{-2v\cdot p_s\,\delta}{\mu^2}-\log^2\frac{-2v\cdot p_s\,\delta}{\mu^2}-\frac{\pi^2}{2}\right]. \end{aligned} \tag{5.43}$$

Adding all the diagrams we find

$$\begin{aligned} A_\delta^{II} &= \frac{\alpha_s C_F}{4\pi}\left[\frac{1}{\epsilon^2}+\frac{2}{\epsilon}\log\frac{\mu}{\bar n\cdot p_c}+\frac{5}{2\epsilon}+\log^2\frac{\delta\bar n\cdot p_c}{\mu^2}-\frac{3}{2}\log\frac{\delta\bar n\cdot p_c}{\mu^2}-2\log\frac{-2v\cdot p_s}{\mu}\right. \\ &\qquad \left.+2\log^2\left(\frac{-2v\cdot p_s}{\mu}\right)-\log^2\left(\frac{-2v\cdot p_s\delta}{\mu^2}\right)+\frac{11}{2}-\frac{\pi^2}{4}\right], \end{aligned} \tag{5.44}$$

which again reproduces the $\mathrm{SCET_I}$ result for $\delta \ll v\cdot p_s$. From this discussion it follows that the presence of the soft collinear messenger mode depends on the precise implementation of the IR regulator in the theory. Since the definition of an effective theory should be independent of the regulator used for an explicit calculation, one can view the soft-collinear messenger mode as part of the IR regulator.

The term added to the gluon Lagrangian breaks gauge invariance. However, in this

regard it is on the same footing as a gluon mass. Since the coupling of gluons to fermions is via a conserved current, this breaking of gauge invariance is only a problem once gluon self-interactions are taken into account. For the renormalization of operators such as the heavy-light current considered in this chapter, this only arises at the two-loop level. In matching calculations, the IR divergences always cancel. Hence any IR regulator, including the one proposed here is applicable to matching calculations at any order in perturbation theory. More care has to be taken when using this regulator to calculate operator mixing, and in this case gauge noninvariant operators have to be included beyond one-loop order. However, all IR regulators proposed so far for SCET break gauge invariance. The main advantage of the new regulator is that it preserves invariance of $\mathrm{SCET_I}$ under the field redefinition given in Eq. (5.4).

5.4 Summary

We have considered the matching of the heavy-light current in $\mathrm{SCET_I}$ onto the corresponding current in $\mathrm{SCET_{II}}$, in particular addressing the question of whether all long distance physics in $\mathrm{SCET_I}$ is correctly reproduced in $\mathrm{SCET_{II}}$. Using the off-shellness of the external heavy and light fermions, it was argued in Ref. [40] that a new collinear–soft messenger mode is required in $\mathrm{SCET_{II}}$ to reproduce all the long distance physics of $\mathrm{SCET_I}$. Regulating the IR in $\mathrm{SCET_{II}}$ with an off-shellness is problematic, since the off-shellness prevents performing the field redefinition required to decouple the usoft gluons from the collinear particles, which allows the matching onto $\mathrm{SCET_{II}}$ easily. In this chapter we investigated the relationship between IR regulators and the definition of $\mathrm{SCET_{II}}$. By performing the k_0 loop integral by contours and then writing the remaining integrals as $\mathrm{d}|\mathbf{k}|\,\mathrm{d}\cos\theta$, we showed explicitly that the off-shellness leaves the IR angular divergence $(1-\cos\theta)\to 0$ unregulated in $\mathrm{SCET_{II}}$.

We then introduced a new regulator for SCET that regulates soft ($|\mathbf{k}|\to 0$) and collinear ($\cos\theta\to 1$) IR divergences in both $\mathrm{SCET_I}$ and $\mathrm{SCET_{II}}$. This regulator modifies the gluon action, much like a gluon mass, and thus preserves the field redefinition required to decouple usoft gluons from collinear particles in SCET. Using this regulator, we showed explicitly that $\mathrm{SCET_{II}}$ as formulated in Refs. [36, 38] reproduces all the IR divergences of $\mathrm{SCET_I}$. We also argued that any cutoff κ regulating the collinear divergence has to satisfy $\kappa \ll$

$n\cdot k_s$. Regulating $\mathrm{SCET_{II}}$ this way therefore naturally requires keeping a formally subleading regulator in the theory.

We also showed that a soft-collinear messenger mode is required in the definition of the IR regulator if one insists on power counting the regulator in the same way as kinetic terms in the action. In this case, there are unregulated IR divergences left in soft diagrams, which are corrected by additional contributions from the soft-collinear mode.

The new regulator introduced in this chapter preserves the invariance of $\mathrm{SCET_I}$ under the field redefinitions (5.4), and is therefore useful in studying factorization theorems beyond tree level.

Chapter 6

Summing logarithms in high-energy unstable heavy fermion pair production

This chapter discusses high-precision predictions for the top-antitop production cross section in electron-positron scattering at very high energies. Much of this material will appear in Ref. [44].

6.1 Introduction

The International Linear Collider (ILC) currently being planned will provide a wealth of precision top quark measurements. For example, a line-shape scan of the threshold top pair production cross section, $\sigma(e^+e^- \to \gamma^*, Z^* \to t\bar{t})$, should provide a measurement of the top mass with an uncertainty of only 100 MeV. It is also interesting to consider high-energy production of top pairs. This regime will also be explored at the ILC. In this limit there are three relevant and widely separated scales: the center-of-mass energy, $\sqrt{s}$; the mass, m; and the decay width, Γ. The large width prevents the top from hadronizing before it decays and thus acts as an infrared cutoff on the strong forces between the t and the $\bar{t}$. This fact allows one to calculate the production perturbatively. But these widely separated scales also lead to enhancements of the QCD corrections to the cross section in the form of logs that must be summed. It is this issue we address here.

Our approach consists of several steps. First the large scale $\sqrt{s}$ is integrated out by matching the production current onto the soft-collinear theory (SCET) [33, 34, 35, 36]. The next scale below $\sqrt{s}$ is m. This fixes the infrared scale so the heavy quark mass must

be retained in the effective theory [45]. Sudakov logarithms are summed by running the current in this theory down to the scale m. The heavy quark mass is integrated out at the scale m by matching onto heavy quark effective theory in a boosted frame (bHQET), where finite width effects are incorporated systematically [47]. The Wilson coefficients of the second matching step can then be run down to the final scale, Γ. This procedure sums all of the relevant logs, and the cross section can then be calculated in the bHQET to get the final resummed result.

6.2 QCD at one loop

The cross section $\sigma(e^+e^- \to \gamma^*, Z^* \to t\bar{t})$ to all orders in the QCD coupling can be written as

$$\begin{aligned} \sigma_0 &= \sum_X (2\pi)^4\, \delta^4(p_e + p_{\bar{e}} - p_X) \sum_{ij} L^{(ij)}_{\mu\nu} H^{\mu\nu}_{(ij)} \quad , \\ H^{\mu\nu}_{(ij)} &= \frac{1}{2}\Big(\langle 0|J_i^\mu(0)|X\rangle\langle X|J_j^\nu(0)|0\rangle + i \leftrightarrow j \Big) , \end{aligned} \tag{6.1}$$

where $L^{(ij)}_{\mu\nu}$ is the leptonic tensor containing leptonic traces and gauge boson propagators, and the state X contains a top quark/antiquark pair and any additional gluons. The sum over i and j is a sum over the different operator contributions of the photon and Z boson. The QCD current for top quark production appearing in the matrix elements above is

$$J_i^\mu = \bar{\psi}(x)\Gamma_i^\mu \psi(x) , \tag{6.2}$$

where $\Gamma_i^\mu = g_i^V \gamma^\mu + g_i^A \gamma^\mu \gamma_5$ involves the couplings of the top quark to the photon and the Z boson. In order to integrate out the hard scale of our process, we need to match this production current onto the appropriate current in SCET. We start by computing matrix elements of the current in QCD. The tree-level contribution and the one-loop correction are computed from the graphs in Fig. 6.1 plus the wave function graphs. These diagrams are both ultraviolet (UV) and infrared (IR) divergent despite the presence of a mass. We will regulate the UV divergences using dimensional regularization. The IR divergences are regulated by taking the external fermion to be off-shell $p^2 \neq m^2$. Taking $p^2 \gg m^2$ means the mass can be dropped from the calculation and the result is the same as for the massless

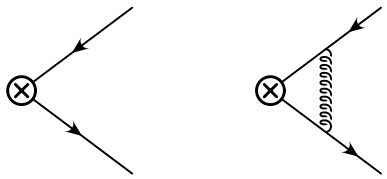

Figure 6.1: Tree-level current (a) and the one-loop correction (b) in QCD.

case regulated with an off-shellness. Also, in this limit the calculation is the same for γ_μ as for $\gamma_\mu\gamma_5$. We take this result from Ref. [48] (after correcting a few typographical errors):

$$\begin{aligned}\langle p1, p2|j^\mu|0\rangle &= \gamma^\mu\bigg[1 + C_F\frac{\alpha_s}{4\pi}\bigg(-\ln\frac{-s}{\mu^2} - 2\ln^2\frac{p^2}{s} \\ &\quad -4\ln\frac{p^2}{s} + \ln\frac{-p^2}{\mu^2} - 1 - \frac{2\pi^2}{3}\bigg)\bigg] + \text{c.t.}\,, \end{aligned} \tag{6.3}$$

where $p^2 \equiv p_1^2 = p_2^2$ and $s \equiv (p_1+p_2)^2$. This result includes the wave function contributions which cancel the poles of the vertex graph, and so the counterterm is zero here. This is because the vector current is conserved in QCD when the mass is taken to zero.

We now repeat the calculation but this time take the external fermions to be nearly on-shell with $\Delta^2 = p^2 - m^2 \approx 0$ to get

$$\begin{aligned}\langle p1, p2|j^\mu|0\rangle &= \gamma^\mu\bigg[1 + \frac{\alpha_s C_F}{4\pi}\bigg(2\ln^2\frac{-s}{m^2} - 4\ln\frac{-s}{m^2}\ln\frac{s}{\Delta^2} + 3\ln\frac{-s}{m^2} \\ &+ \quad 4\ln\frac{m^2}{-\Delta^2} - 4 + \frac{2\pi^2}{3}\bigg)\bigg]\,. \end{aligned} \tag{6.4}$$

Here we have not written the counterterm contribution since it is zero. This calculation is not strictly necessary for our analysis, but it will be a useful check of our results. For instance, this result confirms that SCET with a mass reproduces the full infrared of massive QCD. This will be demonstrated below when we include the mass in SCET.

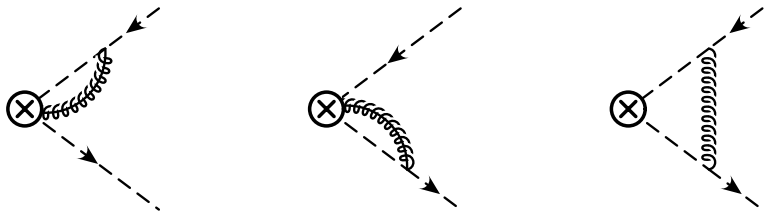

Figure 6.2: One-loop vertex correction in SCET.

6.3 $\mathrm{SCET_I}$ at one loop

Next we integrate out the scale $\sqrt{s}$ by matching onto SCET. The SCET current onto which J^μ matches is [46]

$$J^\mu_{\rm SCET} = C(\mu)\bar\xi_{n,p'} W_n(x)\gamma^\mu_\perp W^\dagger_{\bar n}\xi_{\bar n,p}(x)\,, \tag{6.5}$$

with tree-level matching coefficient

$$C(\sqrt{s}) = 1\,. \tag{6.6}$$

Other operators generated by keeping the quark mass finite are suppressed by $m/\sqrt{s}$. These operators will need to be resummed in the next step; however, they are not needed to match onto QCD and to sum leading logarithms.

The one-loop contributions of the SCET current can be calculated from the diagrams in Fig. 6.2. Note we must include the mass in the calculations [45]. The loop integrals are both UV and IR divergent. We do this calculation twice. In each case we regulate the UV in dimensional regularization, but use a different IR regularization scheme. To start we regulate the IR by taking the external fermions off-shell with $p^2 \gg m^2$. The result of the three diagrams including the wave function contributions is

$$\begin{aligned}\langle p1, p2|J^\mu_{\rm SCET}|0\rangle &= \frac{\alpha_s C_F}{4\pi}\gamma^\mu_\perp\left[\frac{2}{\epsilon^2}+\frac{3}{\epsilon}-\frac{2}{\epsilon}\ln\frac{-s}{\mu^2}\right.\\ &\left.+\ln^2\frac{-s}{\mu^2}-2\ln^2\frac{p^2}{s}-3\ln\frac{-p^2}{\mu^2}+7-\frac{5\pi^2}{6}\right]+\text{c.t.}\end{aligned} \tag{6.7}$$

The counterterm is

$$\text{c.t.} = -\frac{\alpha_s C_F}{4\pi}\left[\frac{2}{\epsilon^2}+\frac{3}{\epsilon}-\frac{2}{\epsilon}\ln\frac{-s}{\mu^2}\right], \tag{6.8}$$

and the one-loop matching coefficient is

$$C(\mu) = 1 + \frac{\alpha_s C_F}{4\pi}\left[3\ln\frac{-s}{\mu^2} - \ln^2\frac{-s}{\mu^2} - 8 + \frac{\pi^2}{6}\right]. \tag{6.9}$$

The counterterm gives the anomalous dimension for the effective theory current, which leads to the renormalization group equation

$$\begin{aligned} \mu\frac{dC(\mu)}{d\mu} &= \gamma_1(\mu)C(\mu)\,, \\ \gamma_1(\mu) &= -\frac{\alpha_s C_F}{4\pi}\left[4\ln\frac{\mu^2}{-s-i\epsilon} + 6\right]. \end{aligned} \tag{6.10}$$

The solution is straightforward:

$$\frac{C(\mu_0)}{C(\sqrt{s})} = \left(\frac{\alpha_s(\mu_0)}{\alpha_s}\right)^{(C_F/\beta_0)(3-2\pi i-8\pi/\beta_0\alpha_s)}\left(\frac{\mu_0^2}{s}\right)^{-2C_F/\beta_0}, \tag{6.11}$$

where $\alpha_s \equiv \alpha_s(\sqrt{s})$, $\beta_0 = 11C_A/3 - 2n_f/3$, and $C(\sqrt{s})$ is given in Eq. (6.6).

We now repeat the one-loop calculation above but this time take the external particles to be nearly on-shell: $\Delta^2 \equiv p^2 - m^2 \approx 0$. We do this for two reasons: first to show that $\mathrm{SCET_m}$ reproduces QCD with a mass, and second because it is a convenient way to calculate the $\mathrm{SCET_m}$ cross section.

The result of the one-loop vertex corrections is the sum of the collinear vertex corrections given in the first two graphs of Fig. 6.2

$$\begin{aligned} V_c &= \frac{\alpha_s C_F}{4\pi}\gamma_\perp^\mu\left[\frac{4}{\epsilon^2} + \frac{4}{\epsilon}\left(\ln\frac{\mu^2}{-\Delta^2} + 1\right) + 2\ln^2\frac{\mu^2}{-\Delta^2}\right. \\ &+ \left. 2\ln^2\frac{m^2}{-\Delta^2} + 4\ln\frac{\mu^2}{m^2} + 8 + \pi^2\right], \end{aligned} \tag{6.12}$$

and the ultrasoft (usoft) vertex correction

$$\begin{aligned} V_{us} &= \frac{\alpha_s C_F}{4\pi}\gamma_\perp^\mu\left[-\frac{2}{\epsilon^2} - \frac{2}{\epsilon}\ln\left(\frac{s\mu^2}{-\Delta^4}\right)\right. \\ &- \left. \ln^2\frac{s\mu^2}{-\Delta^4} - \frac{\pi^2}{2}\right], \end{aligned} \tag{6.13}$$

minus half the wave function renormalization graph for each fermion

$$I_w = \frac{\alpha_s C_F}{4\pi}\left(\frac{1}{\epsilon} + 4 + \ln\frac{\mu^2}{m^2} - 4\ln\frac{m^2}{-\Delta^2}\right). \tag{6.14}$$

The total is

$$\begin{aligned}\langle p1, p2|J^\mu_{\rm SCET}|0\rangle &= \frac{\alpha_s C_F}{4\pi}\gamma^\mu_\perp\bigg[\frac{2}{\epsilon^2} + \frac{3}{\epsilon} - \frac{2}{\epsilon}\ln\frac{-s}{\mu^2} \\ &\quad - \ln^2\frac{-s}{\mu^2} + 2\ln^2\frac{m^2}{\mu^2} + 4\ln\frac{-\Delta^2}{\mu^2}\ln\frac{-s}{m^2} \\ &\quad + \ln\frac{m^2}{\mu^2} - 4\ln\frac{-\Delta^2}{\mu^2} + 4 + \frac{\pi^2}{2}\bigg] + \text{c.t.}\end{aligned} \tag{6.15}$$

Note that the infrared logarithms in this result match those in QCD where all three scales have been kept. This is a check that SCET with a mass reproduces QCD with a mass and confirms the correctness of SCET_m .

6.4 SCET_I cross section

In the previous section, the hard scale was integrated out by matching the QCD current onto the SCET_I current of Eq. (6.5). We can now write the cross section in SCET_I as:

$$\begin{aligned}\sigma_1 &= \Big|C(Q,m)\Big|^2 \sum_{X_n X_{\bar n} X_s} (2\pi)^4\,\delta^4(q - P_{X_n} - P_{X_{\bar n}} - P_{X_s}) \sum_{ij} L^{(ij)}_{\mu\nu}\hat H^{\mu\nu}_{(ij)} \quad , \\ \hat H^{\mu\nu}_{(ij)} &= \frac{1}{2}\Big(\langle 0|\overline\chi_{n,Q}\hat\Gamma^\mu_i\chi_{\bar n,Q}(0)|X_n X_{\bar n} X_s\rangle\langle X_n X_{\bar n} X_s|\overline\chi_{\bar n,Q}\hat\Gamma^\nu_j\chi_{n,Q}(0)|0\rangle + i\leftrightarrow j\Big)\end{aligned} \tag{6.16}$$

The physics of the hard scale is contained in the Wilson coefficient $C(Q,m)$ obtained by current matching at the the hard scale Q followed by RG evolution down to the scale m, with the result in Eq. (6.11). This RG evolution of the hard Wilson coefficient sums logarithms of Q/m. Since the SCET_I current contains only collinear fields and the dynamics of the hadronic matrix elements are now determined by the SCET_I Lagrangian, the complete set of final states involve only usoft (X_s) and collinear (X_n and $X_{\bar n}$) degrees of freedom. Thus, matching the QCD current onto the SCET_I current automatically ensures the final states are restricted to pairs of collinear top quarks.

However, the sum over final states in Eq. (6.16) is still implicitly restricted by the invariant mass constraint. We are only interested in events that have two top-quark jets

each with invariant mass satisfying the constraint $P^2_{X_{n(\bar{n})}} - m^2 \sim m\Gamma \ll m^2$. In this section, this restriction will be made manifest. We will arrive at a cross section with an unrestricted sum over final states with the invariant mass constraints appearing as limits of integration over appropriately defined variables. The unrestricted sum over final states will allow us to use the optical theorem.

Furthermore the usoft-collinear decoupling property of the $\mathrm{SCET_I}$ Lagrangian will allow us to factorize the cross section so that the top quark and antiquark are decoupled from each other. This will be a crucial idea later on when we match the SCET cross section onto HQET in order to sum logarithms of m/Γ. Combining the usoft-collinear factorization and the optical theorem, the $\mathrm{SCET_I}$ cross section can be brought into a simple and transparent form.

6.4.1 Ultrasoft-collinear factorization

Even though we are dealing with an entirely perturbative process, the ideas of usoft-collinear factorization are crucial for correctly summing the large logarithms of m/Γ. In $\mathrm{SCET_I}$ the collinear top quark and antiquark interact with each other through the exchange of usoft gluons. In this section we use the well-known property of usoft-collinear decoupling of the leading-order $\mathrm{SCET_I}$ Lagrangian to decouple the top quark and antiquark from each other. Once this is done we are left with the picture of a massive top quark moving along at high speed oblivious to the existence of the antiquark moving in the opposite direction. The top quark moves in the $\vec{n}$ direction and the antiquark moves in the $\vec{\bar{n}}$ direction, each interacting with A_n and $A_{\bar{n}}$ collinear gluons, respectively. Once we add the constraint $P^2_{X_{n(\bar{n})}} - m^2 \sim m\Gamma \ll m^2$ to force the top quark and antiquark to remain close to their mass shell, the situation looks like two distinct copies of HQET in boosted frames. We will explore this idea in more detail in the next section.

To begin, recall that the leading-order $\mathrm{SCET_I}$ Lagrangian decouples into collinear and usoft parts,

$$\mathcal{L}^{(0)}_{SCET} = \mathcal{L}^{(0)}_{n} + \mathcal{L}^{(0)}_{\bar{n}} + \mathcal{L}^{(0)}_{s}, \tag{6.17}$$

after the field redefinitions

$$\begin{aligned} \xi_{n,\bar{n}}(x) &\to Y^\dagger_{n,\bar{n}}(x)\xi^{(0)}_{n,\bar{n}}(x)\,, \\ A^\mu_{n,\bar{n}}(x) &\to Y^\dagger_{n,\bar{n}}(x)A^{(0)\mu}_{n,\bar{n}}(x)Y_{n,\bar{n}}(x)\,, \end{aligned} \tag{6.18}$$

where the Wilson lines are defined as

$$Y_n(x) = \mathrm{P}\,\mathrm{Exp}\left(\int_{-\infty}^{0} ds\, n\cdot A(ns+x)\right)\,, \quad Y_{\bar{n}}(x) = \mathrm{P}\,\mathrm{Exp}\left(\int_{-\infty}^{0} ds\, \bar{n}\cdot A(\bar{n}s+x)\right). \tag{6.19}$$

Since the top quark mass scales as $m \sim Q\lambda$, the leading-order collinear Lagrangian terms $\mathcal{L}^{(0)}_n$ and $\mathcal{L}^{(0)}_{\bar{n}}$ include the necessary mass terms [45] for the top quark and antiquark, respectively.

In the usoft-collinear decoupling we need to be careful how the final state $\langle X_n X_{\bar{n}} X_s|$ is treated [49]. In particular if we choose the canonical approach of Eqs. (6.18) and (6.19) we must introduce a usoft Wilson line that extends from $+\infty$ to $-\infty$ for each collinear direction in the final state. As a result the $Y_{n,\bar{n}}(x)$ from the field redefinition are turned into

$$\tilde{Y}_n(x) = \mathrm{P}\,\mathrm{Exp}\left(\int_{0}^{\infty} ds\, n\cdot A(ns+x)\right)\,, \quad \tilde{Y}_{\bar{n}}(x) = \mathrm{P}\,\mathrm{Exp}\left(\int_{0}^{\infty} ds\, \bar{n}\cdot A(\bar{n}s+x)\right). \tag{6.20}$$

The hadronic matrix elements now factorize as

$$\begin{aligned} \langle X_n X_{\bar{n}} X_s|\overline{\chi}_{\bar{n},Q}\hat{\Gamma}^\nu_j \chi_{n,Q}(0)|0\rangle &\to \langle X_n X_{\bar{n}} X_s|\overline{\chi}_{\bar{n},Q}{}^{(0)}\tilde{Y}^\dagger_{\bar{n}}\hat{\Gamma}^\nu_j\tilde{Y}_n\chi_{n,Q}{}^{(0)}(0)|0\rangle \\ &\to \langle X_s|\tilde{Y}^\dagger_n\tilde{Y}_{\bar{n}}(0)|0\rangle\langle X_{\bar{n}}|\overline{\chi}^{(0)}_{\bar{n},Q}(0)|0\rangle\langle X_n|\chi^{(0)}_{n,Q}(0)|0\rangle\,\hat{\Gamma}^\nu_j\,, \end{aligned} \tag{6.21}$$

where we have suppressed Dirac indices for clarity. From now on we will drop the (0) superscript. The factorized $\mathrm{SCET_I}$ cross section takes the form

$$\begin{aligned} \sigma_1 &= \Big|C(Q,m)\Big|^2 \sum_{X_n X_{\bar{n}} X_s} (2\pi)^4\,\delta^4(q - P_{X_n} - P_{X_{\bar{n}}} - P_{X_s})\langle 0|\tilde{Y}^\dagger_{\bar{n}}\tilde{Y}_n(0)|X_s\rangle\langle X_s|\tilde{Y}^\dagger_n\tilde{Y}_{\bar{n}}(0)|0\rangle \\ &\times \sum_{ij} L^{(ij)}_{\mu\nu}\frac{1}{2}\Big(\langle 0|\overline{\chi}_{n,Q}(0)|X_n\rangle\langle X_n|\chi_{n,Q}(0)|0\rangle\langle 0|\chi_{\bar{n},Q}(0)|X_{\bar{n}}\rangle\langle X_{\bar{n}}|\overline{\chi}_{\bar{n},Q}(0)|0\rangle\hat{\Gamma}^\mu_i\hat{\Gamma}^\nu_j + i\leftrightarrow j\Big)\,. \end{aligned} \tag{6.22}$$

6.4.2 Final state invariant mass constraints

So far we have managed to restrict the final states to include only usoft and collinear degrees of freedom by matching the QCD production currents onto $\mathrm{SCET_I}$ currents. This has ensured that the final states correspond to high-energy top pairs produced at $\sqrt{s} \gg m$. However we would like to be more restrictive and require that the two top jets have invariant masses close to the top mass (i.e., require that the tops be nearly on-shell):

$$P^2_{X_{n(\bar{n})}} - m^2 \sim m\Gamma \ll m^2. \tag{6.23}$$

This constraint implies an implicit restriction over the sum of final states X_n, $X_{\bar{n}}$, and X_s in Eq. (6.22). In this section we will make this constraint manifest. We will follow a series of steps that allow us to express the cross section as an unrestricted sum over final states, allowing us to exploit the optical theorem, with the invariant mass constraints appearing as limits of integration over appropriately defined variables.

First we insert the identity operator

$$1 = \int d^4p_n \, d^4p_{\bar{n}} \, d^4p_s \, \delta^4(p_n - P_{X_n}) \, \delta^4(p_{\bar{n}} - P_{X_{\bar{n}}}) \, \delta^4(p_s - P_{X_s}) \, . \tag{6.24}$$

We can now restrict the final state jet momenta P_{X_n}, $P_{X_{\bar{n}}}$, and P_{x_s} by applying constraints on the momentum variables p_n, $p_{\bar{n}}$, and p_s. Next we decompose the momenta into label and residual parts:

$$\begin{aligned} p_n &= \tilde{p}_n + k_n, \qquad & p_{\bar{n}} &= \tilde{p}_{\bar{n}} + k_{\bar{n}}, \qquad & p_s &= k_s, \\ P_{X_n} &= \tilde{P}_{X_n} + k_{X_n}, \qquad & P_{X_{\bar{n}}} &= \tilde{P}_{X_{\bar{n}}} + k_{X_{\bar{n}}}, \qquad & P_{X_s} &= k_{X_s}, \end{aligned} \tag{6.25}$$

and likewise decompose delta functions into Kronecker deltas of the labels and integrals over position of exponentials of the residual momentum:

$$\delta^4(p - P_X) = \delta^4_{\tilde{p},\tilde{P_X}} \, \delta^4(k - K_X) = \delta^4_{\tilde{p},\tilde{P_X}} \int \frac{d^4x}{(2\pi)^4} \, e^{i\,(k-K_X)\,\cdot\,x} \, . \tag{6.26}$$

Using Eqs. (6.24), (6.25), and (6.26) in the cross-section formula in Eq. (6.22), the $\mathrm{SCET_I}$ cross

section takes the form

$$\begin{aligned}
\sigma_1 &= \int d^4p_n \int d^4p_{\bar{n}} \int d^4p_s\,(2\pi)^4\delta^4(q-p_n-p_{\bar{n}}-p_s) \sum_{X_nX_{\bar{n}}X_s} \int d^4x\,d^4y\,d^4z \left|C(Q,m)\right|^2 \\
&\times \delta_{\tilde{p}_n,\tilde{P}_{X_n}}\delta_{\tilde{p}_{\bar{n}},\tilde{P}_{X_{\bar{n}}}} e^{i(k_n-K_{X_n})\cdot x} e^{i(k_{\bar{n}}-K_{X_n})\cdot y} e^{i(k_s-K_s)\cdot z} \langle 0|\tilde{Y}_{\bar{n}}^\dagger \tilde{Y}_n(0)|X_s\rangle\langle X_s|\tilde{Y}_n^\dagger\tilde{Y}_{\bar{n}}(0)|0\rangle \quad (6.27) \\
&\times \sum_{ij} L_{\mu\nu}^{(ij)} \frac{1}{2}\Big(\langle 0|\overline{\chi}_{n,Q}(0)|X_n\rangle\langle X_n|\chi_{n,Q}(0)|0\rangle\langle 0|\chi_{\bar{n},Q}(0)|X_{\bar{n}}\rangle\langle X_{\bar{n}}|\overline{\chi}_{\bar{n},Q}(0)|0\rangle \hat{\Gamma}_i^\mu\hat{\Gamma}_j^\nu + i\leftrightarrow j\Big).
\end{aligned}$$

Note there is a sum over label momenta and an integral over residual momenta contained in the integrals over p_n, $p_{\bar{n}}$, and p_s. We will make this explicit at a later stage. We use label momentum conservation to replace the collinear jet momenta labels $\tilde{P}_{X_{n,\bar{n}}}$ in the Kronecker deltas with the label Q of the collinear fields. Furthermore, we pull the exponentials of the residual momenta k_{X_n}, $k_{X_{\bar{n}}}$, and k_{X_s} into the respective matrix elements and translate the fields in position space to get

$$\begin{aligned}
\sigma_1 &= \int d^4p_n \int d^4p_{\bar{n}} \int d^4p_s\,(2\pi)^4\delta^4(q-p_n-p_{\bar{n}}-p_s) \sum_{X_nX_{\bar{n}}X_s} \int d^4x\,d^4y\,d^4z \\
&\times \left|C(Q,m)\right|^2 e^{ik_n\cdot x} e^{ik_{\bar{n}}\cdot y} e^{ik_s\cdot z} \delta_{\tilde{p}_n,Q}\delta_{\tilde{p}_{\bar{n}},Q} \langle 0|\tilde{Y}_{\bar{n}}^\dagger \tilde{Y}_n(z)|X_s\rangle\langle X_s|\tilde{Y}_n^\dagger\tilde{Y}_{\bar{n}}(0)|0\rangle \quad (6.28) \\
&\times \sum_{ij} L_{\mu\nu}^{(ij)} \frac{1}{2}\Big(\langle 0|\overline{\chi}_{n,Q}(x)|X_n\rangle\langle X_n|\chi_{n,Q}(0)|0\rangle\langle 0|\chi_{\bar{n},Q}(y)|X_{\bar{n}}\rangle\langle X_{\bar{n}}|\overline{\chi}_{\bar{n},Q}(0)|0\rangle \hat{\Gamma}_i^\mu\hat{\Gamma}_j^\nu + i\leftrightarrow j\Big).
\end{aligned}$$

At this point there is no longer an explicit dependence on the final state jet momenta. However, we can restrict the final state jet momenta by applying constraints to the momentum variables p_n, $p_{\bar{n}}$, and p_s introduced in Eq. (6.24). We make explicit the invariant mass condition of Eq. (6.23) in the collinear sectors by inserting the identity operator

$$1 = \int ds_n \delta(p_n^2 - m^2 - s_n) \int ds_{\bar{n}} \delta(p_{\bar{n}}^2 - m^2 - s_{\bar{n}}) \tag{6.29}$$

and restricting the range of integration for the variables s_n and $s_{\bar{n}}$ to

$$-m\Gamma \lesssim s_n, s_{\bar{n}} \lesssim m\Gamma. \tag{6.30}$$

This forces the final collinear states X_n and $X_{\bar{n}}$ to have the appropriate invariant mass for the system we are considering. In this manner we have expressed the invariant mass constraint on the top jets by imposing limits on the range of integration of the variables

s_n and $s_{\bar{n}}$. In the end we will have a differential cross section in these variables, and our expression for it will only be valid in the range specified in Eq. (6.30).

6.4.3 Specifying jet momenta and $\mathrm{SCET_I}$ jet functions

Next we need to define the jet momenta relative to an appropriate coordinate system. As before, we can do this by specifying the momentum components of the variables p_n, $p_{\bar{n}}$, and p_s because of Eq. (6.24). It is convenient to align one of the collinear momenta with the vector $\vec{n} = (0, 0, -1)$ [50]. If we choose to do this for p_n, we must have $\tilde{p}_n^\perp = k_n^\perp = 0$. Since $p_n^2 - m^2 = s_n$, there is no other constraint and we get

$$\begin{aligned} p_n^- &= Q + k_n^-, \qquad p_n^\perp = 0, \qquad p_n^+ = k_n^+ , \\ p_{\bar{n}}^+ &= Q + k_{\bar{n}}^+, \quad p_{\bar{n}}^\perp = \tilde{p}_{\bar{n}}^\perp + k_{\bar{n}}^\perp, \quad p_{\bar{n}}^- = k_{\bar{n}}^- , \\ p_s^- &= k_s^-, \qquad p_s^\perp = k_s^\perp, \qquad p_s^+ = k_s^+ . \end{aligned} \tag{6.31}$$

The $\mathrm{SCET_I}$ power counting for the residual momenta is $k_n \sim k_{\bar{n}} \sim k_s \sim Q\lambda^2 \sim m^2/Q$, which allows us to write

$$\delta^4(q - p_n - p_{\bar{n}} - p_s) = 2\delta_{Q,\tilde{p}_n^-}\delta_{Q,\tilde{p}_{\bar{n}}^+}\delta^2_{0,\tilde{p}_{\bar{n}}^\perp}\delta(k_n^- + k_{\bar{n}}^- + k_s^-)\delta(k_n^+ + k_{\bar{n}}^+ + k_s^+)\delta^2(k_{\bar{n}}^\perp + k_s^\perp). \tag{6.32}$$

Furthermore, with the coordinate choice in Eq. (6.31), the phase space integrals are decomposed into sums over label momenta and integrals over residual momenta just as in Ref. [50]:

$$\int d^4p_n \int d^4p_{\bar{n}} \int d^4p_s \to \frac{1}{2}\sum_{\tilde{p}_n^-} \int dk_n^+ dk_n^- \, \frac{1}{2}\sum_{\tilde{p}_{\bar{n}}} \int dk_{\bar{n}}^+ dk_{\bar{n}}^- d^2k_{\bar{n}}^\perp \int d^4k_s. \tag{6.33}$$

Using Eqs. (6.29), (6.31), (6.32) and (6.33) in the cross-section formula in Eq. (6.28), we obtain

$$\begin{aligned}
\sigma_1 &= (2\pi)^4 \sum_{X_n X_{\bar n} X_s} \int ds_n\, ds_{\bar n} \int d^4k_s (2\pi)^4 \int d^4x\, d^4y\, d^4z\, e^{ik_s\cdot z} \langle 0|\tilde{Y}_{\bar n}^\dagger \tilde{Y}_n(z)|X_s\rangle\langle X_s|\tilde{Y}_n^\dagger \tilde{Y}_{\bar n}(0)|0\rangle \\
&\times \quad \Big|C(Q,m)\Big|^2 \,\mathrm{Exp}\Big(\frac{-i}{2}\{k_s^- + \frac{s_{\bar n}+m^2}{Q}\}x^+ + \frac{i}{2}\frac{s_n+m^2}{Q}x^-\Big) \\
&\times \quad \mathrm{Exp}\Big(\frac{-i}{2}\{k_s^+ + \frac{m^2+s_n}{Q}\}y^- + \frac{i}{2}\frac{s_{\bar n}+m^2}{Q}y^+ - ik_{s\perp}\cdot y_\perp\Big) \qquad (6.34) \\
&\times \quad \sum_{ij} L_{\mu\nu}^{(ij)} \frac{1}{2}\Big(\langle 0|\overline{\chi}_{n,Q}(x)|X_n\rangle\langle X_n|\chi_{n,Q}(0)|0\rangle\langle 0|\overline{\chi}_{\bar n,Q}(y)|X_{\bar n}\rangle\langle X_{\bar n}|\chi_{\bar n,Q}(0)|0\rangle \hat\Gamma_i^\mu \hat\Gamma_j^\nu + i\leftrightarrow j\Big)\,.
\end{aligned}$$

Note the sum over final states is now unrestricted, with all final state constraints appearing implicitly as limits over the s_n and $s_{\bar n}$ variables. Next we define jet functions

$$\begin{aligned}
\sum_{X_n}\langle 0|\overline{\chi}_{n,Q}(x)|X_n\rangle\langle X_n|\chi_{n,Q}(0)|0\rangle &= i\int \frac{d^4r_n}{(2\pi)^4} e^{-ir_n\cdot x} J_{n,Q}(r_n^+)\frac{\not n}{2} \\
&= i\delta(x^+)\delta^2(x_\perp)\frac{\not n}{2}\int \frac{dr_n^+}{2\pi} e^{-\frac{i}{2}r_n^+\cdot x^-} J_{n,Q}(r_n^+)\,, \\
\sum_{X_{\bar n}}\langle 0|\overline{\chi}_{\bar n,Q}(y)|X_{\bar n}\rangle\langle X_{\bar n}|\chi_{\bar n,Q}(0)|0\rangle &= i\int \frac{d^4r_{\bar n}}{(2\pi)^4} e^{-ir_{\bar n}\cdot y} J_{\bar n,Q}(r_{\bar n}^-)\frac{\bar{\not n}}{2} \\
&= i\delta(y^-)\delta^2(y_\perp)\frac{\bar{\not n}}{2}\int \frac{dr_{\bar n}^-}{2\pi} e^{-\frac{i}{2}r_{\bar n}^-\cdot y^+} J_{\bar n,Q}(r_{\bar n}^-)\,. \qquad (6.35)
\end{aligned}$$

Since the sums over final states are no longer restricted and are therefore complete, the jet functions are related to the discontinuity of the forward amplitude across the real axis:

$$\begin{aligned}
J_{n,Q}(r_n^+) &= \frac{\bar{\not n}}{4}\sum_{X_n}\int d^4x\, e^{ir_n\cdot x}\langle 0|\overline{\chi}_{n,Q}(x)|X_n\rangle\langle X_n|\chi_{n,Q}(0)|0\rangle \\
&= \int d^4x\, e^{ir_n\cdot x}\,\mathrm{Disc}\,\langle 0|\mathrm{T}\{\overline{\chi}_{n,Q}(x)\frac{\bar{\not n}}{4}\chi_{n,Q}(0)\}|0\rangle\,, \\
J_{\bar n,Q}(r_{\bar n}^-) &= \frac{\not n}{4}\sum_{X_{\bar n}}\int d^4x\, e^{ir_{\bar n}\cdot x}\langle 0|\overline{\chi}_{\bar n,Q}(y)|X_{\bar n}\rangle\langle X_{\bar n}|\chi_{\bar n,Q}(0)|0\rangle \\
&= \int d^4x\, e^{ir_{\bar n}\cdot x}\,\mathrm{Disc}\,\langle 0|\mathrm{T}\{\overline{\chi}_{\bar n,Q}(x)\frac{\not n}{4}\chi_{\bar n,Q}(0)\}|0\rangle\,. \qquad (6.36)
\end{aligned}$$

Substituting these expressions into Eq. (6.34) gives

$$\sigma_1 = \frac{1}{2}\Big(\mathrm{Tr}\Big[\frac{\not n}{2}\hat\Gamma_i^\mu\frac{\bar{\not n}}{2}\hat\Gamma_j^\nu\Big] + i\leftrightarrow j\Big)\frac{1}{2}\Big|C(Q,m)\Big|^2\int ds_n\, ds_{\bar n} J_{n,Q}(s_n+m^2)J_{\bar n,Q}(s_{\bar n}+m^2)\,, \qquad (6.37)$$

where we have used

$$\begin{aligned}
&\int \frac{d^4k_s}{(2\pi)^4} \int d^4z\, e^{ik_s\cdot z} \sum_{X_s} \langle 0|\tilde{Y}_{\bar{n}}^\dagger \tilde{Y}_n(z)|X_s\rangle\langle X_s|\tilde{Y}_n^\dagger \tilde{Y}_{\bar{n}}(0)|0\rangle \\
&= \int \frac{d^4k_s}{(2\pi)^4} \int d^4z\, e^{ik_s\cdot z} \langle 0|\tilde{Y}_{\bar{n}}^\dagger \tilde{Y}_n(z)\tilde{Y}_n^\dagger \tilde{Y}_{\bar{n}}(0)|0\rangle \\
&= \int d^4z\, \delta^{(4)}(z) \langle 0|\tilde{Y}_{\bar{n}}^\dagger \tilde{Y}_n(z)\tilde{Y}_n^\dagger \tilde{Y}_{\bar{n}}(0)|0\rangle \\
&= \langle 0|\tilde{Y}_{\bar{n}}^\dagger \tilde{Y}_n(0)\tilde{Y}_n^\dagger \tilde{Y}_{\bar{n}}(0)|0\rangle \\
&= 1\,. \qquad (6.38)
\end{aligned}$$

The $\mathrm{SCET_I}$ cross section in Eq. (6.37) is the main result of this section. It is given in terms of two decoupled jet functions, J_n and $J_{\bar{n}}$, describing the dynamics of the top quark and antiquark moving in the $\vec{n}$ and $\vec{\bar{n}}$ directions, respectively. As mentioned before and to be described in detail later, each of these jet functions will be matched onto a distinct copy of HQET in a boosted frame.

6.4.4 Computing $\mathrm{SCET_I}$ jet functions

The jet functions J_n and $J_{\bar{n}}$, defined in Eq. (6.36) and appearing in the $\mathrm{SCET_I}$ cross section in Eq. (6.37), can be calculated perturbatively in the strong coupling $\alpha_s(m)$. In this section we give the tree-level and one-loop expressions for the jet functions. It is convenient to work with the dimensionless variables y_n and $y_{\bar{n}}$ defined as

$$1 - y_n = \frac{s_n}{m^2}, \quad 1 - y_{\bar{n}} = \frac{s_{\bar{n}}}{m^2}. \qquad (6.39)$$

From Eq. (6.36), the tree-level jet funtions are simply given by the discontinuity of the collinear propagator:

$$J^{\mathrm{tree}}_{(n,\bar{n}),Q}(y,\mu) \;=\; 2\pi \frac{Q}{m^2}\delta(1-y). \qquad (6.40)$$

At one loop, the jet functions are given by the discontiniuities of the diagrams shown in Fig. 6.3. The result is the collinear quark propagator times V_c given in Eq. (6.12) plus the

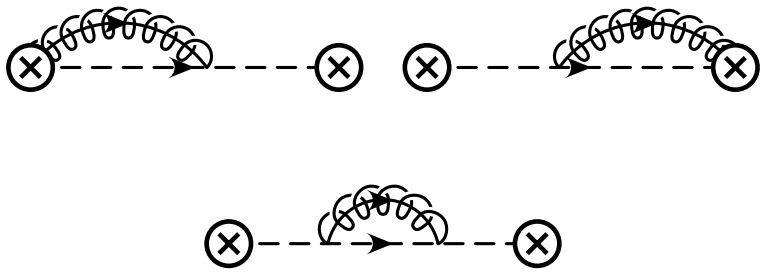

Figure 6.3: Forward scattering amplitudes.

collinear quark propagator times I_w given in Eq. (6.14).

$$\begin{aligned}\delta J_{(n,\bar{n}),Q}(y,\mu) &= 2\pi\frac{Q}{m^2}\frac{\alpha_s C_F}{4\pi}\bigg[8\bigg(\frac{\ln(1-y)}{1-y}\bigg)_+ + \bigg(-\frac{4}{\epsilon}+4\ln\frac{m^2}{\mu^2}+4\bigg)\frac{1}{(1-y)_+} \\ &+ \bigg(\frac{4}{\epsilon^2}+\frac{5}{\epsilon}-\frac{4}{\epsilon}\ln\frac{m^2}{\mu^2}+2\ln^2\frac{m^2}{\mu^2}-\ln\frac{m^2}{\mu^2}+12-\frac{\pi^2}{3}\bigg)\delta(1-y)\bigg] \qquad (6.41)\end{aligned}$$

It should be understood that in computing the cross section in $\mathrm{SCET_I}$, the right-hand side of Eq. (6.41) must be evaluated at $\mu = m$ for the cross section to be scale invariant. This is because we ran the $\mathrm{SCET_I}$ operator J^{μ}_{SCET} in Eq. (6.5) between the scales Q and m before factorizing the cross section into soft and collinear sectors. However, we keep the μ dependence explicit for the purposes of matching onto HQET, the effective theory below m, in the next section. The need for this matching is now apparent from Eq. (6.41) which involves large logarithms of $1 - y_{n,\bar{n}} = s_{n,\bar{n}}/m^2 \sim \Gamma/m$. These large logarithms of the width will be summed by the RG running of the corresponding HQET jet functions after the matching is performed.

In arriving at Eqs. (6.40) and (6.41), we made use of the well-known identities

$$\begin{aligned}\mathrm{Disc}\frac{i}{2\pi}\frac{1}{1-y+i\epsilon} &= \delta(1-y), \\ \mathrm{Disc}\frac{i}{2\pi}\frac{\ln(y-1-i\epsilon)}{1-y+i\epsilon}\theta(y) &= \frac{1}{(1-y)_+}, \\ \mathrm{Disc}\frac{i}{2\pi}\frac{\ln^2(y-1-i\epsilon)}{1-y+i\epsilon}\theta(y) &= -\frac{\pi^2}{3}\delta(1-y)+\Big[\frac{2\ln(1-y)}{1-y}\Big]_+. \qquad (6.42)\end{aligned}$$

In the calculation of the jet functions we were able to insert by hand the necessary step functions $\theta(y)$ appearing on the LHS of the last two identities by noting from Eq. (6.39) that the variables y_n and $y_{\bar{n}}$ must be greater than zero. This is evident from the phase space

restrictions $|s_n/m^2|, |s_{\bar{n}}/m^2| \sim \Gamma/m \ll 1$. Furthermore, there exists an implicit upper bound $y_n, y_{\bar{n}} \leq 1$ in the identities above. This follows from the fact that for $y_n, y_{\bar{n}} > 1$, the discontinuities are trivially zero. There is no contribution to the cross section from this region of phase space. The relevant region of phase space can now be characterized in terms of the range of the dimensionless variables y_n and $y_{\bar{n}}$ as

$$1 - \frac{\Gamma}{m} \leq \ y_{n,\bar{n}} \ \leq 1. \tag{6.43}$$

It is convenient to introduce the dimensionless jet functions $K_{(n,\bar{n})}$ defined as

$$K_{(n,\bar{n})}(y,\mu) = \frac{m^2}{Q}\, J_{(n,\bar{n}),Q}(y,\mu). \tag{6.44}$$

In terms of these dimensionless variables, the $\mathrm{SCET_I}$ cross section takes the form

$$\hat{\sigma} \ = \ \frac{1}{2}\Big(\mathrm{Tr}\Big[\frac{\bar{n}\!\!\!/}{2}\hat{\Gamma}_i^\mu \frac{n\!\!\!/}{2}\hat{\Gamma}_j^\nu\Big] + i \leftrightarrow j\Big)\big|C(Q,\mu)\big|^2\, Q^2 \int dy_n\, dy_{\bar{n}} K_n(y_n,\mu) K_{\bar{n}}(y_{\bar{n}},\mu)\,, \tag{6.45}$$

where the range of integration is restricted as shown in Eq. (6.43) and we have kept the scale dependence of the hard Wilson coefficient and the jet functions manifest.

6.5 Boosted HQET

Using factorization in $\mathrm{SCET_I}$, we have decoupled the top quark and antiquark and can now treat them separately. Our goal is to describe the production of heavy unstable fermions experiencing small momentum fluctuations about their mass shell of order their decay width. We quantify this condition by requiring that the top quark and antiquark each satisfy

$$p^2 - m^2 \sim m\Gamma \ll m^2. \tag{6.46}$$

This invariant mass constraint is identical to that on the virtuality of a heavy quark of mass m described in HQET:

$$p^2 - m^2 \sim 2mv \cdot k \ll m^2, \tag{6.47}$$

where the heavy quark momentum is decomposed according to

$$p^\mu = m v^\mu + k^\mu. \tag{6.48}$$

HQET is usually applied in the context of bottom and charm hadrons ($m = m_b, m_c$) and $k \sim v \cdot k \sim \Lambda_{QCD}$ corresponding to the typical momentum of soft gluons in a hadron of size $1/\Lambda_{QCD}$. The theory and its predictions are then formulated as an expansion in powers of $\Lambda_{QCD}/m_{b,c}$.

Our situation is similar with the identification $\Lambda_{QCD} \to \Gamma$. In addition, we are in a frame in which the quarks are highly boosted. In the rest frame of the top quarks, the soft gluons of HQET have the scaling $k^\mu \sim (\Gamma, \Gamma, \Gamma)$. In the boosted frame the soft gluons acquire a collinear momentum scaling. Similarly, the velocity labels of the top quarks are also boosted. Thus, after the scale m is integrated out, the decoupled evolution of the top quark and antiquark is given by two distinct copies of boosted HQET in the $\vec{n}$ and $\vec{\bar{n}}$ directions, respectively:

$$\begin{aligned} v_n^\mu &= \left(\frac{m}{Q}, \frac{Q}{m}, \mathbf{0}_\perp\right), \quad k_n^\mu \sim \Gamma\left(\frac{m}{Q}, \frac{Q}{m}, \mathbf{1}_\perp\right), \\ v_{\bar{n}}^\mu &= \left(\frac{Q}{m}, \frac{m}{Q}, \mathbf{0}_\perp\right), \quad k_{\bar{n}}^\mu \sim \Gamma\left(\frac{Q}{m}, \frac{m}{Q}, \mathbf{1}_\perp\right). \end{aligned} \tag{6.49}$$

This picture suggests matching the $\mathrm{SCET_I}$ jet functions $K_{n,\bar{n}}(y_n, \mu)$ onto the corresponding boosted HQET jet functions $J_{v_n, v_{\bar{n}}}$.

The HQET cross section is given by Eq. (6.45) after matching the $\mathrm{SCET_I}$ jet functions $K_{n,\bar{n}}(y_n, \mu)$ onto the corresponding jet functions in boosted HQET. The jet functions in boosted HQET are given by

$$\begin{aligned} J_{v_n}(r_n^2) &= \int d^4x\, e^{i r_n \cdot x}\, \mathrm{Disc}\, \langle 0 | T\{\bar{h}_{v_n}(x) W_n(x) W_n^\dagger(0) h_{v_n}(0)\} | 0 \rangle\,, \\ J_{v_{\bar{n}}}(r_{\bar{n}}^2) &= \int d^4x\, e^{i r_{\bar{n}} \cdot x}\, \mathrm{Disc}\, \langle 0 | T\{\bar{h}_{v_{\bar{n}}}(x) W_{\bar{n}}(x) W_{\bar{n}}^\dagger(0) h_{v_{\bar{n}}}(0)\} | 0 \rangle\,. \end{aligned} \tag{6.50}$$

These bHQET jet functions can be calculated using the usual Feynman rules of HQET except that the gluons have collinear scaling as in Eq. (6.49). The Wilson lines in the jet functions above contain these bHQET gluons. The tree-level and one-loop results for the

jet functions $J_{v_n,v_{\bar{n}}}$ are

$$\begin{aligned} J^{\rm tree}_{v_n,v_{\bar{n}}}(y) &= \frac{2}{m}\,2\pi\,\delta(1-y), \qquad (6.51)\\ \delta J_{v_n,v_{\bar{n}}}(y) &= \frac{2}{m}\,2\pi\frac{\alpha_s C_F}{4\pi}\left[8\left[\frac{\ln(1-y)}{(1-y)}\right]_+ + \left(-\frac{4}{\epsilon}+4\ln\frac{m^2}{\mu^2}+4\right)\frac{1}{(1-y)_+}\right.\\ &+ \left.\left(\frac{2}{\epsilon^2}-\frac{2}{\epsilon}-\frac{2}{\epsilon}\ln\frac{m^2}{\mu^2}+\ln^2\frac{m^2}{\mu^2}+2\ln\frac{m^2}{\mu^2}-\frac{\pi^2}{2}\right)\delta(1-y)\right]. \qquad (6.52)\end{aligned}$$

Once again we define dimensionless jet functions:

$$K_{(v_n,v_{\bar{n}})}(y,\mu) = \frac{m}{2}\,J_{(v_n,v_{\bar{n}}),Q}(y,\mu). \qquad (6.53)$$

The equations for matching the $\mathrm{SCET_I}$ jet functions $K_{n,\bar{n}}$ onto the bHQET jet functions $K_{(v_n,v_{\bar{n}})}$ are given by

$$K_{(n,\bar{n})}(y,\mu) = \int dx\, C_{(n,\bar{n})}(y,x,\mu)\, K_{(v_n,v_{\bar{n}})}(x,\mu). \qquad (6.54)$$

The final cross section can now be written as

$$\begin{aligned}\sigma_2 &= \frac{1}{2}\Big(\mathrm{Tr}\Big[\frac{\not{n}}{2}\hat{\Gamma}^\mu_i\frac{\not{\bar{n}}}{2}\hat{\Gamma}^\nu_j\Big]+i\leftrightarrow j\Big)\,\frac{Q^6}{m^2}\,\big|C(Q,m)\big|^2\\ &\times \int dy_n\int dx_n\; C_n(y_n,x_n;m,\mu)K_{v_n}(x_n;m,\mu)\\ &\times \int dy_{\bar{n}}\int dx_{\bar{n}}\, C_{\bar{n}}(y_{\bar{n}},x_{\bar{n}};m,\mu)\, K_{v_{\bar{n}}}(x_{\bar{n}};m,\mu). \qquad (6.55)\end{aligned}$$

The Wilson coefficients of matching the $\mathrm{SCET_I}$ jet functions onto the bHQET jet functions in Eq. (6.54) are given by

$$C_{(n,\bar{n})}(x,y,\mu) = \left[1+\frac{\alpha_s C_F}{4\pi}\left(\ln^2\frac{m^2}{\mu^2}-3\ln\frac{m^2}{\mu^2}+12+\frac{\pi^2}{6}\right)\right]\delta(x-y). \qquad (6.56)$$

Note that the logs are zero at the matching scale: $\mu = m$. This is an important check of our results. The evolution of the Wilson coefficients $C_{n,\bar{n}}$ below m is given by the anomalous dimension of the jet functions $K_{(v_n,v_{\bar{n}})}(y)$

$$\mu\frac{d}{d\mu}C_{n,\bar{n}}(x,z,\mu) = \int dy\,\gamma_{K_{(v_n,v_{\bar{n}})}}(x,y,\mu)\,C_{n,\bar{n}}(y,z,\mu)\,, \qquad (6.57)$$

where the anomalous dimension is

$$\gamma_{K_{(v_n,v_{\bar{n}})}}(x,y,\mu) = \frac{\alpha_s C_F}{4\pi}\left[\left(4\ln\frac{m^2}{\mu^2}+4\right)\delta(y-x) - \frac{8}{(y-x)_+}\theta(y-x)\right]. \tag{6.58}$$

We can use the renormalization group equations to run the Wilson coefficients down to the scale $\mu \sim \Gamma$ and in the process sum logs of m/Γ. We do this by taking moments of Eq. (6.57). First, define the Nth moment:

$$M_N[f(z)] = \int_0^1 dz\, z^{N-1} f(z)\,. \tag{6.59}$$

This turns Eq. (6.57) into the diagonal form

$$\mu\frac{d}{d\mu}C_{n,\bar{n}}(N,\mu) = \gamma_K(N,\mu)C_{n,\bar{n}}(N,\mu)\,, \tag{6.60}$$

where the Nth moment of the jet function anomalous dimension is

$$\begin{aligned}\gamma_K(N,\mu) &= \int_0^1 dz\, z^{N-1}\gamma(z,\mu) \\ &= -\frac{\alpha_s C_F}{\pi}\left[1-2\ln\left(\frac{\mu N}{m}\right)\right]\end{aligned} \tag{6.61}$$

for large N. Taking large moments is appropriate here, since our effective field theory methodology is valid for small Γ, or values of y near 1, and this is the region of y corresponding to large N. This equation can be solved by standard means to give

$$C_{n,\bar{n}}(N,\frac{m}{N}) = C_{n,\bar{n}}(N,m)\left[\frac{\alpha_s(m/N)}{\alpha_s(m)}\right]^{\frac{2C_F}{\beta_0}\left(1+\frac{4\pi}{\beta_0\alpha_s}-2\ln N\right)} N^{\frac{-4C_F}{\beta_0}}\,. \tag{6.62}$$

Eq. (6.62) demonstrates the correct resummation of logs of Γ/m in the Wilson coefficient, since for large N we have $1/N \sim \Gamma/m$. Given the RGE solution for the Nth moment, the inverse Mellin transform can be performed to go from moment space back to y space, but this computation is beyond the scope of this work [51]. Here we will simply calculate the

large-N moments of the cross section in Eq. (6.55). For these we get

$$\begin{aligned}\int_0^1 dy_n\, y_n^{N-1} \int_0^1 dy_{\bar{n}}\, y_{\bar{n}}^{N-1} \frac{\mathrm{d}^2\sigma_2}{\mathrm{d}y_n \mathrm{d}y_{\bar{n}}} &= \frac{1}{2}\Big(\mathrm{Tr}\Big[\frac{\not{n}}{2}\hat{\Gamma}^\mu_i \frac{\bar{\not{n}}}{2}\hat{\Gamma}^\nu_j\Big] + i \leftrightarrow j\Big)\, \frac{Q^6}{m^2}\, \big|C(Q,m)\big|^2 \\ &\times\ C_n(N;\mu) K_{v_n}(N;\mu) \\ &\times\ C_{\bar{n}}(N;\mu)\, K_{v_{\bar{n}}}(N;\mu)\,. \end{aligned} \tag{6.63}$$

We have just derived the resummed versions of the Wilson coefficients $C_{n,\bar{n}}$. Now we must derive an expression for the moments of the bHQET jet functions. Since we are only summing leading logs in this analysis, it will be sufficient to calculate these moments at tree level. At this point we can also add the width to the jet functions, so that we reproduce the standard Breit-Wigner form. Adding the top width to the jet functions $K_{(v_n,v_{\bar{n}})}$, we get

$$K^{\mathrm{tree}}_{(v_n,v_{\bar{n}})}(y;m,\mu) = \frac{\Gamma/m}{(1-y)^2 + \Gamma^2/m^2}\,. \tag{6.64}$$

Note that this reduces to a delta function in the $\Gamma \to 0$ limit as required. Large N moments of this expression are simply

$$K^{\mathrm{tree}}_{(v_n,v_{\bar{n}})}(N;\mu) = \int_0^1 dy\, y^{N-1} \frac{\Gamma/m}{(1-y)^2 + \Gamma^2/m^2} \to \frac{m}{N\Gamma}\,. \tag{6.65}$$

Note that this expression is order one.

The analysis is now complete. We have an expression for moments of the cross section in the limit corresponding to $y_{n,\bar{n}} \sim 1$. The leading logs have been summed and are contained in the coefficient functions.

6.6 Summary

This chapter has explored the application of SCET to top-antitop production at high energy in an e^+e^- environment. The focus was on summing logarithms of the three relevant scales in the problem: $\sqrt{s}$, m_t, and Γ_t. These logarithms occur in the calculation of distributions that are not fully inclusive. This may be necessary in the process we are considering or in a process involving as-yet-undiscovered heavy particles because experimenters will want to know the cross section in a very specific region in order to study the particle properties closely.

Our analysis consisted of four basic parts: matching QCD currents onto SCET currents at the large scale $\sqrt{s}$, running the currents down to the lower scale m_t, matching the SCET jet functions onto boosted HQET jet functions at the scale m_t, and then running the jet functions down to the low scale Γ_t. Because the high-energy degrees of freedom are properly integrated out at each stage, this process correctly sums the logs of the three scales.

Chapter 7

Testing jet definitions in SCET

This chapter discusses the applicability of soft-collinear effective theory to jet physics. That is, what are the correct definitions of jets in the SCET framework. Part of this chapter appeared in Ref. [52].

7.1 The problem of defining jets in SCET

Many processes at high-energy colliders require reliable calculations of differential distributions of kinematic variables defined through the momenta of isolated jets in the detector. One example is the measurement of masses of the gauge bosons in hadronic decays, which require the invariant mass distribution of a pair of jets. Recently it was shown [53, 50] that factorization formulas can be derived for such observables using the soft-collinear effective theory (SCET) [33, 34, 35, 36]. An example is the differential jet energy distribution in the decay of a Z boson to two light quarks, which close to the endpoint of maximal jet energy is predicted at tree level to be [53]

$$\frac{d\Gamma}{dE_J} = \Gamma^{(0)} S(E_J - \frac{m_Z}{2}) \,, \tag{7.1}$$

where $\Gamma^{(0)}$ is the total decay rate at tree level, which can be calculated reliably using quark-hadron duality and the operator product expanision (OPE). The functional dependence on the jet energy is contained in the nonperturbative function

$$S(k) = \frac{1}{N_C} \left\langle 0 \left| \left[\overline{Y}_n^\dagger Y_{\bar{n}}^\dagger \right]_d^a \delta \left(k + \frac{in \cdot \partial}{2} \right) \left[Y_{\bar{n}} \overline{Y}_n \right]_a^d \right| 0 \right\rangle , \tag{7.2}$$

which is defined as the vacuum matrix element of a nonlocal operator containing Wilson lines

$$Y_n(z) = P \exp\left[ig \int_0^\infty \mathrm{d}s \; n \cdot A_u(ns + z)\right] . \tag{7.3}$$

The above calculation of the jet energy distribution requires two crucial assumptions:

1. One needs to factor the final state into a collinear jet and a remaining purely ultrasoft piece, where the ultrasoft piece satisfies the completeness relation

$$|X\rangle = |\text{jet}\rangle \, |X_{\text{us}}\rangle \; , \qquad \sum_{X_{\text{us}}} |X_{\text{us}}\rangle \, \langle X_{\text{us}}| = 1 \, . \tag{7.4}$$

2. The momentum of the jet is required to be equal to the total momentum of all collinear partons in the same direction as the hadronic jet

$$P_j = p_n^c \, . \tag{7.5}$$

One can question both of these assumptions, since the total collinear partonic system in each light like direction is in a color-triplet configuration, while the final hadronic jet is of course color singlet. Thus, color needs to be redistributed between the two collinear systems in order to form the final hadronic system observed experimentally. This implies that the factorization of the final state in Eq. 7.4 is only unambiguously defined at the partonic level, and that the color recombination should move some momentum between the collinear and the remaining soft physics, such that Eq. 7.5 is violated at some level. The assumption made in [53, 50] is that the summation over hadronic and partonic states are equivalent, such that neither of the two assumptions affect the decay rate at order Λ_{QCD}/m_Z.

To understand in more detail whether these assumptions are correct requires a detailed understanding of how energetic partons hadronize and form the observed jets, and how the color gets redistributed between the two jets. Unfortunately this is not feasible with our current understanding of QCD. The best way to gain insight into this question is therefore to test experimentally whether predictions made under the above assumptions are correct. In this chapter we derive an expression for the jet P^+ distribution in the semileptonic or radiative decays of a heavy meson, under the assumption explained above. The jet is defined as before using a particular algorithm, and for simplicity we restrict ourselves to

the Sterman-Weinberg jet definition [54]. We find that the jet P^+ spectrum is directly related to differential distributions in leptonic variables, which can be calculated reliably using the well-known twist expansion. We begin by showing this relation at tree level, using simple kinematical arguments. We then extend this argument by calculating the leading perturbative corrections. This relation will be no surprise to those acquainted with the P^+ distribution used in determining $|V_{ub}|$ [55, 56]. It is well known that that distribution is related to the photon energy spectrum [55, 51]. There is a big difference, however, between the P^+ distribution and our jet P^+ distribution. For our distribution, we have separated the jet momenta from the ultrasoft momenta, based on a jet definition. The P^+ distribution, on the other hand, considers the sum of these two contributions. That is, the total final state momentum after subtracting off the photon or lepton momentum, as the case may be.

7.2 Review of radiative and semileptonic B decay in SCET

The currents describing the currents $b \to u\ell\bar{\nu}$ and $b \to s\gamma$ are

$$\begin{aligned} J^\alpha_{(s)} &= \frac{1}{m_b} \bar{s} P_R \, \sigma^{\alpha\beta} \, b \; q_\beta, \\ J^\alpha_{(u)} &= \bar{u} P_R \, \gamma^\alpha \, b, \end{aligned}$$

respectively. To describe the processes in the shape function region, where the hadronic final state has small invariant mass and large energy, we match these currents onto operators in SCET:

$$\begin{aligned} j^{\rm eff}_{1\mu} &= \bar{\chi}^{(0)}_n Y_n P_R \gamma^\perp_\mu b_v \,, \\ j^{\rm eff}_2 &= \bar{\chi}^{(0)}_n Y_n P_R b_v \,, \end{aligned} \tag{7.6}$$

where the matching coefficients are given in Eqs. (8) and (9) of [57]. The collinear fields $\chi^{(0)}_n$ include the collinear Wilson line W_n and are related to the standard collinear fields through the usual field redefinition [35] $\chi_n \to Y_n \chi^{(0)}_n$ and have no interactions with ultrasoft fields at leading order in the SCET Lagrangian. Choosing the assignments of momenta as illustrated in Fig 7.1, the fact that the collinear quark is massless gives the relation

$$0 \sim m_b^2 - 2 m_b v \cdot q + 2(m_b v - q) \cdot (k - l) \,, \tag{7.7}$$

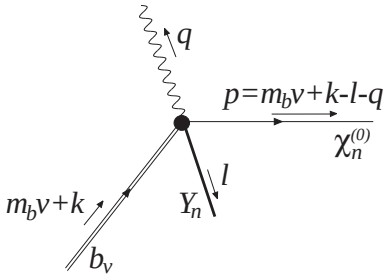

Figure 7.1: Kinematics of the current in the effective theory. The heavy quark b_v has momentum $m_b v + k$, the gauge boson has q and the total momentum of the usoft Wilson line Y_n is l.

where we have dropped terms of order $\Lambda^2_{\rm QCD}$. Thus, for the process $B \to X_s\gamma$ the photon energy spectrum is given by the expectation value $\langle k^+ - l^+ \rangle$, which is given by the well-known shape function.

The kinematics of this process are shown in Fig. 7.1. There are two momenta of order $\Lambda_{\rm QCD}$. The first is the residual momentum k, which describes classically the small recoil of the heavy b quark inside a B meson at rest. The second is the momentum l, which gives the total momentum which the energetic light quark loses to soft radiation.

7.3 Standard observables

We begin by reviewing the derivation of the inclusive observables, which can be defined purely from leptonic kinematics. These calculations are known to one-loop order in the QCD coupling constant and are now usually done in the framework of SCET. We will follow closely the discussion in [57]. All strong interaction effects for the inclusive B decays studied here can be encoded in the hadronic tensor

$$W^{\alpha\beta} = -\frac{1}{\pi}\text{Im}\ T^{\alpha\beta},$$

where

$$T^{\alpha\beta}_{(f)} \;=\; -i\int d^4x e^{-iq\cdot x}\frac{\left\langle \bar{B}\left|T\left[J^{\dagger\alpha}_{(f)}(x)J^{\beta}_{(f)}(0)\right]\right|\bar{B}\right\rangle}{2m_B},$$

and $J^\alpha_{(u)}$ and $J^\alpha_{(s)}$ are the quark currents mediating the $b \to u\ell\bar\nu$ and $b \to s\gamma$ transition, respectively,

$$\begin{aligned} J^\alpha_{(s)} &= \frac{1}{m_b}\bar s P_R\, \sigma^{\alpha\beta}\, b\; q_\beta, \\ J^\alpha_{(u)} &= \bar u P_R\, \gamma^\alpha\, b. \end{aligned}$$

The most general tensor structure possible for $W^{\alpha\beta}$ is

$$\begin{aligned} W^{\alpha\beta} &= -g^{\alpha\beta}W_1 + v^\alpha v^\beta W_2 + i\epsilon^{\alpha\beta\rho\sigma}v_\rho q_\sigma W_3 \\ &\quad + q^\alpha q^\beta W_4 + \Big(q^\alpha v^\beta + q^\beta v^\alpha\Big) W_5\,, \end{aligned} \tag{7.8}$$

and the $W_i's$ are different for $b \to u\ell\bar\nu$ and $b \to s\gamma$ transition.

The inclusive differential decay rates for the decays $B \to X_s\gamma$ and $B \to X_u\ell\bar\nu$ are

$$\begin{aligned} \frac{\mathrm{d}\Gamma^s}{\mathrm{d}x_\gamma} &= 2\, m_b\, \Gamma_0^{(s)} x_\gamma \left[4W_1^{(s)} - W_2^{(s)} - x_\gamma\, m_b\, W_5^{(s)}\right], \\ \frac{\mathrm{d}\Gamma^u}{\mathrm{d}x_\ell\, \mathrm{d}z\, \mathrm{d}\hat p^2} &= 12\, m_b\, \Gamma_0^{(u)} \Big[2(1 - z + \hat p^2)W_1^{(u)} \\ &\quad + (\bar x_\ell(z - \bar x_\ell) - \hat p^2)W_2^{(u)} \\ &\quad + m_b(1 - z + \hat p^2)(z - 2\bar x_\ell)W_3^{(u)}\Big], \end{aligned} \tag{7.9}$$

where

$$\begin{aligned} \Gamma_0^{(s)} &= \frac{G_F^2\, |V_{tb}V_{ts}|^2\, \alpha\, \left|c_7^{\mathrm{eff}}\right|^2 m_b^5}{32\pi^4}, \\ \Gamma_0^{(u)} &= \frac{G_F^2\, |V_{ub}|^2\, m_b^5}{192\pi^3}, \end{aligned}$$

and we have defined the dimensionless variables

$$x_\gamma = \frac{2E_\gamma}{m_b}\,, \quad x_\ell = \frac{2E_\ell}{m_b}\,, \quad \hat p^2 = \frac{p^2}{m_b^2}\,, \quad z = \frac{2v\cdot p}{m_b}\,,$$

and $\bar x_\ell = 1 - x_\ell$. c_7^{eff} is the coefficient of the $b \to s\gamma$ operator O_7 in the weak Hamiltonian at the scale μ_1. At next-to-leading order $c_7(m_b) = -0.311$ [58].

To obtain expressions for the scalar functions $W_i^{(f)}$ involves three steps: (1) Match from QCD to SCET currents at $\mu_1 \sim m_b$. (2) Run from μ_1 to μ_2 using the SCET anomalous

dimension. (3) Integrate out the final hadronic states at $\mu_2 \sim \sqrt{m_b \Lambda_{\rm QCD}}$ by computing the time-ordered product of currents, and match onto bilocal operators. All these three steps have been carried out in sections V.A–V.C of Ref. [57] and we refer the reader to this reference for all details of the calculation. Here we will only give the final result for the functions $W_i^{(f)}$. For the decay $B \to X_u \ell \bar{\nu}$ one finds

$$\begin{aligned}
W_1^{(u)} &= \frac{C_1^2}{4} \frac{\langle \bar{B} \,|\mathcal{W}(p^+)|\, \bar{B}\rangle}{2m_B}, \\
W_2^{(u)} &= \left[\frac{\bar{n}\cdot\hat{p}-1}{\bar{n}\cdot\hat{p}^2}\, C_1^2 + \left(\frac{C_2}{\bar{n}\cdot\hat{p}} + \frac{C_3}{2}\right)^2\right] \frac{\langle \bar{B} \,|\mathcal{W}(p^+)|\, \bar{B}\rangle}{2m_B}, \\
W_3^{(u)} &= \frac{1}{2m_b \bar{n}\cdot\hat{p}}\, C_1^2 \frac{\langle \bar{B} \,|\mathcal{W}(p^+)|\, \bar{B}\rangle}{2m_B}, \\
W_4^{(u)} &= \frac{1}{m_b^2(\bar{n}\cdot\hat{p})^2}(C_2^2 - C_1^2) \frac{\langle \bar{B} \,|\mathcal{W}(p^+)|\, \bar{B}\rangle}{2m_B}, \\
W_5^{(u)} &= \frac{1}{2m_b(\bar{n}\cdot\hat{p})^2}\Big[C_1^2(2-\bar{n}\cdot\hat{p}) - 2C_2^2 \\
&\quad - C_2 C_3 \bar{n}\cdot\hat{p}\Big] \frac{\langle \bar{B} \,|\mathcal{W}(p^+)|\, \bar{B}\rangle}{2m_B}\,.
\end{aligned} \tag{7.10}$$

For the decay $B \to X_s \gamma$ one finds

$$\begin{aligned}
W_1^{(s)} &= \frac{C_4^2}{4} \frac{\langle \bar{B} \,|\mathcal{W}(p^+)|\, \bar{B}\rangle}{2m_B}, \\
W_2^{(s)} &= 0\,, \\
W_3^{(s)} &= \frac{C_4^2}{2m_b} \frac{\langle \bar{B} \,|\mathcal{W}(p^+)|\, \bar{B}\rangle}{2m_B}, \\
W_4^{(s)} &= \frac{1}{4m_b^2}\left(C_5^2 - 4C_4^2\right) \frac{\langle \bar{B} \,|\mathcal{W}(p^+)|\, \bar{B}\rangle}{2m_B}, \\
W_5^{(s)} &= \frac{C_4^2}{2m_b} \frac{\langle \bar{B} \,|\mathcal{W}(p^+)|\, \bar{B}\rangle}{2m_B}.
\end{aligned} \tag{7.11}$$

The matrix element $\langle \bar{B} \,|\mathcal{W}(p^+)|\, \bar{B}\rangle$ is given by

$$\langle \bar{B} \,|\mathcal{W}(p^+)|\, \bar{B}\rangle_{\rm lept} = \int {\rm d}r^+ \mathcal{C}(p^+ - r^+, \mu) f(r^+, \mu)\,, \tag{7.12}$$

where the function $f(r^+)$ is a nonperturbative distribution function, which physically gives the probability of finding a b quark with lightlike momentum r^+ inside the B meson. It is

defined by

$$f(r^+,\mu) = \frac{1}{2\pi}\int_{-\infty}^{\infty} du^- e^{-iu^-r^+} \left\langle \bar{B}\left|\bar{b}_v(0)Y(0,u^-)b_v(u^-)\right|\bar{B}\right\rangle|_\mu\,. \tag{7.13}$$

The coefficient $\mathcal{C}$ is the jet function, which can be calculated using perturbation theory at the scale $\mu_2 \sim \sqrt{m_b\Lambda_{\rm QCD}}$. To order α_s it is given by

$$\begin{aligned}
\mathcal{C}(q^+,\mu) &= \delta(q^+) + \frac{\alpha_s(\mu)C_F}{4\pi}\mathcal{C}^{(1)}(q^+,\mu),\\
\mathcal{C}^{(1)}(q^+,\mu) &= 4\left[\frac{\ln(q^+/\mu)\;\theta(q^+)}{q^+}\right]_\mu\\
&\quad + \left[4\ln\frac{\bar{n}\cdot p}{\mu} - 3\right]\left[\frac{\theta(q^+)}{q^+}\right]_\mu\\
&\quad + \left[2\ln^2\frac{\bar{n}\cdot p}{\mu} - 3\ln\frac{\bar{n}\cdot p}{\mu} + 7 - \pi^2\right]\delta(q^+).
\end{aligned} \tag{7.14}$$

7.4 Jet P^+ distribution

Next, we calculate the jet P^+ distribution. The calculation can be divided into the same three steps as for the calculation of the fully inclusive observables. Furthermore, the steps (1) and (2), the matching from QCD onto SCET and the running of the SCET currents, are the same as before, so we again obtain the results given in Eqs. (7.10) and (7.11), albeit with a different expression for the matrix element $\left\langle \bar{B}\left|\mathcal{W}(p^+)\right|\bar{B}\right\rangle$. For the jet P^+ distribution, this matrix element depends on the precise definition of the jet. There are several jet definitions available [59], and in this chapter we restrict ourselves to the original definition by Sterman and Weinberg (SW) [54]. While this definition has some problems when multiple jets are present [59], it is simplest to use theoretically and will suffice for the work presented here. Defining a SW jet requires specifying a cone angle δ and an energy cut $\beta E_{\rm max}$, where $E_{\rm max}$ is the maximum hadronic energy allowed in the process. In the work considered here, we want events with a single jet in the final state, thus we require all particles with energy above $\beta E_{\rm max}$ to lie within the cone angle δ. The combination of all the particles within the cone angle are called the jet, and the jet P^+ is thus the sum of the p^+ momentum components of all the particles within the cone angle δ.

Under the two assumptions mentioned at the beginning of this letter, we find that the matrix element $\left\langle \bar{B}\left|\mathcal{W}(p^+)\right|\bar{B}\right\rangle$ is given by an expression very similar to the one in the fully

inclusive case

$$\left\langle \bar{B} \left| \mathcal{W}(p^+) \right| \bar{B} \right\rangle_{\text{jet}} = \int \mathrm{d}r^+ \mathcal{D}(p^+ - r^+, \mu) f(r^+, \mu) \,, \tag{7.15}$$

where $f(r^+, \mu)$ is the *same* nonperturbative distribution function as before. To see this, we go back to the original definition of the matrix element of $\mathcal{W}$. For this calculation, we will restrict ourselves to the radiative B decay case, although it is straightforward (but more tedious with more particles in the final state) to do the leptonic decay as well. Our derivation follows the derivation for Z decay in Ref. [50] closely.

We start with the definition of the B meson differential decay rate. Somewhat schematically we have

$$\mathrm{d}\Gamma = \frac{1}{2m_B} \sum_{\text{final}} \left| \left\langle J X_u \left| \bar{\chi}_n \Gamma^\mu \epsilon_\mu^* b_v(0) \right| \bar{B} \right\rangle \right|^2 (2\pi)^4 \delta^4(p_B - p_J - q - l) \,, \tag{7.16}$$

where ϵ is the polarization vector of the photon and the sum over final states includes all the phase space integrals. As usual, we perform the following field redefinitions to decouple soft and collinear degrees of freedom:

$$\xi \;\to\; Y_n^\dagger \xi_n \,, \tag{7.17}$$

$$A_n \;\to\; Y_n^\dagger A_n Y_n \,. \tag{7.18}$$

This allows us to factorize the matrix element and make the dubious assumption. We split the final state into a jet final state and an ultrasoft final state containing any additional QCD radiation that occurs beyond leading order in perturbation theory. We need to insert a delta function into our decay rate expression to specify the distribution we are considering. Since we are looking at the jet P^+ distribution, we insert the following:

$$\delta(P_J^+ - n{\cdot}p_J) = \delta(P_J^+ - p_B^+ + q^+ + l^+) \,, \tag{7.19}$$

where we have used the momentum-conserving delta function in the decay rate above. For now choose coordinates such that the photon momentum is along the $\bar{n}$ lightlike vector. This implies that

$$q^+ = m_B x \,, \tag{7.20}$$

where x is defined to be the photon energy fraction in units of $m_B/2$. With all of these definitions, our expression for the differential decay rate becomes

$$\begin{aligned}\frac{\mathrm{d}\Gamma}{\mathrm{d}P_J^+} &= \frac{3|\mathcal{M}^{(0)}|^2}{32\pi m_B}\sum_{X_u}\delta\left[P_J^+ - m_B(1-x) - (k^+ - l^+)\right] \\ &\quad\times\left\langle \bar{B}(k)\middle|Y_n(0)\middle|X_u(l)\right\rangle\left\langle X_u(l)\middle|Y_n^\dagger(0)\middle|\bar{B}(k)\right\rangle . \end{aligned} \tag{7.21}$$

We have labeled the B states with the residual momentum k instead of the full b quark momentum because we are thinking of this calculation in HQET, where the large part of the momentum has been removed and is no longer dynamical. Therefore the momentum operator acting on these states gives the residual momentum rather than the total.

In order to do the sum over ultrasoft states, we must remove the l^+ momentum from the delta function. We do this in the standard way by writing the delta function as

$$\delta\left[P_J^+ - m_B(1-x) - (k^+ - l^+)\right] = \int\frac{\mathrm{d}u^-}{2\pi}\exp\left[i\left(P_J^+ - m_B(1-x) - (k^+ - l^+)\right)u^-\right] . \tag{7.22}$$

We can now use this expression to translate the starting position of the second Wilson line and then do the sum over ultrasoft states. The result is

$$\frac{\mathrm{d}\Gamma}{\mathrm{d}P_J^+} = \Gamma^{(0)} f(P_J^+ - m_B(1-x)) , \tag{7.23}$$

where the shape function f is given in Eq. (7.13). Our result above is a product of the perturbative part and the shape function because we have done the perturbative part only at leading order. Extending the perturbative calculation beyond leading order shows that the real expression for the differential decay rate is a convolution of these two parts, and therefore the expression for the matrix element we want is simply given by Eq. (7.15).

It remains only to calculate the distribution $\mathcal{D}$ in Eq. (7.15). This is a straightforward calculation now that all the notation is in place. For this calculation we follow the example of Appendix B of Ref. [50].

We find

$$\begin{aligned}
\mathcal{D}(q^+,\mu) &= \delta(q^+) - \frac{\alpha_s(\mu)C_F}{4\pi}\mathcal{D}^{(1)}(q^+,\mu), \\
\mathcal{D}^{(1)}(q^+,\mu) &= \delta(q^+)\bigg(2\ln\frac{\mu^2}{m_b^2} - \ln^2\beta^2 + 3\ln\beta^2 + 3\ln\frac{\delta^2}{4} \\
&\quad + 2\ln\beta^2\ln\frac{\delta^2}{4} + 2\pi^2 - 5\bigg) \\
&\quad + \theta(\delta^2/2 - 2P_J^+/m_b)\theta(P_J^+)\left[\frac{1}{P_J^+}\ln\left(\frac{4P_J^+}{m_b\delta^2}\right)\right]_+ . \qquad (7.24)
\end{aligned}$$

With both perturbative results in hand, the two distributions can be compared. Different moments of the two matrix elements will be easiest to compare. Since the standard leptonic and photonic distributions are well studied, any discrepancies will probably be due to unknown features of the jet P^+ distribution. This is precisely the information we are interested in. Good measurements of these moments will be an excellent consistency check on the procedures in the SCET jet P^+ distribution derivation.

7.5 Summary

This chapter has explored possible difficulties with defining jets in SCET. The philosophy taken here has been to proceed naively in SCET and then construct an observable that can be compared with well-known results. This way we avoid the considerable difficulty of trying to prove SCET jet definitions from first-principles QCD. The assumptions required in the procedure of defining the SCET jets can then be checked with experimental results.

The first section of this chapter illustrated the problem. Typically, SCET applications to jet physics must factorize a final state into separate collinear and ultrasoft states. At first glance it is not clear whether this is a reasonable thing to do. Surely at some stage hadronization occurs and color must be rearranged between the supposedly separate states. They cannot really be physical states in their own right.

The second and third sections then reprised the derivation of the standard leptonic and photonic distributions for comparison. These distributions are widely used and well-tested in B decays. Results based on them are on firm ground and can serve as a benchmark for testing the SCET jet assumptions. The fourth section then computed the corresponding distributions in jet P^+ momentum for B decays. Since the nonperturbative parts are the

same, moments of each distribution can be taken and compared with experiment. Any discrepancies will answer some of our questions about the SCET jet procedure.

Chapter 8

Conclusions

This thesis has shown several applications of effective theories involving heavy particles. The first main chapter has presented order α_s corrections to two new sum rules derived in Refs. [12, 13, 14] in the context of HQET. Section 3.2 repeated the tree-level derivation of a generic sum rule depending on three velocity transfer variables and included one-loop corrections. Section 3.3 studied the axial vector and vector sum rules that result from choosing specific currents in the generic equation. These led to α_s-corrected versions of the sum rules of Le Yaouanc *et al.* for the curvature of the Isgur-Wise function. There were no corrections suppressed by the heavy quark masses because the infinite-mass limit was used. Section 3.4 translated these HQET bounds into bounds on physical form factors by including perturbative and finite-mass corrections associated with matching HQET onto the full theory. Numerical estimates were given and compared with experimental values and dispersive constraints. The bounds produced here are less powerful than dispersive constraints but may provide an important check on those constraints.

We have also considered the matching of the heavy-light current in $\mathrm{SCET_I}$ onto the corresponding current in $\mathrm{SCET_{II}}$, in particular addressing the question whether all long-distance physics in $\mathrm{SCET_I}$ is correctly reproduced in $\mathrm{SCET_{II}}$. Using the off-shellness of the external heavy and light fermions, it was argued in Ref. [40] that a new collinear–soft messenger mode is required in $\mathrm{SCET_{II}}$ to reproduce all the long-distance physics of $\mathrm{SCET_I}$. Regulating the IR in $\mathrm{SCET_{II}}$ with an off-shellness is problematic, since the off-shellness prevents performing the field redefinition required to decouple the usoft gluons from the collinear particles, which allows the matching onto $\mathrm{SCET_{II}}$ easily. In this chapter we investigated the relationship between IR regulators and the definition of $\mathrm{SCET_{II}}$. By performing the k_0 loop integral by contours and then writing the remaining integrals as

$\mathrm{d}|\mathbf{k}|\,\mathrm{d}\cos\theta$, we showed explicitly that the off-shellness leaves the IR angular divergence $(1-\cos\theta)\to 0$ unregulated in $\mathrm{SCET_{II}}$.

We then introduced a new regulator for SCET that regulates soft ($|\mathbf{k}|\to 0$) and collinear ($\cos\theta\to 1$) IR divergences in both $\mathrm{SCET_I}$ and $\mathrm{SCET_{II}}$. This regulator modifies the gluon action, much like a gluon mass, and thus preserves the field redefinition required to decouple usoft gluons from collinear particles in SCET. Using this regulator, we showed explicitly that $\mathrm{SCET_{II}}$ as formulated in Refs. [36, 38] reproduces all the IR divergences of $\mathrm{SCET_I}$. We also argued that any cutoff κ regulating the collinear divergence has to satisfy $\kappa \ll n{\cdot}k_s$. Regulating $\mathrm{SCET_{II}}$ this way therefore naturally requires keeping a formally subleading regulator in the theory.

We also showed that a soft–collinear messenger mode is required in the definition of the IR regulator if one insists on power counting the regulator in the same way as kinetic terms in the action. In this case, there are unregulated IR divergences left in soft diagrams, which are corrected by additional contributions from the soft-collinear mode.

The new regulator introduced in this chapter preserves the invariance of $\mathrm{SCET_I}$ under the field redefinitions (5.4), and is therefore useful in studying factorization theorems beyond tree level.

The fifth chapter explored the application of SCET to top-antitop production at high energy in an e^+e^- environment. The focus was on summing logarithms of the three relevant scales in the problem: $\sqrt{s}$, m_t, and Γ_t. These logarithms occur in the calculation of distributions that are not fully inclusive. This may be necessary in the process we are considering or in a process involving as-yet-undiscovered heavy particles because experimenters will want to know the cross section in a very specific region in order to study the particle properties closely.

Our analysis consisted of four basic parts: matching QCD currents onto SCET currents at the large scale $\sqrt{s}$, running the currents down to the lower scale m_t, matching the SCET jet functions onto boosted HQET jet functions at the scale m_t, and then running the jet functions down to the low scale Γ_t. Because the high-energy degrees of freedom are properly integrated out at each stage, this process correctly sums the logs of the three scales.

The sixth chapter explored possible difficulties with defining jets in SCET. The philosophy taken here has been to proceed naively in SCET and then construct an observable that can be compared with well-known results. This way we avoid the considerable difficulty of

trying to prove SCET jet definitions from first-principles QCD.

The first section of this chapter illustrated the problem. Typically, SCET applications to jet physics must factor a final state into separate collinear and ultrasoft states. A first glance it is not clear whether this is a reasonable thing to do. Surely at some stage hadronization occurs and color must be rearranged between the supposedly separate states. They cannot really be physical states in their own right.

The second and third sections then reprised the derivation of the standard leptonic and photonic distributions for comparison. The fourth section then computed the corresponding distribution in jet P^+ momentum for B decays. Since the nonperturbative parts are the same, moments of each distribution can be taken and compared with experiment. Any discrepancies will answer some of our questions about the SCET jet procedure. This analysis is left to a subsequent publication.

Bibliography

[1] A. V. Manohar and M. B. Wise, Cambridge Monogr. Part. Phys. Nucl. Phys. Cosmol. **10**, 1 (2000).

[2] M. P. Dorsten, Phys. Rev. D **70**, 096013 (2004).

[3] E. Eichten and B. Hill, Phys. Lett. B **234**, 511 (1990); H. Georgi, Phys. Lett. B **240**, 447 (1990).

[4] N. Isgur and M. B. Wise, Phys. Lett. B **232**, 113 (1989); Phys. Lett. B **237**, 527 (1990).

[5] S. Nussinov and W. Wetzel, Phys. Rev. D **36**, 130 (1987).

[6] M. A. Shifman and M. B. Voloshin, Sov. J. Nucl. Phys. **47**, 511 (1988) [Yad. Fiz. **47**, 801 (1988)].

[7] M. E. Luke, Phys. Lett. B **252**, 447 (1990).

[8] A. Czarnecki, Phys. Rev. Lett. **76**, 4124 (1996); A. Czarnecki and K. Melnikov, Nucl. Phys. B **505**, 65 (1997).

[9] S. Stone, in *B Decays, 2nd Edition*, edited by S. Stone (World Scientific, Singapore 1994), p. 283.

[10] C. G. Boyd, B. Grinstein and R. F. Lebed, Phys. Lett. B **353**, 306 (1995); Nucl. Phys. B **461**, 493 (1996); Phys. Rev. D **56**, 6895 (1997).

[11] I. Caprini and M. Neubert, Phys. Lett. B **380**, 376 (1996); I. Caprini, L. Lellouch and M. Neubert, Nucl. Phys. B **530**, 153 (1998).

[12] A. Le Yaouanc, L. Oliver and J. C. Raynal, Phys. Rev. D **67**, 114009 (2003).

[13] A. Le Yaouanc, L. Oliver and J. C. Raynal, Phys. Lett. B **557**, 207 (2003).

[14] A. Le Yaouanc, L. Oliver and J. C. Raynal, Phys. Rev. D **69**, 094022 (2004).

[15] I. Bigi, M. Shifman, N. G. Uraltsev and A. Vainshtein, Phys. Rev. D **52**, 196 (1995).

[16] A. Kapustin, Z. Ligeti, M. B. Wise and B. Grinstein, Phys. Lett. B **375**, 327 (1996).

[17] C. G. Boyd and I. Z. Rothstein, Phys. Lett. B **395**, 96 (1997).

[18] C. G. Boyd, Z. Ligeti, I. Z. Rothstein and M. B. Wise, Phys. Rev. D **55**, 3027 (1997).

[19] N. Uraltsev, Phys. Lett. B **501**, 86 (2001).

[20] E. C. Poggio, H. R. Quinn and S. Weinberg, Phys. Rev. D **13**, 1958 (1976).

[21] A. F. Falk, Nucl. Phys. B **378**, 79 (1992).

[22] N. Isgur and M. B. Wise, Phys. Rev. D **43**, 819 (1991).

[23] J. D. Bjorken, SLAC-PUB-5278 *Invited talk given at Les Rencontres de la Valle d'Aoste, La Thuile, Italy, Mar 18-24, 1990;* J. D. Bjorken, I. Dunietz and J. Taron, Nucl. Phys. B **371**, 111 (1992).

[24] M. Neubert, Phys. Rept. **245**, 259 (1994).

[25] C. G. Boyd, B. Grinstein and A. V. Manohar, Phys. Rev. D **54**, 2081 (1996).

[26] B. Grinstein and Z. Ligeti, Phys. Lett. B **526**, 345 (2002).

[27] M. Neubert, Phys. Rev. D **46**, 3914 (1992); M. Neubert, Z. Ligeti and Y. Nir, Phys. Lett. B **301**, 101 (1993); Phys. Rev. D **47**, 5060 (1993); Z. Ligeti, Y. Nir and M. Neubert, Phys. Rev. D **49**, 1302 (1994).

[28] M. B. Voloshin, Phys. Rev. D **46**, 3062 (1992).

[29] K. Abe *et al.* [Belle Collaboration], Phys. Lett. B **526**, 258 (2002).

[30] K. Abe *et al.* [Belle Collaboration], Phys. Lett. B **526**, 247 (2002).

[31] C. W. Bauer, "Mini Lecture on SCET," *unpublished.*

[32] C. W. Bauer, M. P. Dorsten and M. P. Salem, Phys. Rev. D **69**, 114011 (2004).

[33] C. W. Bauer, S. Fleming and M. E. Luke, Phys. Rev. D **63**, 014006 (2001).

[34] C. W. Bauer, S. Fleming, D. Pirjol and I. W. Stewart, Phys. Rev. D **63**, 114020 (2001).

[35] C. W. Bauer and I. W. Stewart, Phys. Lett. B **516**, 134 (2001).

[36] C. W. Bauer, D. Pirjol and I. W. Stewart, Phys. Rev. D **65**, 054022 (2002).

[37] C. W. Bauer, D. Pirjol and I. W. Stewart, Phys. Rev. D **67**, 071502 (2003) [arXiv:hep-ph/0211069].

[38] C. W. Bauer, D. Pirjol and I. W. Stewart, Phys. Rev. D **68**, 034021 (2003).

[39] R. J. Hill and M. Neubert, Nucl. Phys. B **657**, 229 (2003) [arXiv:hep-ph/0211018].

[40] T. Becher, R. J. Hill and M. Neubert, arXiv:hep-ph/0308122; T. Becher, R. J. Hill, B. O. Lange and M. Neubert, arXiv:hep-ph/0309227.

[41] R. J. Hill, private communication.

[42] For a recent discussion on this point see I. Z. Rothstein, arXiv:hep-ph/0308266.

[43] M. Beneke and T. Feldmann, arXiv:hep-ph/0311335.

[44] C. W. Bauer, M. P. Dorsten, S. P. Fleming, S. Mantry, and I. Stewart, *in preparation.*

[45] A. K. Leibovich, Z. Ligeti and M. B. Wise, Phys. Lett. B **564**, 231 (2003) [arXiv:hep-ph/0303099].

[46] C. W. Bauer, S. Fleming, D. Pirjol, I. Z. Rothstein and I. W. Stewart, Phys. Rev. D **66**, 014017 (2002) [arXiv:hep-ph/0202088].

[47] M. Beneke, A. P. Chapovsky, A. Signer and G. Zanderighi, Nucl. Phys. B **686**, 205 (2004) [arXiv:hep-ph/0401002]; Phys. Rev. Lett. **93**, 011602 (2004) [arXiv:hep-ph/0312331].

[48] A. V. Manohar, Phys. Rev. D **68**, 114019 (2003) [arXiv:hep-ph/0309176].

[49] C. M. Arnesen, J. Kundu and I. W. Stewart, Phys. Rev. D **72**, 114002 (2005) [arXiv:hep-ph/0508214].

[50] C. W. Bauer, C. Lee, A. V. Manohar and M. B. Wise, Phys. Rev. D **70**, 034014 (2004) [arXiv:hep-ph/0309278].

[51] A. K. Leibovich and I. Z. Rothstein, Phys. Rev. D **61**, 074006 (2000); A. K. Leibovich, I. Low and I. Z. Rothstein, *ibid.* **61**, 053006 (2000); A. K. Leibovich, I. Low and I. Z. Rothstein, Phys. Lett. B **486**, 86 (2000).

[52] C. W. Bauer and M. P. Dorsten, *unpublished*.

[53] C. W. Bauer, A. V. Manohar and M. B. Wise, Phys. Rev. Lett. **91**, 122001 (2003) [arXiv:hep-ph/0212255].

[54] G. Sterman and S. Weinberg, Phys. Rev. Lett. **39**, 1436 (1977).

[55] S. W. Bosch, B. O. Lange, M. Neubert and G. Paz, Nucl. Phys. B **699**, 335 (2004).

[56] S. W. Bosch, B. O. Lange, M. Neubert and G. Paz, Phys. Rev. Lett. **93**, 221801 (2004).

[57] C. W. Bauer and A. V. Manohar, Phys. Rev. D **70**, 034024 (2004)

[58] M. Misiak, Nucl. Phys. B **393**, 23 (1993) [Erratum-ibid. B **439**, 461 (1995)]; A. J. Buras and M. Munz, Phys. Rev. D **52**, 186 (1995).

[59] G. C. Blazey *et al.*, arXiv:hep-ex/0005012.